



2007

INFLUENCE OF SURFACE ROUGHNESS OF COPPER SUBSTRATE ON WETTING BEHAVIOR OF MOLTEN SOLDER ALLOYS

Dinesh Reddy Nalagatla
University of Kentucky, drnala2@uky.edu

[Click here to let us know how access to this document benefits you.](#)

Recommended Citation

Nalagatla, Dinesh Reddy, "INFLUENCE OF SURFACE ROUGHNESS OF COPPER SUBSTRATE ON WETTING BEHAVIOR OF MOLTEN SOLDER ALLOYS" (2007). *University of Kentucky Master's Theses*. 488.
https://uknowledge.uky.edu/gradschool_theses/488

This Thesis is brought to you for free and open access by the Graduate School at UKnowledge. It has been accepted for inclusion in University of Kentucky Master's Theses by an authorized administrator of UKnowledge. For more information, please contact UKnowledge@sv.uky.edu.

ABSTRACT OF THESIS

INFLUENCE OF SURFACE ROUGHNESS OF COPPER SUBSTRATE ON WETTING BEHAVIOR OF MOLTEN SOLDER ALLOYS

The objective of this study is to understand the effect of surface roughness of the *Cu* substrate on the wetting of molten solder alloys. Eutectic *Sn-Pb*, pure *Sn* and eutectic *Sn-Cu* solder alloys and *Cu* substrates with different surface finish viz., highly polished surface, polished surface and unpolished surface were used in this work. Highly polished surface was prepared in Metallography lab, University of Kentucky while other two substrates were obtained from a vendor. Surface roughness properties of each substrate were measured using an optical profilometer. Highly polished surface was found to be of least surface roughness, while unpolished surface was the roughest.

Hot-stage microscopy experiments were conducted to promote the wetting behavior of each solder on different *Cu* substrates. Still digital images extracted from the movies of spreading recorded during hot-stage experiments were analyzed and data was used to generate the plots of relative area of spread of solder versus time. The study of plots showed that surface roughness of the *Cu* substrate had major influence on spreading characteristics of eutectic *Sn-Pb* solder alloy. Solder showed better spreading on the *Cu* substrate with least surface roughness than the substrates with more roughness. No significant influence of surface roughness was observed on the wetting behavior of lead free solders (pure *Sn* and eutectic *Sn-Cu*).

Keywords: Wetting, surface roughness, hot-stage microscopy, lead solders, lead-free solders

Dinesh Reddy Nalagatla

12/11/2007

INFLUENCE OF SURFACE ROUGHNESS OF COPPER SUBSTRATE ON
WETTING BEHAVIOR OF MOLTEN SOLDER ALLOYS

By

Dinesh Reddy Nalagatla

Dr. Dusan P. Sekulic

(Director of Thesis)

Dr. L. S. Stephens

(Director of Graduate studies)

12/11/2007

RULES FOR USE OF THESIS

Unpublished theses submitted for the Master's Degree and deposited in the University of Kentucky Library are a rule open for inspection, but are to be used only with due regard to the rights of the author. Bibliographical references may be noted, but quotations or summaries of parts may be published only with the permission of the author, and with the usual scholarly acknowledgements.

Extensive copying or publication of the thesis in whole or in part also requires the consent of the Dean of the Graduate School of the University of Kentucky.

THESIS

Dinesh Reddy Nalagatla

The Graduate School
University of Kentucky

2007

INFLUENCE OF SURFACE ROUGHNESS OF COPPER SUBSTRATE ON
WETTING BEHAVIOR OF MOLTEN SOLDER ALLOYS

THESIS

A thesis submitted in partial fulfillment of the requirements
for the degree of Master of Science in Mechanical Engineering
from the College of Engineering at the University of Kentucky

By

Dinesh Reddy Nalagatla

Lexington, Kentucky

Director: Dr. Dusan P. Sekulic, Professor

Center for Manufacturing, Department of Mechanical Engineering

Lexington, Kentucky

2007

Copyright © Dinesh Reddy Nalagatla, 2007

Dedicated to my Parents

(Dr. N. RamaSubba Reddy and Mrs. N. Lakshmi Devi)

ACKNOWLEDGEMENTS

This thesis work was achieved through constant encouragement and guidance from a number of people. First and foremost, I would sincerely like to acknowledge the support and mentorship extended by my Advisor, Dr. Dusan P. Sekulic throughout the course of this work. I am thankful that he was a major influence in my Masters' experience. I also thank him for funding me during my MS. I would like to thank my Director of Graduate studies, Dr. L. S. Stephens for giving me an opportunity to pursue my Masters' in Mechanical engineering at University of Kentucky. I am also grateful to him for giving permission to use Optical surface profilometer present in his laboratory.

I would then like to extend my sincere thankfulness to Dr. I. S. Jawahir and Dr. Marwan Khraisheh for agreeing to be on my advisory committee. I would also like to acknowledge and thank Dr. Hui Zhao for her guidance during this study. I am also thankful to her for helping me with experiments and data collection during the work. I am also grateful to my friends for their suggestions and advise in organizing the material.

Above all, I would like to thank my parents, Dr. N. RamaSubba Reddy and Mrs. N. Lakshmi Devi, for supporting and motivating me throughout my life and making me able to achieve success in life. I am ever grateful for their unconditional support.

Dinesh Reddy Nalagatla

TABLE OF CONTENTS

ACKNOWLEDGEMENTS.....iii

List of Figures.....vii

List of Tables.....xi

List of Files.....xii

Chapter 1 Introduction.....1

 1.1 Soldering.....3

 1.2 Solders.....5

 1.2.1 Lead solders.....6

 1.2.2 Health and environmental concerns involving lead.....7

 1.2.3 Lead free solders.....8

 1.3 Wetting.....15

 1.3.1 Wetting in soldering process.....17

 1.3.2 Factors influencing wetting in soldering process.....19

 1.4 Objective of this study.....20

Chapter 2 Problem Formulation.....21

 2.1 An influence of surface roughness of a substrate on wetting.....21

 2.1.1 Research studies related to soldering process.....24

 2.1.2 Summary of review.....24

 2.2 Hypothesis for the current study.....25

 2.3 The study approach to be used in current work.....25

Chapter 3 Materials and Surface Characterization.....27

 3.1 Materials used in current work.....27

 3.1.1 Solders.....27

 3.1.2 *Cu* substrates.....27

3.2 Surface characterization.....	29
3.2.1 Substrate's characterization by profilometer.....	30
3.2.2 Profilometer results.....	32
Chapter 4 Experimental Setup and Procedures.....	34
4.1 Hot-stage microscopy.....	34
4.1.1 Hot-stage system.....	35
4.1.2 Microscope and data acquisition unit.....	36
4.2 Sample preparation.....	36
4.3 Experimental procedure and post-processing.....	37
Chapter 5 Hot-stage experiments involving eutectic Sn-Pb solder alloy.....	40
5.1 Eutectic Sn-Pb alloy spreading over highly polished Cu surface (Met. Lab)....	40
5.2 Eutectic Sn-Pb alloy spreading over polished Cu surface (vendor).....	45
5.3 Eutectic Sn-Pb alloy spreading over unpolished Cu surface.....	50
Chapter 6 Hot-stage experiments involving lead-free solders.....	55
6.1 Pure Sn spreading over highly polished Cu surface (Met. Lab).....	55
6.2 Pure Sn spreading over polished Cu surface (vendor).....	59
6.3 Pure Sn spreading over unpolished Cu surface.....	63
6.4 Eutectic Sn-Cu solder alloy spreading over highly polished Cu surface (Met. Lab).....	67
6.5 Eutectic Sn-Cu solder alloy spreading over polished Cu surface (vendor).....	71
Chapter 7 Summary of Results and Discussion.....	75
7.1 Effect of surface roughness of Cu substrates on the wetting behavior of eutectic Sn-Pb solder alloy.....	75
7.2 Effect of surface roughness of Cu substrates on the wetting behavior of lead-free solder alloys.....	77

Chapter 8 Conclusions and Future work.....	80
8.1 Summary and conclusions.....	80
8.2 Future work.....	81
References.....	83
Appendix A Surface characterization using optical profilometer.....	88
Appendix B Temperature uncertainty in hot-stage experiments.....	90
Appendix C Temperature vs. time data for hot-stage experiments involving eutectic Sn-Pb alloy.....	91
Appendix D Temperature vs. time data for hot-stage experiments involving lead-free solder alloys.....	94
Appendix E A/A_o vs. time data for hot-stage experiments involving eutectic Sn-Pb alloy.....	99
Appendix F A/A_o vs. time data for hot-stage experiments involving lead-free solder alloys.....	102
Appendix G Final A/A_o vs. Cu substrates data for spreading of solder alloys on different copper substrates.....	106
Nomenclature.....	107
Vita.....	109

LIST OF FIGURES

Figure 1.1: Principle of wave soldering technique.....	4
Figure 1.2: Reflow soldering technique.....	5
Figure 1.3: Phase diagram of <i>Sn-Pb</i> system.....	7
Figure 1.4: Phase diagram of <i>Sn-Cu</i> system.....	11
Figure 1.5: Phase diagram of <i>Ag-Sn</i> system.....	12
Figure 1.6: Phase diagram of <i>Bi-Sn</i> system.....	13
Figure 1.7: Phase diagram of <i>Sn-Ag-Cu</i> system.....	14
Figure 1.8: Phase diagram of <i>Sn-Ag-Bi</i> system.....	15
Figure 1.9: Spreading of sessile drop on solid surface.....	16
Figure 1.10: Schematic representation of drop after spreading and dissolution.....	18
Figure 1.11: Resolidified solder on <i>Cu</i> substrate with intermetallic compound formation at the interface.....	19
Figure 2.1: Schematic representation of liquid drop over rough surface.....	22
Figure 3.1: Highly polished surface (Met. lab).....	28
Figure 3.2: Polished surface (vendor).....	28
Figure 3.3: Unpolished surface.....	29
Figure 3.4: Zygo NewView™ 5000 Optical Profilometer.....	29
Figure 3.5: Schematic representation of surface profile.....	30
Figure 3.6: Surface map and profile of highly polished surface (Met. lab).....	31
Figure 3.7: Surface map and profile of polished surface (vendor).....	31
Figure 3.8: Surface map and profile of unpolished surface.....	32
Figure 3.9: Comparison plots of surface roughness measurements of the surfaces: average roughness (R_a) and Peak to Valley distance (PV).....	33
Figure 4.1: Hot-stage microscope equipment.....	34
Figure 4.2: Schematic representation of hot-stage microscopy system.....	35

Figure 4.3: Photo and Schematic of hot-stage chamber setup.....	35
Figure 4.4: Setup of sample used.....	37
Figure 4.5: Temperature cycle plot during a hot-stage experiment involving eutectic <i>Sn-Pb</i> solder alloy and a <i>Cu</i> substrate.....	38
Figure 4.6: Computer screen capture of Image pro [®] software.....	39
Figure 5.1: Eutectic <i>Sn-Pb</i> over highly polished surface (Met. lab).....	40
Figure 5.2: Heating and Cooling cycle, eutectic <i>Sn-Pb</i> alloy on highly polished surface (Met. Lab).....	41
Figure 5.3: Extracted images representing the sequence of spreading of eutectic <i>Sn-Pb</i> solder alloy on a highly polished surface (Met. Lab).....	42
Figure 5.4: Schematic representation of spreading of eutectic <i>Sn-Pb</i> solder alloy on highly polished surface (Met. Lab).....	44
Figure 5.5: A/A_0 Vs time (sec), eutectic <i>Sn-Pb</i> solder alloy spreading on highly polished surface (Met. Lab).....	44
Figure 5.6: Eutectic <i>Sn-Pb</i> over Polished Surface (vendor).....	45
Figure 5.7: Heating and Cooling cycle, eutectic <i>Sn-Pb</i> alloy on polished surface (vendor).....	46
Figure 5.8: Extracted images representing the sequence of spreading of eutectic <i>Sn-Pb</i> solder alloy on a polished surface (vendor).....	47
Figure 5.9: Schematic representation of spreading of eutectic <i>Sn-Pb</i> solder alloy on polished surface (vendor).....	49
Figure 5.10: A/A_0 vs time (sec), eutectic <i>Sn-Pb</i> solder alloy spreading on a polished surface (vendor).....	49
Figure 5.11: Eutectic <i>Sn-Pb</i> over unpolished Surface.....	50
Figure 5.12: Heating and Cooling cycle, eutectic <i>Sn-Pb</i> alloy on unpolished surface.....	51
Figure 5.13: Extracted images representing the sequence of spreading of eutectic <i>Sn-Pb</i> solder alloy on unpolished surface.....	52
Figure 5.14: Schematic representation of spreading of eutectic <i>Sn-Pb</i> solder alloy on unpolished surface.....	54

Figure 5.15: A/A_0 Vs time (sec), eutectic $Sn-Pb$ solder alloy spreading on unpolished Surface.....	54
Figure 6.1: Pure Sn over highly polished Surface (Met lab).....	55
Figure 6.2: Heating and cooling cycle, pure Sn over highly polished surface (Met. lab).....	56
Figure 6.3: Extracted images representing the sequence of spreading of pure Sn on highly polished surface (Met. Lab).....	57
Figure 6.4: Schematic representation of pure Sn spreading on highly polished surface (Met. lab).....	58
Figure 6.5: A/A_0 Vs time (sec), pure Sn spreading on highly polished surface (Met. lab).....	58
Figure 6.6: Pure Sn over Polished Surface (vendor).....	59
Figure 6.7: Heating and cooling cycle, pure Sn over polished surface (vendor).....	60
Figure 6.8: Extracted images representing the sequence of spreading of pure Sn on polished surface (vendor).....	60
Figure 6.9: Schematic representation of pure Sn spreading on a polished surface (vendor).....	62
Figure 6.10: A/A_0 Vs time (sec), pure Sn spreading on a polished surface (vendor).....	62
Figure 6.11: Pure Sn over unpolished Surface.....	63
Figure 6.12: Heating and cooling cycle, pure Sn over an unpolished surface.....	64
Figure 6.13: Extracted images representing the sequence of spreading of pure Sn on an unpolished surface.....	64
Figure 6.14: Schematic representation of pure Sn spreading on an unpolished surface...66	66
Figure 6.15: A/A_0 Vs time (sec), pure Sn spreading on an unpolished surface.....	66
Figure 6.16: Eutectic $Sn-Cu$ solder alloy over a highly polished surface (Met. Lab).....	67
Figure 6.17: Heating and cooling cycle, eutectic $Sn-Cu$ solder alloy over a highly polished surface (Met. lab).....	68

Figure 6.18: Extracted images representing the sequence of spreading of eutectic <i>Sn-Cu</i> solder alloy on a highly polished surface (Met. lab).....	68
Figure 6.19: Schematic representation of eutectic <i>Sn-Cu</i> solder alloy spreading on a highly polished surface (Met. lab).....	70
Figure 6.20: A/A_o Vs time (sec), eutectic <i>Sn-Cu</i> solder alloy spreading on a highly polished surface (Met. lab).....	70
Figure 6.21: Eutectic <i>Sn-Cu</i> solder alloy over polished Surface (vendor).....	71
Figure 6.22: Heating and cooling cycle, eutectic <i>Sn-Cu</i> solder alloy over a polished surface (vendor).....	72
Figure 6.23: Extracted images representing the sequence of spreading of eutectic <i>Sn-Cu</i> solder alloy on a polished surface (vendor).....	72
Figure 6.24: Schematic representation of eutectic <i>Sn-Cu</i> solder alloy spreading on polished surface (vendor).....	74
Figure 6.25: A/A_o Vs time (sec), eutectic <i>Sn-Cu</i> solder alloy spreading on polished surface (vendor).....	74
Figure 7.1: Spreading behavior of eutectic <i>Sn-Pb</i> on <i>Cu</i> substrate with different surface Roughnesses.....	75
Figure 7.2: Final A/A_o vs Average roughness (R_a).....	76
Figure 7.3: Final area spread by eutectic <i>Sn-Pb</i> solder alloy on a) highly polished surface(Met. lab.) b) polished surface (vendor) c) unpolished surface.....	77
Figure 7.4: Spreading behavior of pure <i>Sn</i> and eutectic <i>Sn-Cu</i> on <i>Cu</i> substrates with different surface roughness.....	78
Figure 7.5: Final A/A_o vs <i>Cu</i> substrates, Lead-free solders spreading on different <i>Cu</i> Substrates.....	79
Figure 7.6: Final A/A_o vs <i>Cu</i> substrates, Eutectic <i>Sn-Pb</i> and Lead-free solders spreading on different <i>Cu</i> substrates.....	79

LIST OF TABLES

Table 1.1: Lead free solders.....	9
Table 3.1: Solders used in present work.....	27
Table 3.2: Profilometer results.....	32

LIST OF FILES

Thesis_nalagatla.pdf

Chapter 1 Introduction

Technology development at the cost of environment has been the case in past and also now in present. Increase in pollution of air, water and land from automobiles, manufacturing industries and energy production using fossil fuels resulted in risks of global warming, ozone depletion and human health problems. Manufacturing industries are significant participants in releasing toxic chemical wastes, contaminating ground water and land. These impacts prompted a change in the traditional approach of societal development. New approach involves sustainability concerns in development for next generations. This approach is termed “sustainable development”. Sustainable development is defined by the World commission on Environment and Sustainability 1987 as the broader approach to the development that meets the needs of present without compromising the ability of future generations to meet their needs [Glasby, 2002]. This approach’s focus is not limited to environmental issues but also focuses on social and economical development.

In manufacturing industries, environmentally conscious manufacturing is gaining importance for sustainable development. Environmentally Benign Manufacturing [EBM] involves technologies, strategies and practices necessary for sustainable production of products [Charles, 2003]. This aims at protecting environment. Many industries in 21st century are taking the issue of environmental protection seriously and are adopting EBM approach for manufacturing products. This approach particularly becomes important for electronics industry, as electronic products have very short useful life span, with emphasis placed on the ecological issues surrounding soldering and electronic waste disposal [Charles, 2003].

World market for electronic products is vast and fast growing. Total estimated worldwide market sale of electronic products was 96.6 billion US dollars in year 2000. It rose to 135.4 billion US dollars in 2006 and is estimated to reach 158.4 billion US dollars in year 2008, about 65% growth from 2000 [Worldwide consumer electronics market, 2006]. Due to relatively short useful life span of electronic products, rate of electronic waste disposed is raising with growing market. For example, Environmental protection Agency (EPA) in its report on Electronic waste management in US [EPA, 2007], estimated about

1.9 million tons of electronic waste generated in US itself in year 2005 which was about 11.7% more than in year 2003. These electronic wastes, which include computers and other electronic products, are either disposed of in large landfills or sent for recycling. According to EPA's report on electronic waste management in US about 80-85% of electronic wastes are disposed to large landfills and 15-20% is sent for recycling process.

Electronic waste landfills are considered a threat to environment. It is considered as one of the sources of contaminating soil and ground water with lead (*Pb*). Printed circuit boards (PCBs), part of waste electronic products, consists of lead bearing solders used for electronic assemblies. The threat of leaching of lead from landfills raised the issue of usage of lead bearing solders for soldering process in manufacturing products. This issue was taken seriously by in particular European Union and Japan, major electronic product manufacturers in the world, and legislations were proposed to eliminate lead from electronics industry. USA, a leading consumer and manufacturer of electronic products, still does not have a comprehensive legislation approved to the elimination of lead solders. Elimination of lead from electronics industry will automatically eliminate the issue of lead contamination. Discussion on this issue started from 1990. Initial driving force was a proposed legislative ban on lead in electronics industry in US [Sattiraju, 2002]. At that time no potential solder alloy replacement for *Sn-Pb* solder alloy was identified and legislation was dropped under strong pressure from electronics industry [Sattiraju, 2002]. Later European Union with Legislations in the form of Waste Electrical and Electronic equipments (WEEE) directives [European Parliament and the Council, WEEE directives, 2003] and Restriction of Hazardous Substance (RoHs) [European Parliament and the Council directives, RoHS directives, 2003] and Japan with proposed legislation of prohibiting lead from being sent to landfills [Abteu et al., 2000], made elimination of lead from electronic products necessary. But determining the best alternative is very complex. Lot of research studies has been done in determining the best alternative. Mechanical, physical and chemical properties of lead free solders are well studied and documented in literatures [Abteu et al., 2000] [Lee, 1999] [Moser et al., 2005] [JCAA/JG-PP report, 2006].

Surface roughness of the substrate is considered one of important factors which influence wetting and spreading characteristics of molten solder flowing over it [Manko, 1979]. But limited literature data is available on how it influences wetting. Current research aims at understanding the effects of surface roughness of a substrate on the wettability of a solder.

This chapter will discuss soldering processes, types of solders (lead and lead-free solders), impact of lead on human health and environment and wetting mechanism of solder on a copper substrate.

1. 1 Soldering

Soldering is one of several methods used for joining materials. Other methods include mechanical fastening, welding, brazing, diffusion bonding and adhesive bonding. Soldering process is defined as a metallurgical bonding method using a filler metal with melting temperature less than 425°C [Manko, 1979]. The process primarily relies on wetting ability of filler metal for bond formation. Heat is applied on base metal parts and solder alloy, alloy melts, and is drawn by surface tension in between the base metals to form a joint upon solidification. When compared to other metallurgical bonding methods, i.e. brazing and welding, soldering is a low cost method and can easily be automated to achieve simultaneous bonding. Thus, soldering is the best method used when high density of joints to be made at low cost, if operating temperatures are not high [Manko, 1979]. Printed circuit boards (PCBs) are best examples of simultaneous bonding of multiple joints. Solder joint provides electrical, thermal and mechanical continuity among the electronic assemblies. Extensive use of PCBs in electronic products was made possible by the ability of a solder to bond electronic component leads to circuit board conductors [Abtew et al., 2000].

Soldering in electronics industry is different from hand soldering techniques, as a number of joints needed to be formed in electronics mass production is roughly in hundreds of millions. For example, a standard radio receiver has about 500 joints; large computer systems have over 10^5 soldered joints [Wassink, 1984].

There are two primary soldering techniques used more often in electronics industry. These are Wave Soldering Technique and Reflow Soldering Technique:

Wave soldering Technique: Wave soldering is the major technique used for soldering of PCBs. In wave soldering, a continuous wave of molten solder is generated, and the boards to be soldered are moved in one direction across the wave, Figure 1.1 [Wassink, 1984], shows the principle of wave soldering.

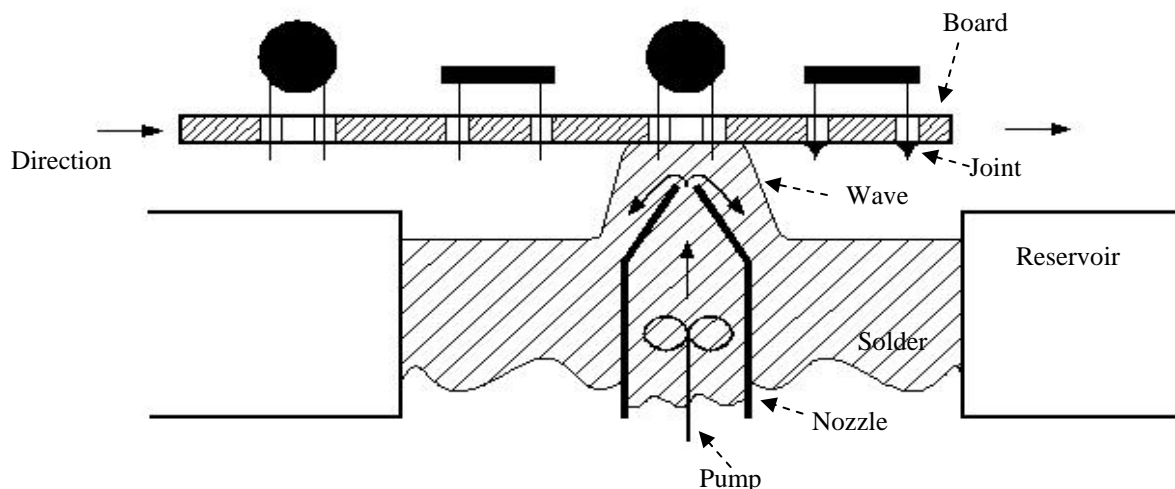


Fig. 1.1 Principle of wave soldering technique [Wassink, 1984]. The board is moved across over the wave of solder pumped out through the nozzle. Joints are formed and excessive solder falls back into the rectangular reservoir for reuse.

Reflow Soldering Technique: Reflow soldering is another technique used in electronics industry. In this process, joints are formed by melting previously applied solder paste to a board [Wassink, 1984]. Electronic components that are needed to be mounted on the surface of the circuit board are placed with solder paste in between. Solder paste is a mixture of flux and small solder particles. This system of electronic components on a printed circuit board is moved through the reflowing oven. Solder particles in the paste melt and produced liquid metal flows over the interface, forming strong metallurgical bond upon solidification. A schematic of a reflow soldering method is shown in figure 1.2. The reflow soldering method is used for electronic components which are needed to be mounted on a board surface.

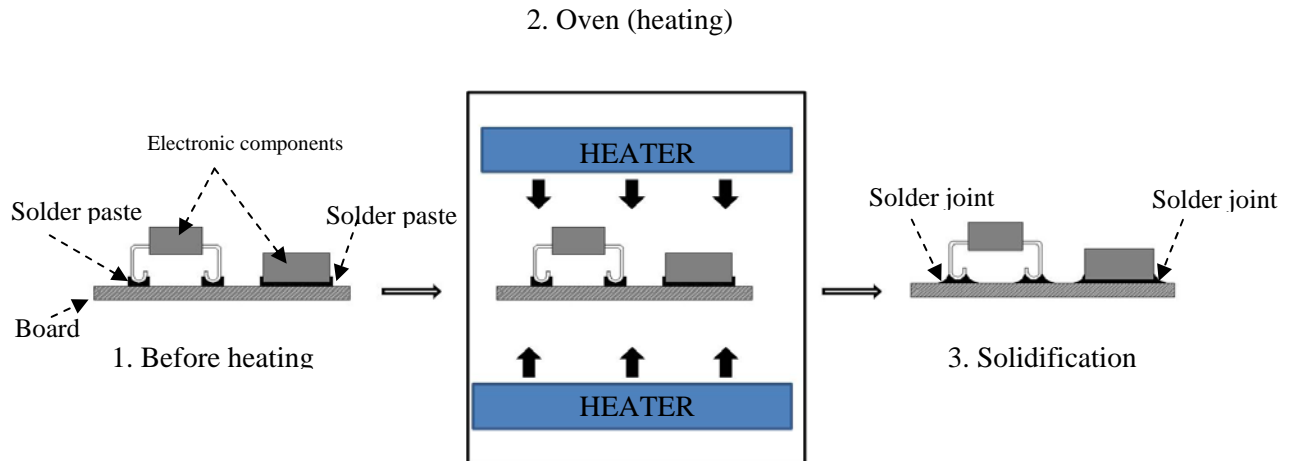


Fig. 1.2 Reflow soldering technique. 1.) Before heating solder paste is placed in between electronic components and circuit board. 2.) The system is then placed in an oven, where solder particles present in solder paste melt and spread over the interface. 3.) Joints are formed upon cooling.

A selection of soldering techniques for manufacturing of electronic components depends upon the design of printed circuit boards and electronics components needed to be soldered with it. Reflow technique is used for joining components that are needed to be mounted on the surface, while components to be mounted through-hole are joined using wave soldering technique.

1.2 Solders

Solder constitutes a filler metal alloy used for joining two metal surfaces in a soldering process. Selection of a solder alloy depends upon following important factors:

- Compatibility with base metals
- Availability and affordability
- Acceptable processing temperature
- Good wetting characteristics
- Forming reliable joints
- Environment friendly

The eutectic combination of tin (*Sn*) and lead (*Pb*) alloy has been most often used solder alloy. With low melting temperature, 183°C, the eutectic alloy (*63Sn-37Pb*) allows soldering conditions that are compatible with most substrates and devices [Abteu et al., 2000]. But usage of lead, considered to be one of the most toxic elements for humans, opened a debate on elimination of it from electronics industry. With the implementation of legislations in Europe and Japan, as discussed earlier, elimination of lead from electronic assemblies became necessary in the rest of the world including USA.

1.2.1 Lead solders

63Sn-37Pb, eutectic composition, and *60Sn-40Pb*, near eutectic composition, are primary used lead solders in electronics industry. Figure 1.3 shows the phase diagram of the *Sn-Pb* alloy system. Tin is a shiny soft metal, which can easily be shaped and moulded without breaking. Tin plays an important role in intermetallic bond formation, due to its ability to dissolve nearly any other metal, Like copper (*Cu*), in the molten state [Cox et al., 2000]. Thus tin is an important part of the alloy. Addition of 37% of lead to 63% of tin results in the formation of alloy with melting temperature of 183°C, very low when compare to the melting temperature of pure tin, 232°C, and pure lead, 327°C [Cox et al., 2000]. Other than forming an alloy with the low melting temperature, lead provides technical advantages to *Sn-Pb* alloys as follows:

- *Sn-Pb* solder alloy has low surface tension due to the addition of lead, lower than the surface tension of pure tin. Lower surface tension facilitates wetting [Vianco, 1993].
- Lead serves as a solvent metal, enabling other constituents, *Sn* and *Cu*, to form intermetallic bonds by diffusing in liquid state [Allenby et al., 1992].

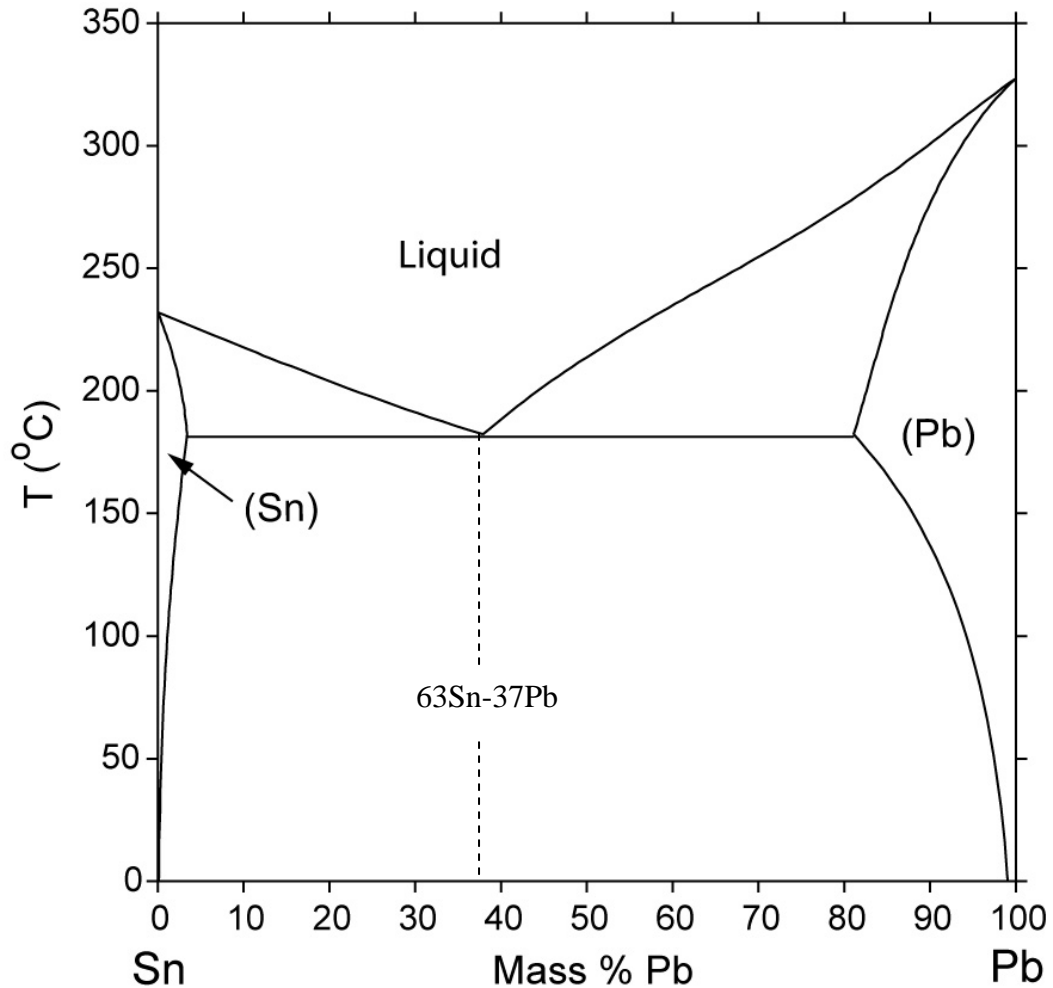


Fig. 1.3 Phase diagram of *Sn-Pb* system [NIST, 2007a]

In addition to these advantages, *Pb* is readily available and is a low cost metal, which makes it an ideal alloying metal with tin. With good wetting properties and low cost, the eutectic *Sn-Pb* solder alloy was considered the best for board level soldering systems in electronics industry.

1.2.2 Heath and environmental concerns involving lead

Lead is soft, heavy and toxic metal. It is very abundant and can easily be extracted from its ores. It is predominantly used in Storage Batteries and was used excessively in paints and petroleum products in past [Lee, 1999]. Lead being toxic in nature, its usage was banned in paints and petroleum products. Accumulation of lead into the body can have adverse effects on the health. It is found that lead, which is a divalent metal, often

competes with the divalent ions such as iron, calcium and Zinc with respect to absorption and biochemical physiological processes. It may also substitute for the normal roles of some other ions, but with deleterious consequences [Edwin, 2004]. Exposure to lead harms the central nervous system, causing memory loss, a damage of brain cells, and decrease of learning ability. This also led to cardiovascular problems and affects kidney, bones and blood. Exposure of children to even a small amount of lead can affect their learning process [Edwin, 2004]. The consumption of lead by humans can take place in three forms, either by air, by drinking water or by direct ingestion.

The concern regarding use of lead in electronics relates primarily to occupational exposure during the manufacturing process and the disposal of electronic assemblies' waste. The potential source of occupational exposure to lead in electronics manufacturing is wave soldering process [Abteu et al., 2000]. Inhalation of lead vapors or lead bearing dusts generated during the process is a possible danger. Occupational Safety and Health Administration (OSHA) requires a worker to have not more than 50mg/dl of lead in blood [Abteu et al., 2000]. Other big concern in industry is the leaching of lead through landfills of electronic wastes into ground. Lead reacts with rain water, which is acidic in nature, and leaches into underground water. Through this process lead can indirectly enter into the food chain system. The Japan environmental agency observed that the amount of leaching of lead through the waste of cathode tubes and other electronic assemblies far exceeds the environmental standards [Lee, 1999]. These impacts on the human health prompted its elimination from electronics industry. Thus, a lot of studies were done for determining the best alternative for lead solders. Next section will discuss some of the lead free solder investigation so far.

1.2.3 Lead free solders

As discussed earlier, eutectic lead-tin alloy has been used in electronic packages and assemblies for many years to bond electronic components to printed circuit boards (PCBs). This has been because of low melting temperature, good wetting and low cost. Issues of the health concerns drive the need for replacement of the lead solders with a better alternative. Also, there is a worldwide pressure to support the growing movement to remove lead from processes and products, to demonstrate environmental

consciousness. Following are the important criterion in determining the best lead free solder [Lee, 1999]:

- Nontoxic
- Available and affordable
- Acceptable wettability
- Acceptable Processing Temperature
- Form reliable Joints

Majority of lead-free solder alloys have tin as the primary component, and copper, bismuth, silver, gold or indium replacing lead in a binary system of alloy. There are even ternary and quaternary solder alloys, consisting of three and four alloying elements respectively. Addition of third and fourth element to the binary system of a solder alloy lowers the melting point and improves wettability and reliability of the alloy [Lee, 1999]. Table 1.1 provides a list of some of the lead free solders.

Table 1.1 Lead-free solders [Lee, 1999]

Solder Alloy	Composition	Melting Temperature (°C)	Eutectic
<i>Au-Sn</i>	<i>80Au-20Sn</i>	280	Eutectic
<i>Bi-Cd</i>	<i>60Bi-40Cd</i>	144	Eutectic
<i>Bi-In</i>	<i>67Bi-33In</i>	109	Eutectic
<i>Bi-In-Sn</i>	<i>57Bi-26In-17Sn</i>	79	Eutectic
<i>Bi-Sn</i>	<i>58Bi-42Sn</i>	138	Eutectic
<i>Bi-Sn</i>	<i>95Bi-5Sn</i>	251	
<i>Bi-Sn-Fe</i>	<i>54.5Bi-43Sn-2.5Fe</i>	137	
<i>Bi-Sn-In</i>	<i>56Bi-42Sn-2In</i>	138	
<i>Bi-Sb</i>	<i>95Bi-5Sb</i>	308(approx.)	
<i>In-Ag</i>	<i>97In-3Ag</i>	143	Eutectic
<i>In-Ag</i>	<i>90In-10Ag</i>	237	
<i>In-Bi-Sn</i>	<i>48.8In-31.6Bi-19.6Sn</i>	59	
<i>In-Bi-Sn</i>	<i>51.0In-32.5Bi-16.5Sn</i>	60	Eutectic
<i>In-Sn</i>	<i>60In-40Sn</i>	127(approx.)	
<i>In-Sn</i>	<i>52In-48Sn</i>	118	Eutectic
<i>In-Sn</i>	<i>50In-50Sn</i>	125	
<i>Sn</i>	<i>100Sn</i>	232	
<i>Sn-Ag</i>	<i>96.5Sn-3.5Ag</i>	221	Eutectic
<i>Sn-Ag</i>	<i>95Sn-5Ag</i>	250(approx.)	
<i>Sn-Ag-Cu</i>	<i>93.6Sn-4.7Ag-1.7Cu</i>	216	
<i>Sn-Ag-Cu-Sb</i>	<i>96.2Sn-2.5Ag-0.8Cu-0.5Sb</i>	217	

<i>Sn-Ag-Sb</i>	<i>65Sn-25Ag-10Sb</i>	233	
<i>Sn-Ag-Zn</i>	<i>95.5Sn-3.5Ag-1.0Zn</i>	217	
<i>Sn-Bi-Ag</i>	<i>91.8Sn-4.8Bi-3.4Ag</i>	211	
<i>Sn-Bi-Ag-Cu</i>	<i>91.0Sn-4.5Bi-3.5Ag-1.0Cu</i>	210	
<i>Sn-Cd</i>	<i>67.8Sn-32.2Cd</i>	177	Eutectic
<i>Sn-Cu</i>	<i>99.3Sn-0.7Cu</i>	227	
<i>Sn-Cu</i>	<i>99Sn-1Cu</i>	227	Eutectic
<i>Sn-Cu</i>	<i>97Sn-3Cu</i>	330(approx.)	
<i>Sn-Cu-Ag</i>	<i>95.5Sn-4Cu-0.5Ag</i>	349	
<i>Sn-Cu-Sb-Ag</i>	<i>95.5Sn-3Cu-1Sb-0.5Ag</i>	256	
<i>Sn-In</i>	<i>70Sn-30In</i>	175(approx.)	
<i>Sn-In</i>	<i>58Sn-42In</i>	145	
<i>Sn-In-Ag</i>	<i>77.2Sn-20.0In-2.8Ag</i>	187	
<i>Sn-In-Ag-Sb</i>	<i>88.5Sn-10.0In-1.0Ag-0.5Sb</i>	211	
<i>Sn-In-Bi</i>	<i>80Sn-10In-10Bi</i>	199	
<i>Sn-In-Bi-Ag</i>	<i>80Sn-10In-9.5Bi-0.5Ag</i>	201	
<i>Sn-Sb</i>	<i>95Sn-5Sb</i>	240	
<i>Sn-Zn</i>	<i>91Sn-9Zn</i>	199	Eutectic
<i>Sn-Zn-In</i>	<i>87Sn-8Zn-5In</i>	188	

Table 1.1 Lead-free solders [Lee, 1999] (Contd.)

Eutectic *Sn-Cu*, eutectic *Sn-Ag* and eutectic *Bi-Sn* alloys as the binary systems and *Sn-Ag-Cu*, *Sn-Ag-Bi* alloys as ternary systems are considered as potential alternatives for lead bearing solders. Brief description of each of these major alloys is given below:

Cu-Sn alloy:

Sn-Cu has an eutectic composition of *Sn* – 0.7 wt% *Cu* and the melting temperature of 227°C. Figure 1.4 shows the phase diagram of *Sn-Cu* solder. This alloy might be also suitable for high temperature applications required by the automotive industry [Lee, 1999]. It is a candidate especially for applications involving lead and silver free alloys. Preliminary testing conducted on this alloy has shown a significant improvement in creep/fatigue data over standard *Sn-Pb* alloys [Lee, 1999].

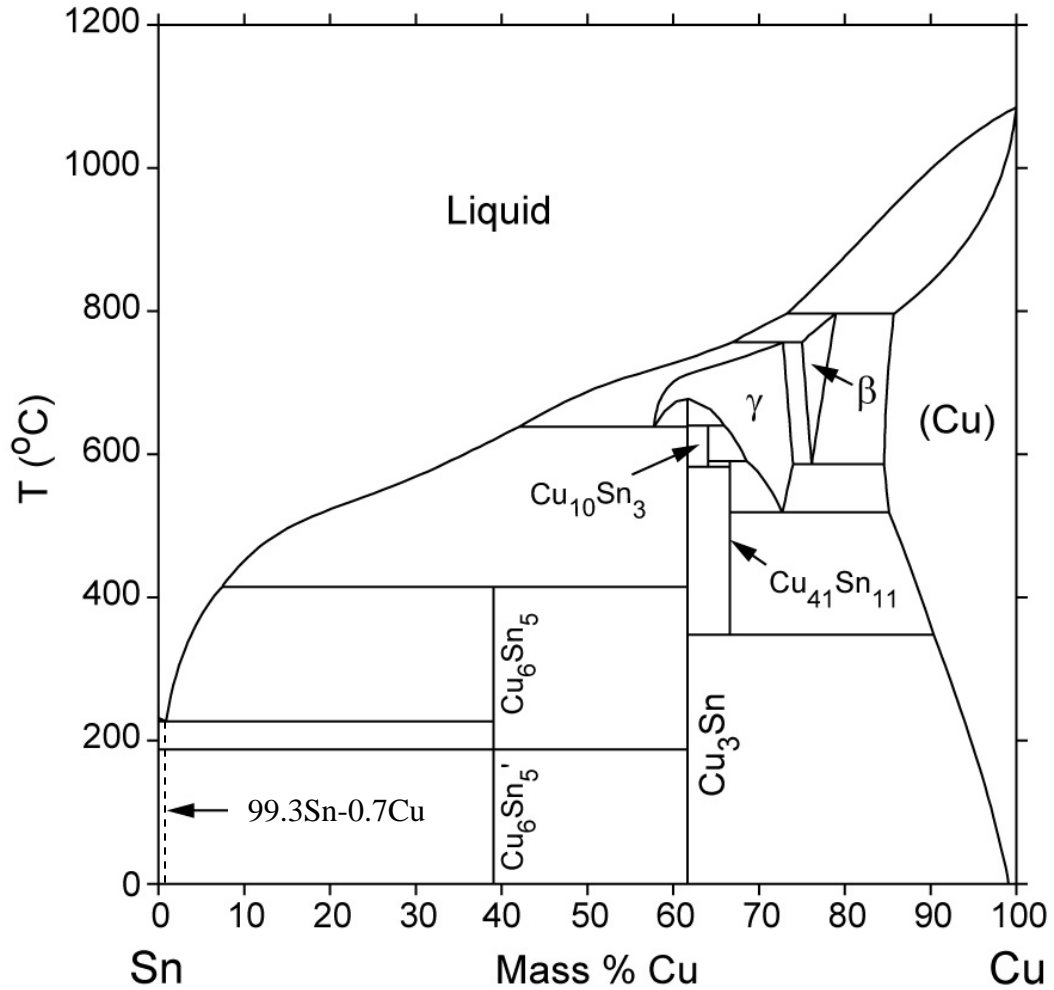


Fig. 1.4 Phase diagram of Sn-Cu system [NIST, 2007b]

Ag-Sn alloy:

The composition of this alloy is Sn – 3.5 wt% Ag, has an eutectic melting temperature of 221°C [Puttliz, 2004]. Figure 1.5 gives the phase diagram of this system. It is better in high temperature applications due to its high melting temperature and exhibits good wetting behavior on copper substrates [Puttliz, 2004]. It offers better mechanical properties than eutectic Sn-Pb [Lee, 1999].

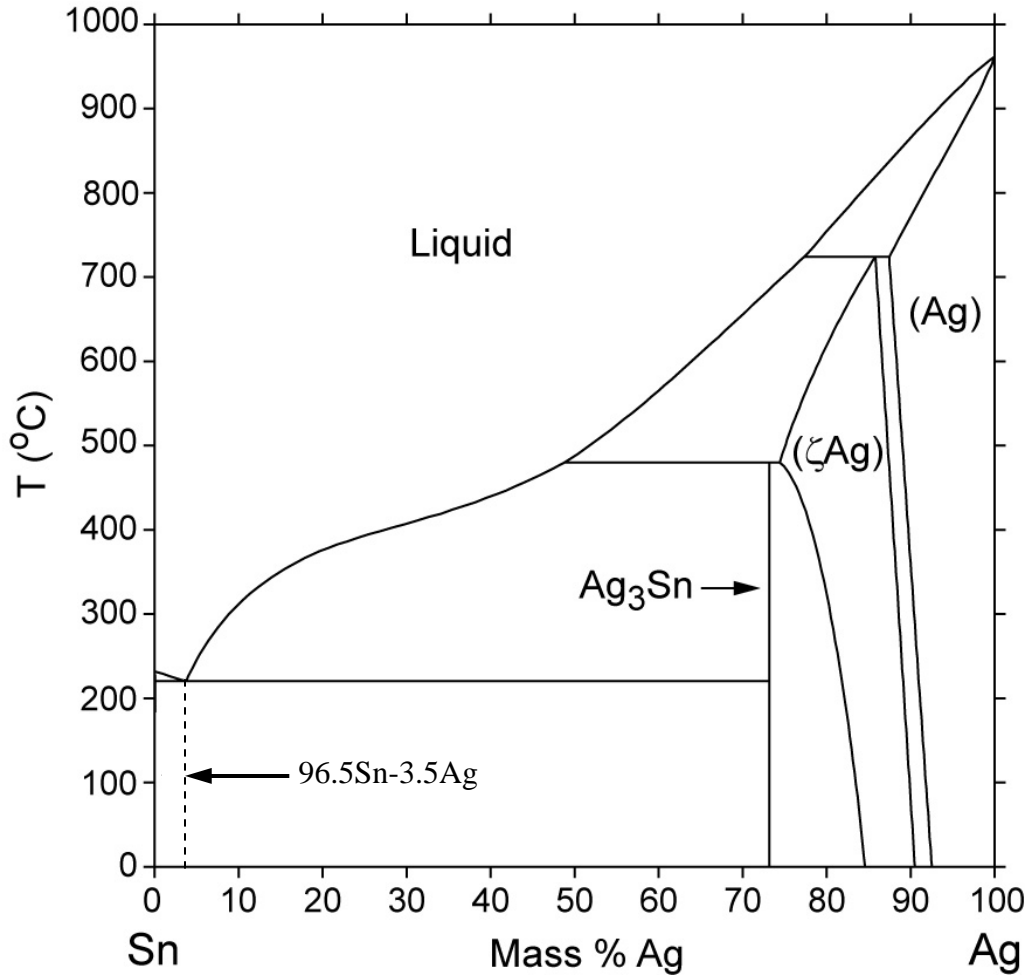


Fig. 1.5 Phase diagram of Ag-Sn system [NIST, 2007c]

Bi-Sn alloy:

Sn-Bi has eutectic composition of 42 *Sn*- 58 *Bi* and relatively low eutectic temperature of 139°C than eutectic *Sn-Pb* [Abteu et al., 2000]. Low melting point of this alloy makes it suitable for soldering temperature-sensitive components and substrates. It is recommended by National Center for Manufacturing Sciences (NCMS, US) as promising replacement [Lee, 1999]. Figure 1.6 represents the phase diagram of this alloy system.

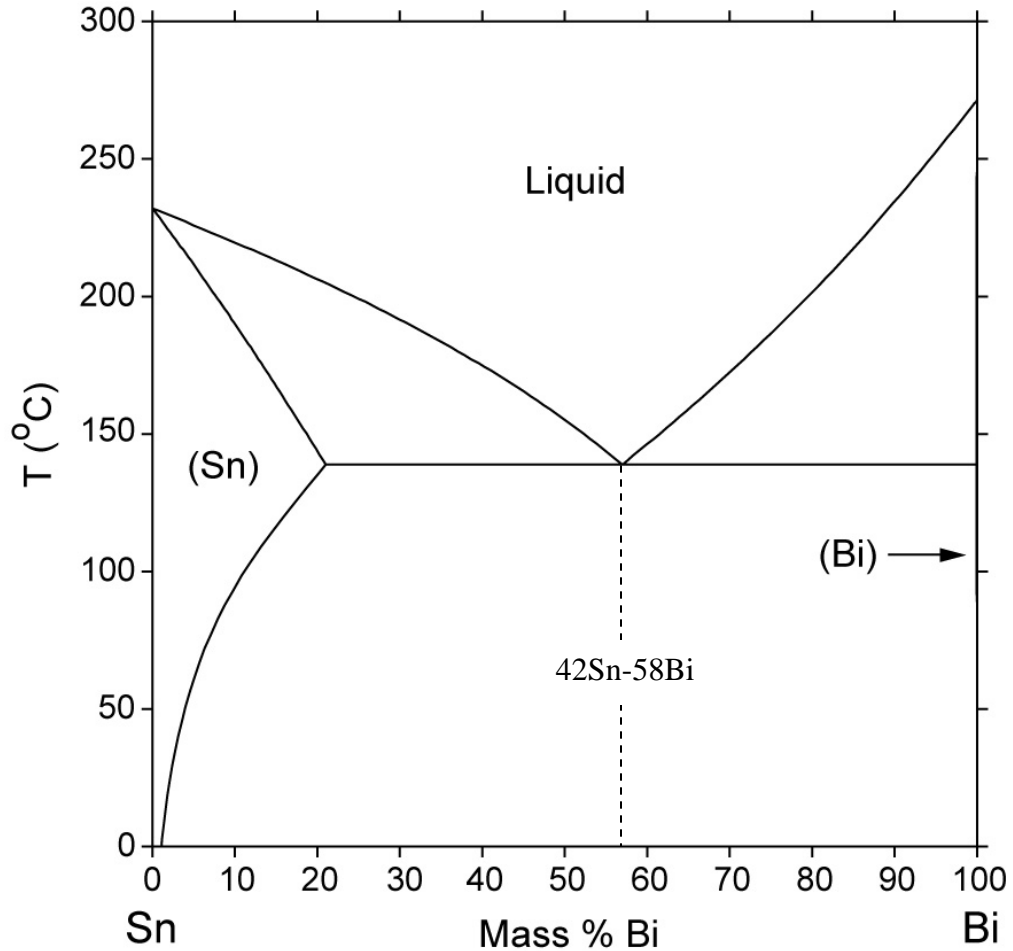


Fig. 1.6 Phase diagram of *Bi-Sn* system [NIST, 2007d]

Sn-Ag-Cu:

Melting point of the eutectic ternary alloy, $95.6\text{Sn}-3.5\text{Ag}-0.9\text{Cu}$, is about 217°C . Figure 1.7 shows the region in the phase diagram of this system where concentration of *Sn* is rich. Addition of *Cu* to *Sn-Ag*, slows down *Cu* dissolution, lowers the melting temperature and improves wettability. As reported in [Lee, 1999] this alloy has better reliability and solderability than *Sn-Cu* and *Sn-Ag* alloy and is recommended as the potential alternative for lead solders. Following are some of the examples of compositions of this alloy as solder alloys [Lee, 1999]:

- $93.6\text{Sn}-4.7\text{Ag}-1.7\text{Cu}$
- $95\text{Sn}-4\text{Ag}-1\text{Cu}$
- $96.5\text{Sn}-3\text{Ag}-0.5\text{Cu}$
- $95.5\text{Sn}-3.8\text{Ag}-0.7\text{Cu}$

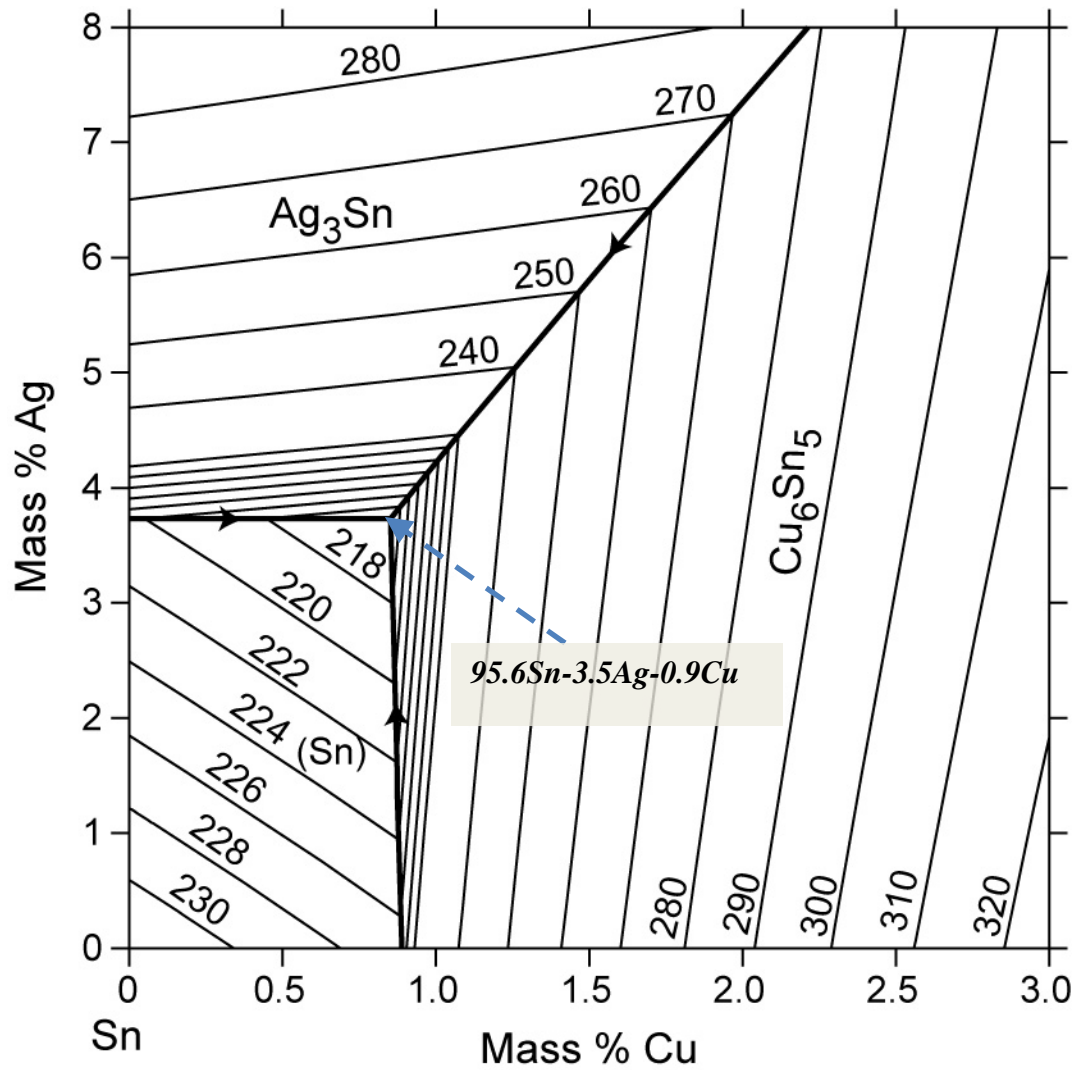


Fig. 1.7 Phase diagram of *Sn-Ag-Cu* system [NIST, 2007e]

Sn-Ag-Bi:

Addition of *Bi* to *Sn-Ag* reduces the melting temperature and improves the wettability of the alloy. *91.8Sn-3.4Ag-4.8Bi* alloy with melting temperature between 202-215°C is considered as the most promising alloy by National Center for Manufacturing Sciences (NCMS, US) [Lee, 1999]. Figure 1.8 gives the region in phase diagram of this system where *Sn* concentration is rich.

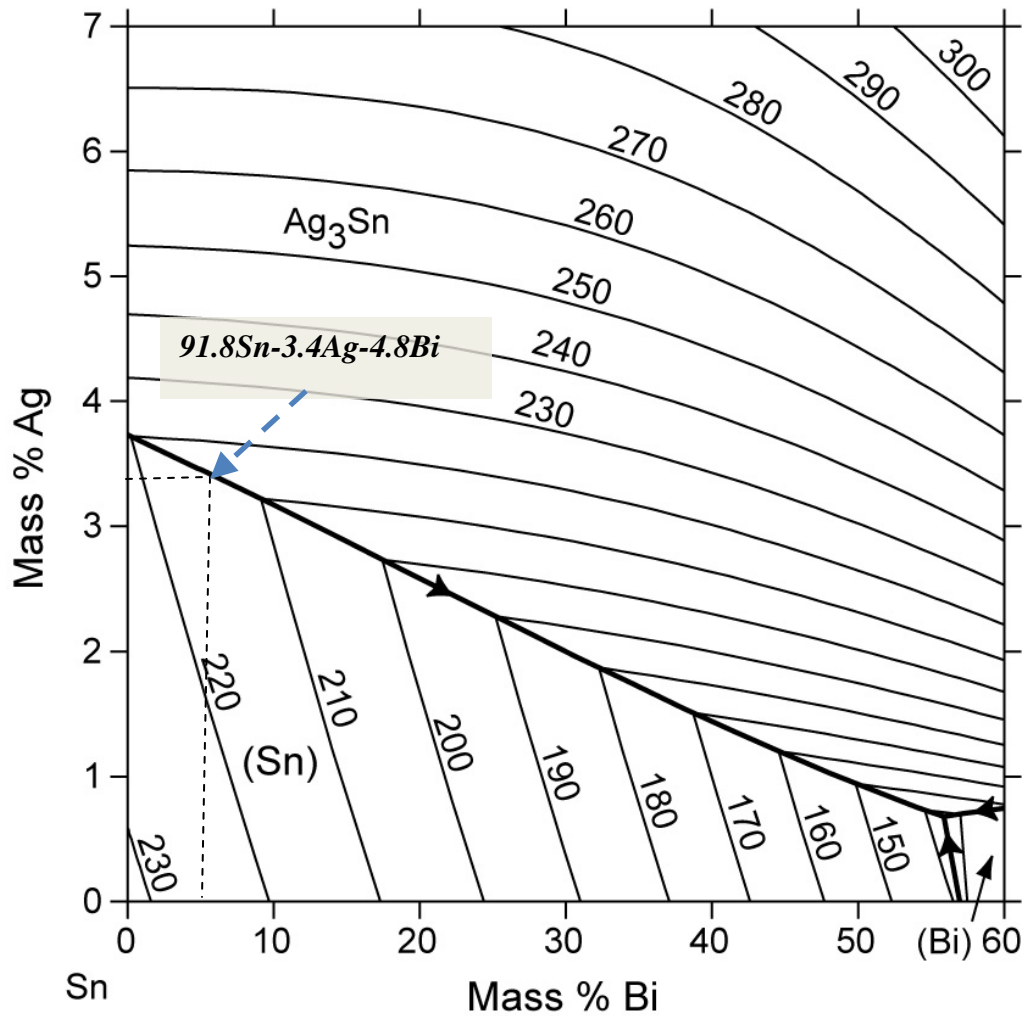


Fig. 1.8 Phase diagram of *Sn-Ag-Bi* system [NIST, 2007f]

1.3 Wetting

Wetting is a property of fluid to spread over a solid surface, when brought in contact, as shown in figure 1.9. It is generally described by the position of contact line, rate of advance and contact angle [Manko, 1979].

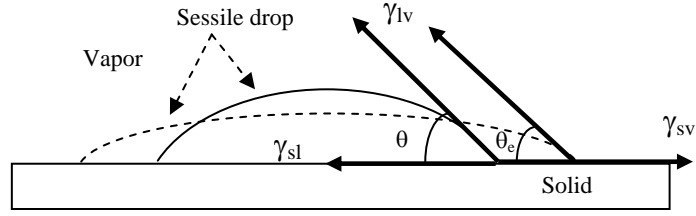


Fig. 1.9 Spreading of sessile drop on solid surface

γ_{lv} is surface tension between liquid and vapor acting tangent to the curvature of the liquid. θ is the dynamic contact angle between the substrate and the liquid and θ_e is the equilibrium contact angle attained after spreading. This surface tension is an energy that tends to minimize surface area of liquid drop in a particular atmosphere. In absence of other forces, surface tension of liquid will draw it into a sphere, which has smallest surface area. γ_{sv} is the interfacial tension acting between solid base metal and the vapor and γ_{sl} is the interfacial tension acting between solid surface and liquid. γ_{sv} and γ_{sl} act in opposite directions along the solid surface.

The condition for spreading to take place is given by the relation:

$$\gamma_{sv} > \gamma_{sl} + \gamma_{lv} \cos \theta \quad (1.1)$$

Sessile drop spreads over the substrate until it reaches the equilibrium state. During spreading dynamic contact angle θ changes with time, usually decreases in the case of wetting system, and reaches to equilibrium angle θ_e . At equilibrium state forces are balanced and are given by relation:

$$\gamma_{sv} = \gamma_{sl} + \gamma_{lv} \cos \theta_e \quad (1.2)$$

Equilibrium contact angle θ_e measures the extent of wetting. If it is between 0° and 90° , good wetting occurs, and if it is more than 90° a lack of wetting takes place. If the contact angle is equal or closer to 0° , total wetting appears.

1.3.1 Wetting in soldering process

During soldering processes, as the temperature raises melting of solder occur. Temperature is usually maintained a little higher than the melting temperature, known as peak temperature. During the peak temperature, the molten solder spreads over the substrate. During spreading of the solder in addition to action of interfacial energies, intermetallic reaction between solder alloy and the surface metal is present [Yost et al., 1993]. During the solder flow, molten solder dissolves the substrate metal by a diffusion process. Dissolution of the substrate affects the flow, often reducing the viscosity of the solder [Evans et al., 2007].

Spreading of solder over a metallic substrate involves a number of complex processes including fluid flow, heat flow and chemical reactions [Warren, 1998]. There can be a number of intermetallic compounds formations during the process. Interfacial energy lowers as a consequence of compounds formation, indicating wetting has taken place. Both formation of intermetallic compounds and wetting are driven by interfacial energy [Abtew et al., 2000]. Wetting involving chemical reactions and diffusion of chemical species is referred as reactive wetting [Warren et al., 1998].

Kinetics of reactive wetting is much more complex when compared to that of non-reactive systems. In addition to the action of the interfacial energy, chemical reactions between solder and the substrate plays a role on wetting dynamics. Extensive research work is done with an objective of determining the kinetics of reactive wetting in brazing and soldering processes [Warren et al., 1998] [Yost, 2000] [Landry et al., 1997]. According to [Warren et al., 1998] reactive wetting can be differentiated into two cases, (1) no new compounds form during the reaction between the liquid metal and the substrate, and (2) new compounds form during the interaction between the molten metal and substrate and layer is formed in between the liquid metal and substrate. Work by [Warren et al., 1998] focuses on the first case, with experiments conducted on the spreadability of *Sn-Bi* over a pure *Bi* substrate. During experiments, molten *Sn-Bi* spreads over a pure *Bi* substrate, dissolves the *Bi* and diffuses into the substrate. The paper describes dissolution phenomenon as a concentration change of the two phases, occurring usually by partial melting of the substrate. No new phase is formed between the two phases. According to [Warren et al., 1998], dissolution of *Bi* in *Sn-Bi* affects the

microscopic contact angle. This happens because of diffusion driven by the differences in the concentration at the substrate-solder interface. According to this study, the dissolution process increases the total volume of molten solder at equilibrium. Figure 1.10 shows the schematic representation of a reactive wetting in this case [Warren et al., 1998].

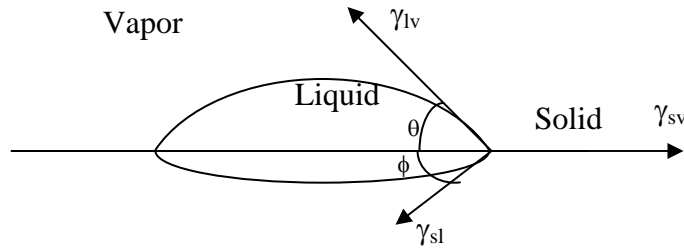


Fig. 1.10 Schematic representation of drop after spreading and dissolution

From fig 1.10, θ is considered as the upper contact angle at equilibrium and ϕ is assumed to be the contact angle of the lower spherical cap representing the portion of substrate dissolved into molten solder. Under equilibrium state, interfacial forces are balanced and represented by relation:

$$\gamma_{sv} = \gamma_{lv}\cos\theta + \gamma_{sl}\cos\phi \quad (1.3)$$

Equation (1.3) is Neumann's description of three phase capillary equilibrium of dissolutive flow, as explained in [Yost et al., 1997]. Kinetics of dissolution wetting is well studied in literature [Yost et al., 1997] [Warren et al., 1998].

Formation of intermetallic compounds (IMC) during the interaction between the molten metal and substrate is the second kind of reactive wetting as mentioned earlier in this section. An intermetallic compound forms an interlayer between the molten metal and the surface. Flow of *Pb-Sn* over the copper substrate is an example of this case. Figure 1.11 gives the Scanning Electron Microscope (SEM) image of the cross-section of a resolidified solder after spreading over a copper substrate. It clearly shows the presence of the IMC formation at the interface between the solder and *Cu* substrate.

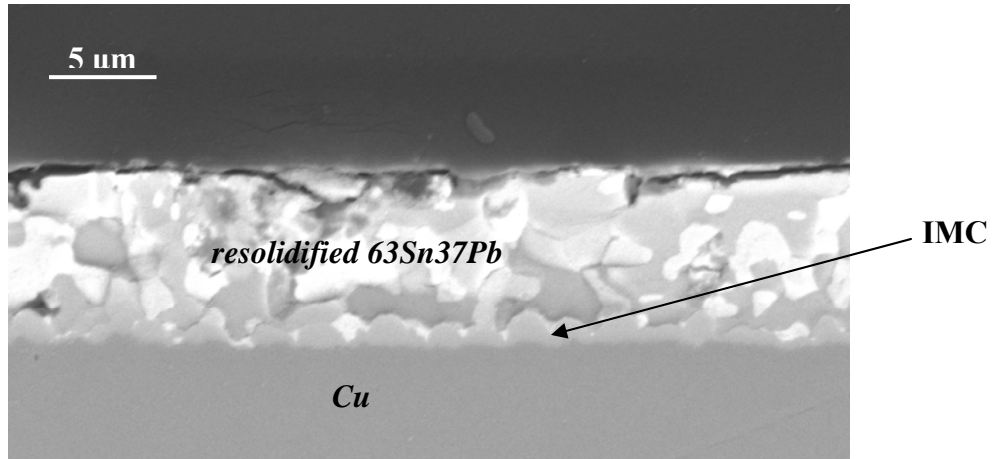


Fig. 1.11 Resolidified solder on *Cu* substrate with intermetallic compound formation at the interface [Wang et al., 2007b]

During the spread of molten *Pb-Sn* solder over a *Cu* surface, *Sn* reacts with *Cu* resulting in the formation of Cu_3Sn and Cu_6Sn_5 intermetallic compounds at the interface [Abteu et al., 2000]. Studies of, [Wang et al., 2006] and [Wang et al., 2007a], give extensive information about reactive wetting of *Sn*-based solders over copper substrate and the influence of an intermetallic compound formation on the wettability of solders. In [Wang et al., 2006], the influence of the composition of *Sn* in the solder alloy during wetting of the solders on two substrates, *Cu* and $Cu_6Sn_5/Cu_3Sn/Cu$ (intermetallic Compound Substrates), was studied. This study was performed by using wetting balance technique. The second study focuses on reactive wetting of lead free solders on the *Cu* substrate. Both wetting balance technique and hot-stage microscopy techniques were used in this investigation. These complex phenomena will not be the subject of the present study. The kinetics of the spreading will be the only objective.

1.3.2 Factors influencing wetting in soldering process

As discussed, good solder joint formation depends upon good wetting by molten solder over the metal substrate. Wettability of solder in soldering process depends on multiple factors such as flux, process temperature and surface roughness, in addition to intermetallic compounds formation and dissolution.

Flux is used to protect substrate surface from atmosphere, thus avoiding formation of oxides on the surface during heating. Oxide formation is not desirable during soldering because it hinders proper wetting. Flux used reacts with the vapor phase and forms a protective layer over the substrate. Flux provides an oxide free surface and makes it available for total contact with a solder. Furthermore, flux improves spreading of molten metal by reducing the contact angle [Manko, 1979]. Process temperature is an important factor that affects spreading. Rising temperature decreases liquid viscosity and liquid surface tension, which assists the good spreading [Singler et al., 2004]. Wetting rate increases with rise in temperature. This trend is observed during all the experiments done in this work. Solder melts and spreads uniformly with a rising temperature.

Surface roughness of the substrate is an important factor that has an influence on the kinetics of solder flow. But, there is no consensus on how in general it influences wetting [Singler et al., 2004]. According to [Manko, 1979] wetting over rough surface exceeds wetting on smooth surface, due to presence of open channel capillaries in the form of grooves on a rough surface. But work done by [Hitchcock et al., 1981] and [Chen et al., 2000] suggested that increase in surface roughness of the substrate hampers the spreading of molten metal on it. According to those studies asperities present on a rough surface acts as barriers needed to be overcome by molten metal while spreading.

1.4 Objective of this study

Present work focuses on the influence of surface roughness on the spreading kinetics of molten solder alloy. Inconsistencies in conclusions of different studies regarding the influences of surface roughness on wetting were one of the motivations for this research work. Primary objective of this study is as follows:

- (1) To observe the influence of surface roughness of substrates over the flow of solders.
- (2) To study the kinetics of wetting of solders during a flow over copper substrates having different surface roughness values.

Chapter 2 Problem Formulation

In this chapter the problem studied in the current research work will be formulated. Problem formulation involves a review of different research studies done regarding the influence of surface roughness on spreading. A working hypothesis based on this review will be formulated. Approach of the study will provide a description of the steps involved to verify the hypothesis.

2.1 An influence of the surface roughness of a substrate on wetting

Surface roughness of a surface, defined as the deviation of actual surface from an ideal, atomically smooth and planar surface, is considered to be an important factor effecting spreading. Extensive research studies have been done and various theories were proposed in this area. Majority of works concentrated on the influence of roughness on contact angle.

Theoretical model developed by Wenzel [Wenzel, 1936], is one of the first models of the influence of roughness on wetting. According to the model, additional area produced due to surface roughening was effective in raising surface energy, and resulting in good wetting. Model predicts that a surface that does have good wetting characteristics when smooth will wet even better when rough. Thus, increase in surface roughness of the substrate will result in smaller contact angle. Model holds good for systems with equilibrium contact angle less than 90° , i.e. for wetting systems. The behavior predicted by this model is expressed by the relation below.

$$\cos \theta_r = r \cos \theta_o \quad (2.1)$$

In equation (2.1), r is the roughness area ratio also known as Wenzel's roughness ratio, given by ratio of true surface area to projected surface area. θ_r and θ_o are the equilibrium contact angles over rough surface and smooth surface, respectively. This relation implies that if roughness ratio r is increased, the apparent contact angle θ_r will decrease.

However, Shuttleworth and Bailey [Shuttleworth et al., 1948] predicted a different behavior as emphasized next.

Shuttleworth and Bailey pointed out that rough surface causes contact line to distort locally, giving rise to a spectrum of micro-contact angles near solid surface and resulting in an increase in contact angle with an increase in surface roughness. According to this hypothesis asperities of a rough surface could act as barriers to the flow of fluid. The model is given by relation

$$\theta_r = \theta_o + \alpha \quad (2.2)$$

In eq. (2.2), θ_r is the apparent contact angle, θ_o is the contact angle formed between rough surface and a liquid drop and α is the steepness of the rough surface as shown in figure 2.1.

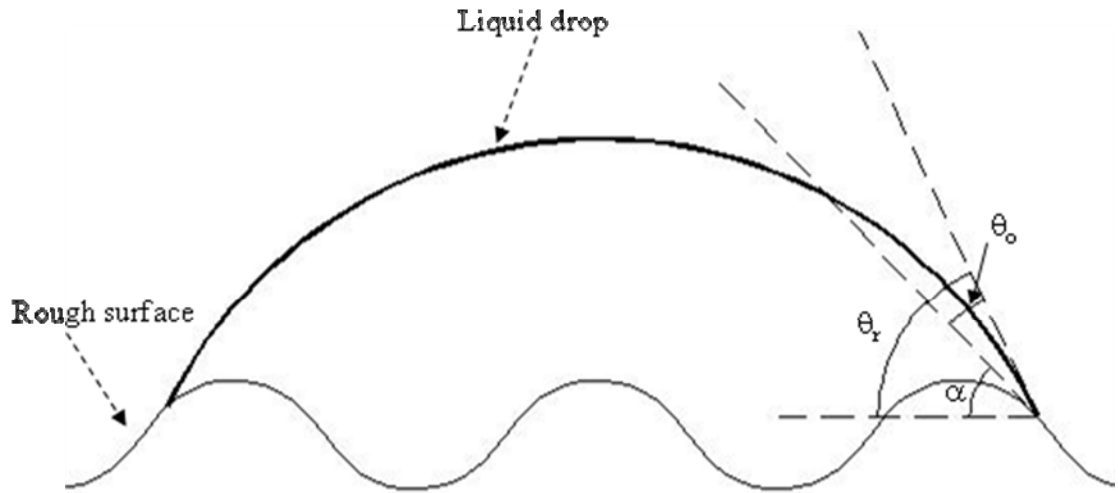


Fig. 2.1 Schematic representation of liquid drop over rough surface

Mathematically, α can be positive and negative depending upon liquid front. Advancing liquid front comes to rest on descending slopes and thus, α will be positive with θ_r greater

than θ_o . Similarly, receding liquid comes to rest on ascending slopes with negative α values, resulting in θ_r less than θ_o .

Contradicting predictions from both the models lead to more research in this area. [Hitchcock et al., 1981], experimentally studied Wenzel's theoretical model and model suggested by Shuttleworth and Bailey on effect of surface roughness. The studies were undertaken to provide information on the effect of surface texture on the behavior of high energy liquid and surface. The study investigated the effect of substrates' surface roughness on wettability at room as well as high temperature using sixteen material combinations, mostly liquid metals and ceramics substrates but also water, glycerol and nickel substrate. The author of this study used mechanical surface profilometer to characterize solid surfaces and measure average roughness R_a and average distance between peaks λ_a . The approximated Wenzel's roughness ratio r and steepness of rough surface α are related as follows

$$r = 1 + k_1(R_a/\lambda_a)^2 \text{ and } \alpha = \tan^{-1} k_2(R_a/\lambda_a) \quad (2.3)$$

In eq. (2.3), k_1 and k_2 are constants. This relationship enabled a comparison of Wenzel's predictions with Shuttleworth and Bailey's approach. From all the experiments, they found that roughening usually causes wettability of both wetting and non-wetting liquids to decrease. Glycerol on abraded silica and Easy-flo braze on electroformed nickel were the exceptions, showing decreasing contact angle with increasing roughness. These exceptions were for two very well wetting systems. They also found that contact angles of both wetting and non-wetting liquids often increase linearly with surface texture parameter R_a/λ_a . The findings were in agreement with Shuttleworth and Bailey approach. Later work by Nicholas and Crispin [Nicholas et al., 1986], studied influence of surface roughness in a well wetting system (Contact angle, $\theta_o < 20^\circ$) such as the exceptions mentioned above. This was the study of the the behavior of sessile drop of liquid copper on mild steel and stainless steel. This study found a decrease in contact angle with

increasing surface roughness. This work was in agreement with Wenzel's model on the influence of surface roughness.

2.1.1 Research studies related to soldering process

A small number of research studies were done concentrating on surface roughness and soldering processes. [Yost et al., 1995], studied experimentally the influence of surface roughness of *Cu* substrate on wettability of a molten eutectic *Sn-Pb* solder alloy. This work intended to demonstrate remarkable effects of the roughness on wetting, and to provide an insight on validity of Wenzel's model. This work involved a study of spreading of eutectic *Sn-Pb* alloy over rough copper substrate prepared by a plating process. Substrates were prepared by depositing copper on a nickel substrate using alkaline electro-plating process. The surface morphology of a thick copper layer deposited on a nickel surface was very rough, with an average peak to valley distance larger than 50 μm . The surface consisted of large spherical nodules. *Sn-Pb* alloy was found to spread extensively over this rough copper surface during wetting experiments due to flow along large groove-like valleys of the nodular structure. This behavior was in agreement with Wenzel's model. The authors also illustrated that for a spontaneous flow assisted by roughness, the surface geometry must feature local angles that are larger than equilibrium contact angle ($\theta_0 < \alpha$). According to the study, the flow through open channel capillaries is the driving force for extensive wetting of eutectic *Sn-Pb* solder.

Later, Chen and Duh [Chen et al., 2000] worked on spreading of a lead free solder over copper substrate. Eutectic *Sn-Bi* solder alloy was the lead free solder used in this study. Different *Cu* substrate surfaces were prepared using sandpapers with different abrasive numbers. The study concludes that the static equilibrium contact angle increases with an increase in surface roughness of the substrate. The findings were in agreement with Shuttleworth and Bailey's approach.

2.1.2 Summary of review

It must be clear that there is no consensus over general trends of influence of surface roughness on wetting. Most of the wetting and non-wetting liquids, as studied in

[Hitchcock et al., 1981], suggested that a liquid to wet a surface well the surface has to be smooth rather than rough. But good well wetting systems like eutectic *Sn-Pb* solder alloy and *Cu* substrate, discussed in [Yost et al., 1995], demonstrate an opposite behavior.

2.2 Hypothesis for the current study

The current work involves a study of the kinetics of spreading of the eutectic *Sn-Pb*, eutectic *Sn-Cu*, and pure *Sn* solder alloys on *Cu* substrates with different surface roughnesses. Spreading of eutectic *Sn-Pb* alloy on copper, as discussed by [Yost et al., 1995], is a good wetting system with the contact angle θ_0 in the range of 15-20° ($\theta_0 < 20^\circ$, a condition for well wetting system [Nicholas et al., 1986]). Thus, eutectic *Sn-Pb* alloy, as inferred from [Yost et al., 1995], was expected to wet well a rough copper surface when compared to a polished surface. Whereas lead free solders, eutectic *Sn-Cu*, and pure *Sn*, which doesn't spread well on *Cu* substrate when compared to *Sn-Pb* alloy [Abteu et al., 2000], are expected to spread better over the smooth surface than rough surface, as inferred from [Hitchcock et al., 1981].

2.3 The study approach to be used in current work

Current work intends to offer a phenomenological understanding of the influence of surface roughness on wetting characteristics of selected solders and to resolve whether the hypothesis, as discussed above, can be verified.

Eutectic *Sn-Pb*, and lead-free solder alloys, eutectic *Sn-Cu*, and Pure *Sn*, are used. *Cu* substrates with different surface finish are prepared. An optical profilometer is used to do the characterization of the surfaces. Next chapter discusses in detail about the materials used in this study and explains surface characterization of *Cu* substrates.

All the experiments were conducted using a hot-stage microscopy system. Hot-stage system provides necessary heat for the phase change of solder through conduction from Joule heated silver substrate block. Spreading mechanism is observed through microscope. Data is recorded in the form of video and still images. The experimental facility and procedures used in this work are described in Chapter 4.

The still images extracted from the movies are analyzed using image processing software to assess the kinetics of the solder flow. Details and analysis of data are presented and explained in Chapters 5 and 6.

Chapter 7 discusses the results. Chapter 8 gives the conclusion, offers verification of the main hypothesis and describes about the future work that should be done.

Chapter 3 Materials and Surface Characterization

3.1 Materials used in the present work

3.1.1 Solders

Three different solder materials were used in this work. They were: 1) Eutectic *Sn-Pb* solder alloy, 2) eutectic *Sn-Cu* alloy and 3) pure *Sn*. Table 3.1 gives the composition and melting temperature of these solders.

Table 3.1 Solders used in present work

S.No.	Solder alloy	Composition	Melting Temperature(°C)
1.	Eutectic <i>Sn-Pb</i>	63%wt <i>Sn</i> – 37%wt <i>Pb</i>	183°C
2.	Pure <i>Sn</i>	100%wt <i>Sn</i>	232°C
3.	Eutectic <i>Sn-Cu</i>	99.3%wt <i>Sn</i> – 0.7%wt <i>Cu</i>	227°C

When received, solders were in the form of thin sheets. A square plate of 0.5 mm x 0.5mm solder was cut from the thin sheet with thickness around 0.05mm. Solder plate was cleaned in the solution of 3.7%*HCL* + Methanol for about 10 seconds, and subsequently ultrasonically cleaned in methanol for 10 seconds. After that, surface was dried off by wiping with a clean tissue paper. Flux was immediately applied on both solder plate and copper substrate by a brush. Solder plate was then placed on the copper substrate, and the sample was carried into the hot-stage chamber.

3.1.2 Cu substrates

Three copper substrates with different surface finish were used in this work. They were: 1) Highly polished surface (Met. lab), 2) Polished surface (vendor), and 3) Unpolished

surface. Naming of the substrates was done based on their surface finish. Description of each surface is as follows:

1) Highly polished surface (Met. lab.): This surface was prepared at the Metallography Laboratory of Brazing R&D program at the Center for Manufacturing, University of Kentucky. This surface was obtained by polishing copper surface with a sequence of polishing grits (320, 500, 1200 and 4000), followed by $1\mu\text{m}$ and the $0.04\mu\text{m}$ diamond suspensions. Struer's Rotopol-22 grinding/polishing machine was used during this process. An image of this surface is shown in figure 3.1



Fig. 3.1 Highly Polished surface (Met. lab)

2) Polished surface (vendor): Polished surface (vendor) was one of the two surfaces obtained from the vendor, McMaster-Carr. The surface was polished by the vendor to obtain a mirror-like finish. Figure 3.2 shows an image of this surface.

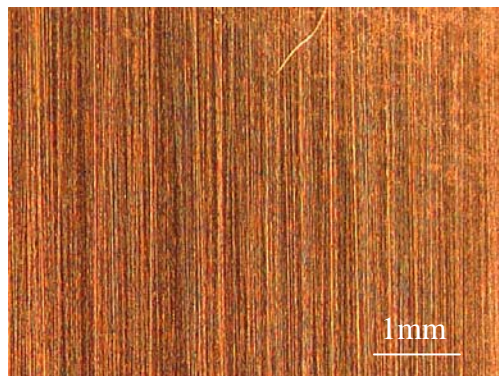


Fig. 3.2 Polished surface (vendor)

3) Unpolished surface: Unpolished surface was also obtained from the vendor, McMaster-Carr. No finish was applied to the surface of the substrate, see figure 3.3. This substrate was received as fabricated by the mill.

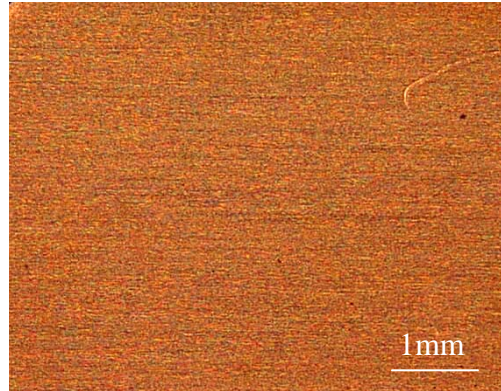


Fig. 3.3 Unpolished surface

3.2 Surface Characterization

Surface roughness measurements aimed at the understanding of the texture of the surface was an important part of the laboratory work. For the present work, three *Cu* substrates, mentioned in previous section, were studied under an optical surface profilometer, Zygo NewView™ 5000. Figure 3.4 shows the setup of the instrument used.

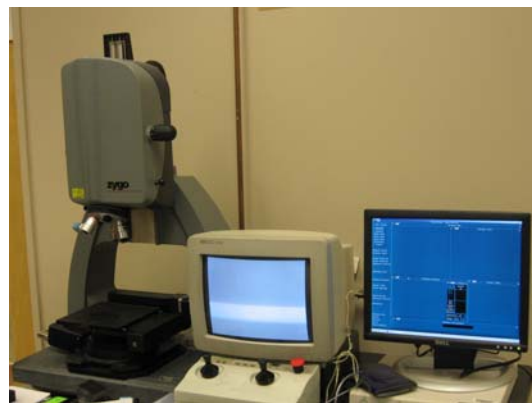


Fig. 3.4 Zygo NewView™ 5000 Optical Profilometer

Zygo NewView™ instrument is capable of characterizing and quantifying surface roughness, step heights, critical dimensions and topographical features with high accuracy and precision. It can measure profile heights ranging from 1nm to 5000 μ m at

vertical scan speed of 10 μ m/s. Arithmetic average surface roughness (R_a), and maximum peak to valley height (PV) are the surface parameters measured using this instrument for the present work. Following is the definition of surface parameters studied by profilometer:

Arithmetic average roughness (R_a): It is defined as the average deviation of surface points from the mean plane. It is given by the relation:

$$R_a = \frac{1}{L} \int |z(x)| dx \quad (3.1)$$

In eq. (3.1), L is the sampling length and $z(x)$ is the deviation of surface point at a given distance x .

Maximum Peak to Valley height (PV): It is defined as the sum of maximum peak height value and largest valley depth value from the mean plane (see figure 3.5).

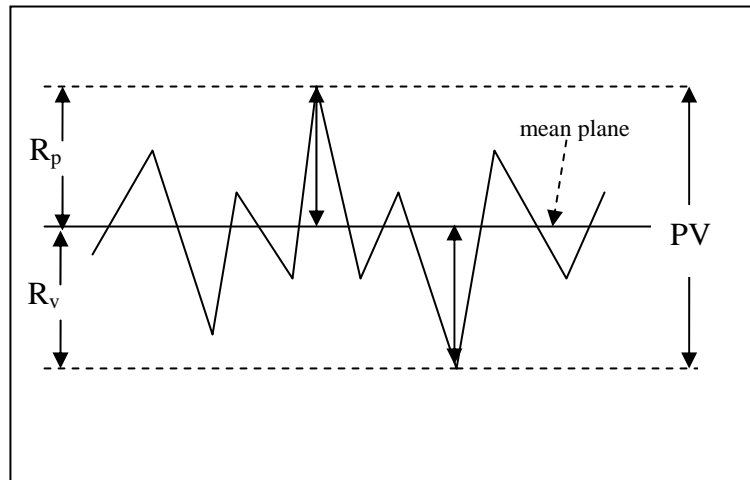


Fig. 3.5 Schematic representation of a surface profile

3.2.1 Substrate's characterization by profilometer

Highly polished surface (Met. Lab.): Figure 3.6, shows surface map and the profile of the surface obtained by the profilometer. It was observed that the surface was smooth and regular. There were very few scratches and irregularities present on the surface. Note that the overall peak-to-valley distance is roughly in the range of 1.5 μ m to 3 μ m. See section 3.2.2 for details.

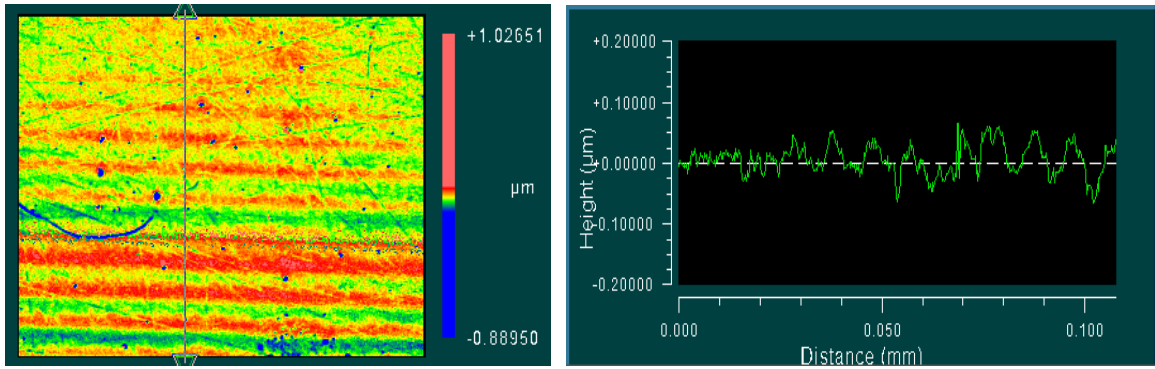


Fig. 3.6 Surface map and profile of polished surface(Met. lab.)

Polished surface(vendor): Surface map and profile of this polished surface shows the presence of few micro-groove lines (Fig. 3.7). The circular regions on the surface map highlight micro-groove lines present in the surface. These lines might be produced in the surface during the polishing of it by the vendor. Note that the overall peak-to-valley distance is roughly in the range of 3.5 μm to 5.5 μm .

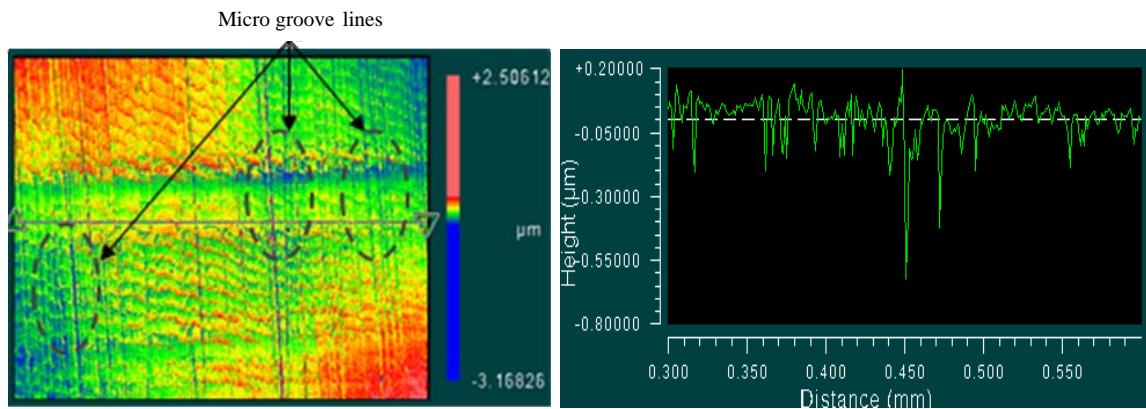


Fig. 3.7 Surface map and profile of polished surface(vendor)

Unpolished surface: Figure 3.8 represents the surface map and profile of this surface obtained from profilometer. Surface was rougher than previous two surfaces, as no work was done on it. Surface profile shows irregularities in the form of peaks and valleys present in it. Those are expected to influence the wetting behavior of solder spreading. Note that the overall peak-to-valley distance is roughly in the range of 6 μm to 8.5 μm .

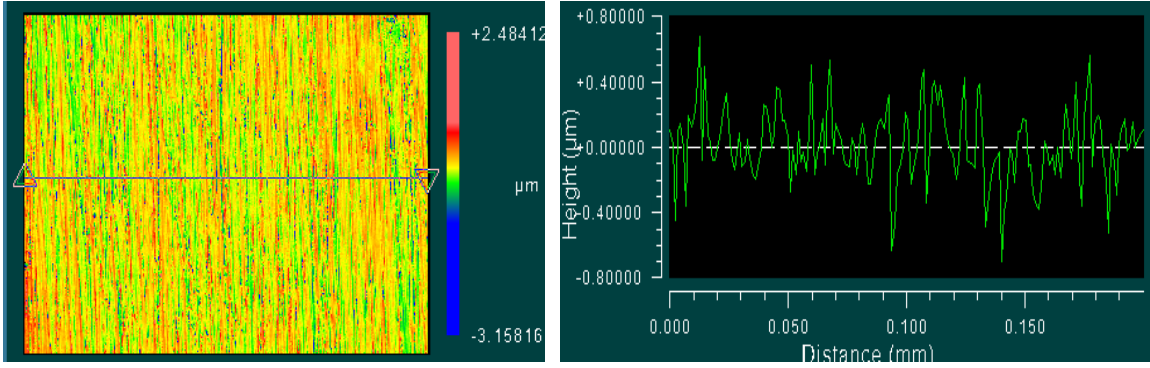


Fig. 3.8 Surface map and profile of unpolished surface

3.2.2 Profilometer results

Surface roughness measurement results obtained from profilometer studies are shown in table 3.2. Plots showing the comparison of roughness values of each surface are presented in figure 3.9.

Table 3.2 Profilometer results

S.No	Surface	Surface Roughness	
		<i>PV</i> (μm)	<i>R_a</i> (μm)
1	Highly polished surface (Met. Lab)	2.788	0.038
2	Polished Surface (vendor)	4.920	0.087
3	Unpolished Surface	6.461	0.178

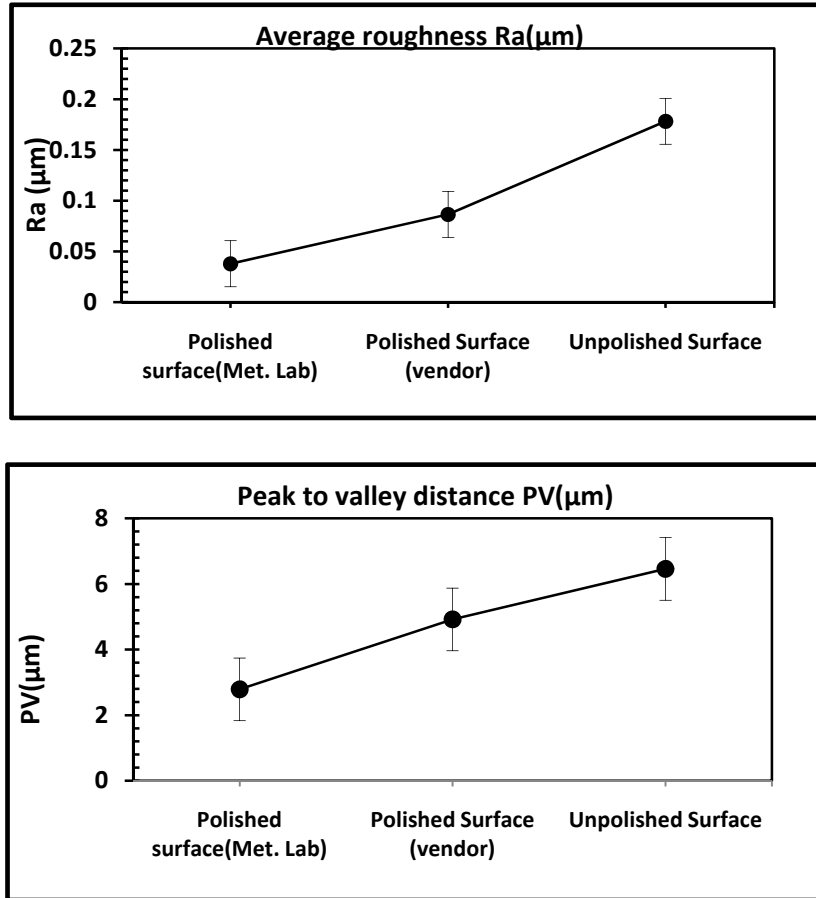


Fig. 3.9 Comparison plots of surface roughness measurements of the surfaces: average roughness (R_a) and Peak to Valley distance (PV)

Table 3.2 and plots in figure 3.9, confirm the fact that unpolished surface is the roughest of the three surfaces studied. It has maximum R_a and PV values. Polished surface (vendor) is the next rough surface, with R_a and PV values around $0.09\mu\text{m}$ and $4.9\mu\text{m}$ respectively. Roughness in this case can be attributed to a large extent to the presences of micro-groove lines present in the surface. Highly polished surface (Met. lab.) with least R_a and PV values (see table 3.2), is the smoothest among the surfaces used in this study.

Chapter 4 Experimental setup and procedures

This chapter describes the experimental setup and procedures involved in this study. It includes description of Hot-stage microscopy, Experimental procedures and post-processing procedures.

4.1 Hot-stage microscopy

Hot-stage microscopy system consists of of two important units. They are 1) hot-stage system and 2) microscope and data acquiring unit. Figure 4.1 and 4.2 shows the Hot-stage Microscope equipment and schematic diagram respectively.

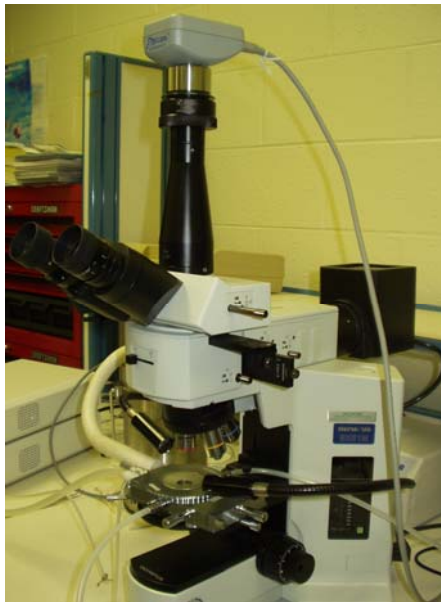


Fig. 4.1 Hot-stage microscope equipment

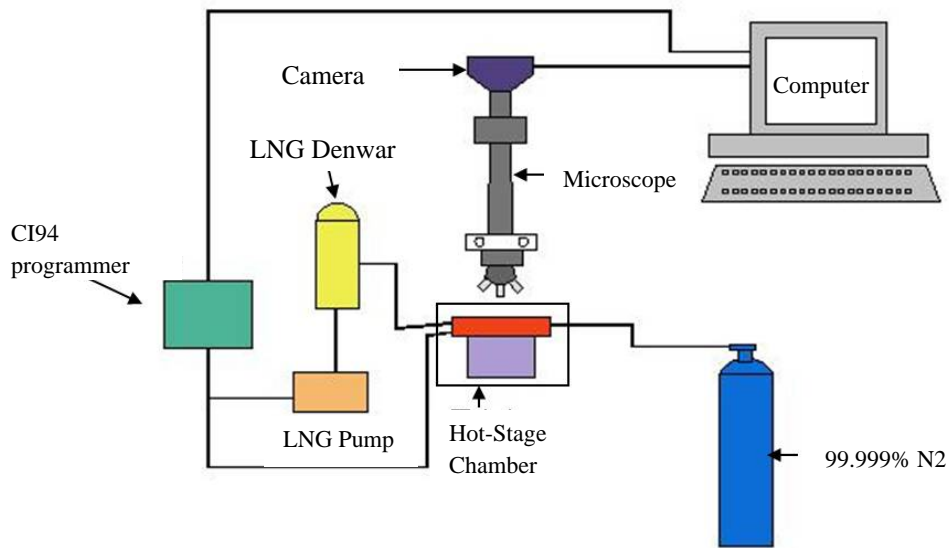


Fig. 4.2 Schematic representation of hot-stage microscopy system

4.1.1 Hot-stage system

THMS 600 hot-stage system (see figure 4.3), manufactured by Linkman Corp. UK, was used in this study. This system has a temperature range of -196°C to 600°C . The inner dimensions of hot-stage chamber are 70mm in diameter and 30mm in height. Silver block is used as the heating element in this system. Conduction mechanism is used to transfer heat to the base plate. Silver block responds well and quickly to heating and cooling cycles. Liquid nitrogen dewar and a cooling pump connected to hot-stage are used for cooling operations.



Fig. 4.3 Photo and schematic representation of Hot-stage chamber setup

CI94 programming unit run by a computer software, Pax-It[®], is used to control the heating element and the cooling system. Sample gets heated evenly by conduction from bottom and by radiations from side. Hot-stage chamber is also connected to ultra pure nitrogen gas (99.999% N_2) supply. This gas is used to provide inert atmosphere in the chamber during the tests. Before conducting the hot-stage tests, sample in the chamber was purged with N_2 gas for minimum of 2 hrs.

4.1.2 Microscope and data acquisition unit

A sample in the hot-stage chamber is observed through a metallurgical microscope, Olympus MX51. The stage is attached to the platform under the microscope, which can be moved along Z-axis using a focusing knob to focus the sample. Observations during the tests were made under different magnifications. A video camera, PaxCam, attached to the microscope was used to capture real-time images of sample. Pax-It[®] computer software was used to capture and store the data in the computer. The images were captured at the rate of 21.818 frames/sec. This software was also used to control heating and cooling cycles during experiments.

Videos and images captured by the camera were analyzed to determine the behavior of solder on the substrate. Real-time imaging and video capturing with Hot-stage microscopy system is of great advantage. The system is easy to operate and provides sharp image under different magnifications. A main disadvantage of this system is the uncertainty in temperature readings. This uncertainty is caused due to a thin glass plate inserted in between sample and the silver block to protect the silver block. This glass acts as thermal resistance, slightly reducing conduction from the heating source to sample. A brief description of temperature uncertainty observed in the experiments is provided in Appendix B.

4.2 Sample preparation

Basic sample used for hot-stage experiments consists of two parts 1) Metal substrate and 2) solder alloy. Figure 4.4 illustrates the configuration of the sample used. Copper surfaces discussed in chapter 3 were used in the experiments. They were cut manually to dimensions approximately 1cm x 1cm and have thickness of 0.5 mm. Eutectic

combinations of *Sn-Pb*, *Sn-Cu* and pure *Sn* solder alloys were used in the test. They were of the dimensions approximately 0.5mm x 0.5mm and 0.05 mm thickness. Flux was applied over both solder and substrate.

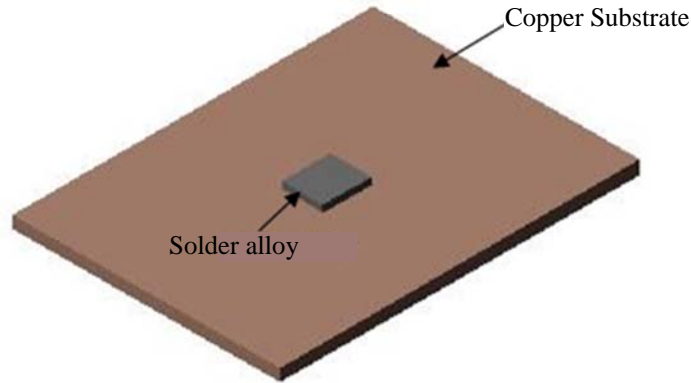


Fig. 4.4 Setup of sample used

4.3 Experimental procedure and post-processing

Sample was placed in the hot-stage chamber over a circular quartz glass desk positioned on the silver block. The chamber was then purged with ultra pure nitrogen gas for minimum of 2 hours. The flow rate used in most of the tests was 39.54 cm³/min at atmospheric pressure and room temperature (1 atm and 23°C). This was done to create inert atmosphere in the chamber. Pax-it[®] software controlling the heating element in hot-stage starts element to heat up after initiation of the heating cycle. The temperature of the sample raises and as it reaches to temperature 30°C lower than the melting point of the solder alloy, video capturing is initiated. Solder placed over the substrate melts when temperature reaches to a value slightly higher than melting temperature of solder alloy (caused due to thermal contact resistance between the base plate and silver block). Finally temperature reaches the peak point set about 30°C above the melting point of the solder alloy. This temperature is maintained for about 30 seconds during which the molten solder flows over the substrate surface temperature is stable. After that duration, cooling cycle starts automatically and temperature of the system drops. Cooling cycle involves

blowing of liquid nitrogen into the hot-stage substrate using a cryogenic system. Figure 4.5 gives an example of a typical temperature cycle in the experiments.

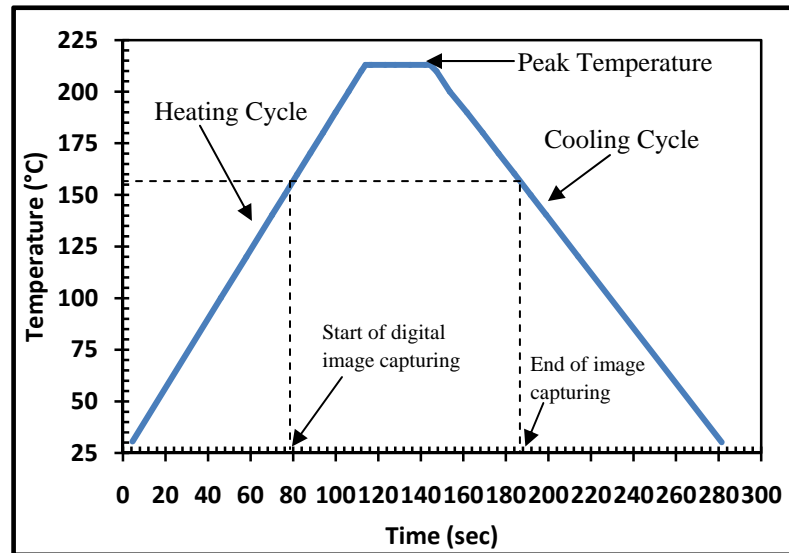


Fig. 4.5 Temperature cycle plot during a hot-stage experiment involving eutectic *Sn-Pb* solder alloy and a *Cu* substrate.

Movie was captured during heating and cooling cycles, and was stopped when solder solidification over the substrate started taking place. Later images were extracted from the video at the rate of approximately 22 frames per second for data analysis. Images obtained from the movie were then studied using Image Pro[®] software. A computer image of Image pro[®] software platform is shown in figure 4.6. The objective of this image analysis was to determine kinetics of solder flow over the substrate during hot-stage experiments, i.e. to determine the triple line movement. Area of instantaneous solder spread over the substrate was measured using this software.

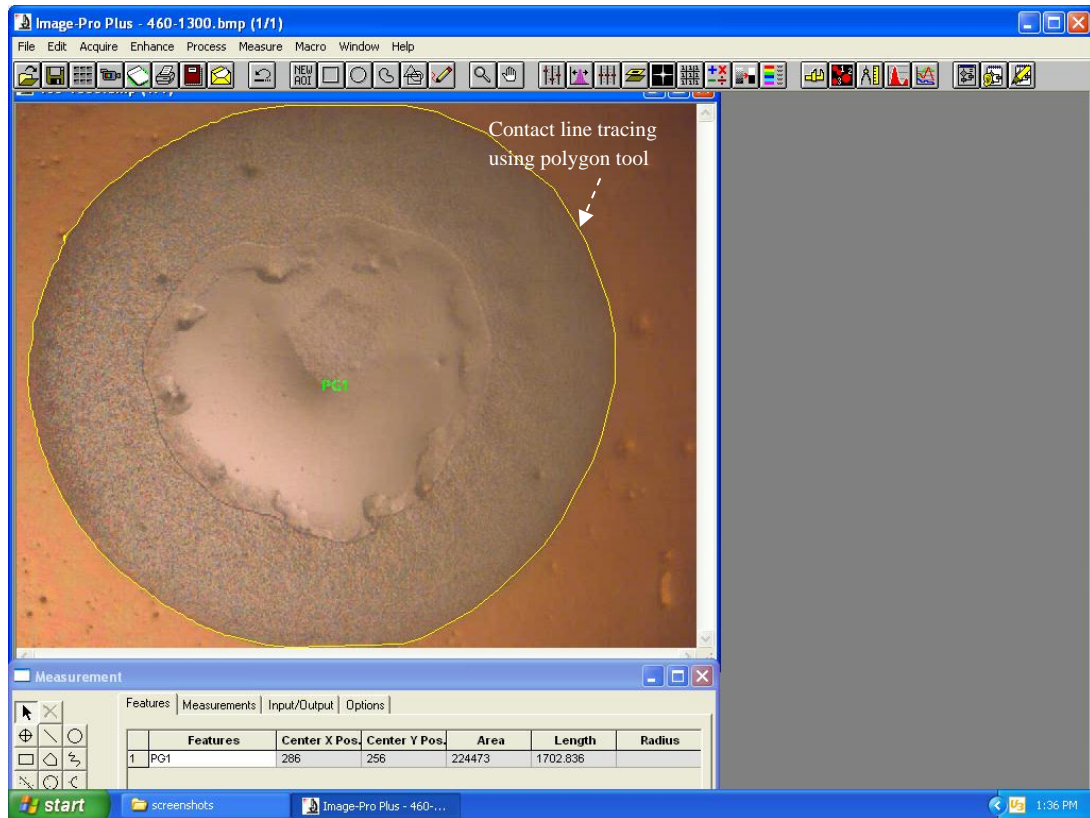


Fig. 4.6 Computer screen capture of Image pro[®] software

Following are the steps involved during the image analysis using the Image pro[®] software

- 1.) Image needed to be analyzed was imported into the software.
- 2.) Polygon measurement tool was selected for performing measurements.
- 3.) The triple line of the contact of the solder alloy and substrate is traced using the tool.
- 4.) Software analyses the area of the region enclosed in the traced boundary.
- 5.) The measured data was stored in a Microsoft excel sheet.

About 90-100 images were extracted from each video and analyzed using the Image Pro[®] software. All data was stored in the excel spreadsheet files. This data was later used to understand the spreading kinetics of solder flow in the experiment.

Chapter 5 Hot-stage experiments involving eutectic *Sn-Pb* solder alloy

5.1 Eutectic *Sn-Pb* alloy spreading over highly polished *Cu* surface (Met lab)

Sample description:

Figure 5.1 shows the sample used in this experiment, as positioned on the substrate covered with flux.

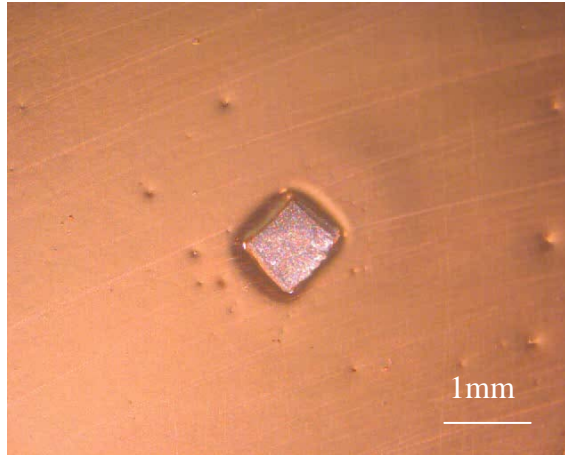


Fig. 5.1 Eutectic *Sn-Pb* over highly polished Surface (Met lab)

Solder alloy: 63Sn-37Pb Dimension: 0.5 mm x 0.5mm x 0.05 mm (approximately)

Substrate: Copper Dimension: 10 mm x 10 mm x 0.5 mm (approximately)

Surface: Highly polished Surface (Met. Lab)

Duration of ultra pure N_2 flow: 120 mins

Observations:

The sample placed in the hot-stage chamber was heated at the rate of $100^\circ\text{C}/\text{min}$ upto to the peak temperature. Solder melts around 187°C which is the temperature higher than nominal melting temperature of alloy i.e. 183°C (due to temperature uncertainty caused by thermal resistance as discussed in Chapter 4). Temperature of the hot-stage was maintained at peak temperature of 213°C for a duration of 30 sec. Solder spreads over the substrate during this period. The sample was then cooled down to the room temperature

at the rate of 80°C/min. Movie recording during the experiment was started when the temperature was 150°C during the heating segment of the cycle and stopped at the same temperature in cooling segment of the cycle.

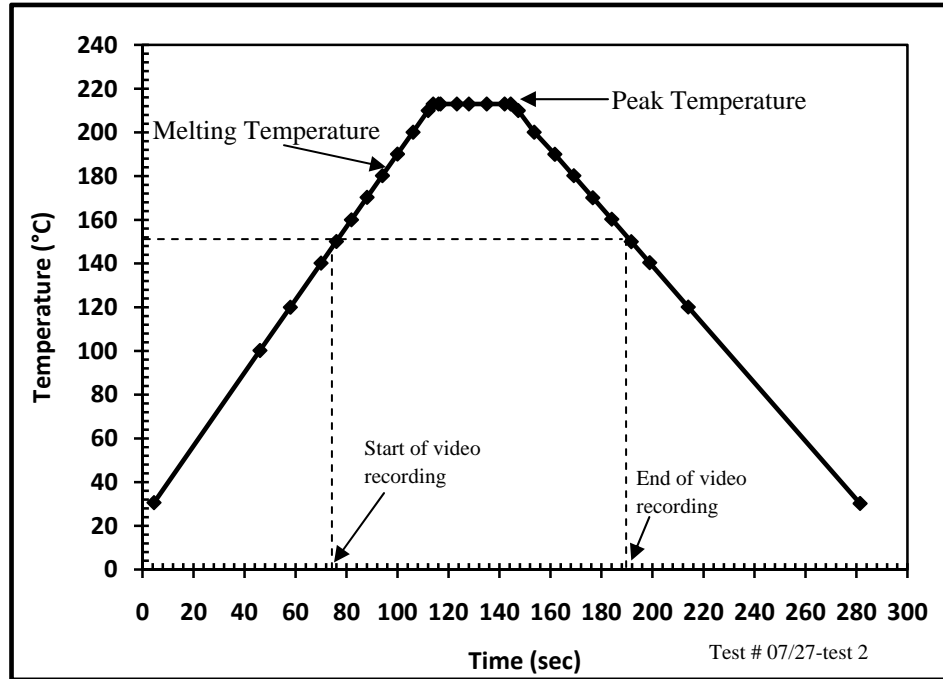


Fig. 5.2 Heating and Cooling cycle, eutectic *Sn-Pb* alloy on highly polished surface (Met. Lab)

Figure 5.3 presents a series of photos, extracted from the movie. These frames represent spreading of eutectic *Sn-Pb* solder alloy over the highly polished surface. These images show regular spreading of molten solder. It advances in form of almost circular liquid front as it flows on the surface.

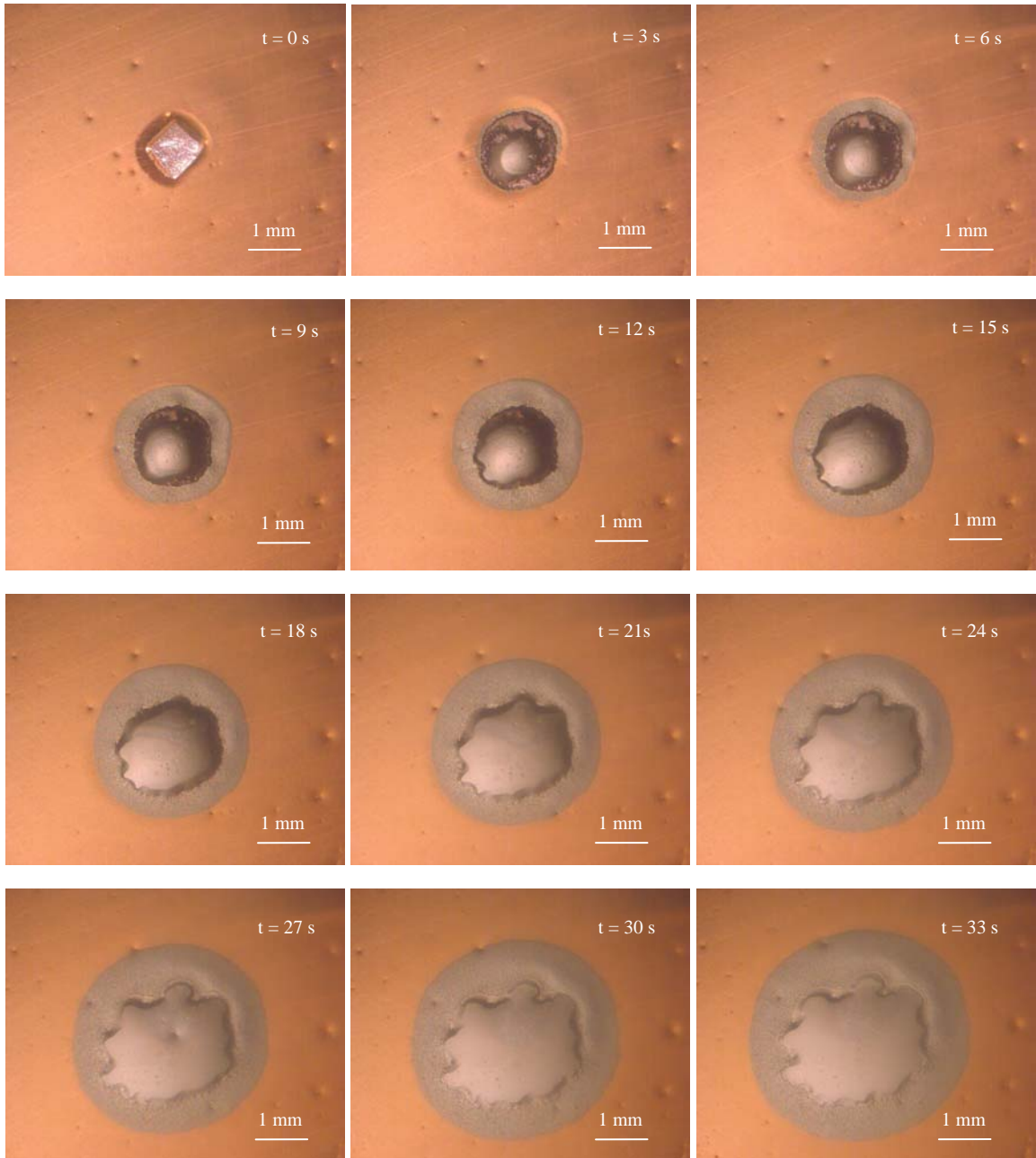


Fig. 5.3 Extracted images representing the sequence of spreading of eutectic *Sn-Pb* solder alloy on a highly polished surface (Met. Lab)

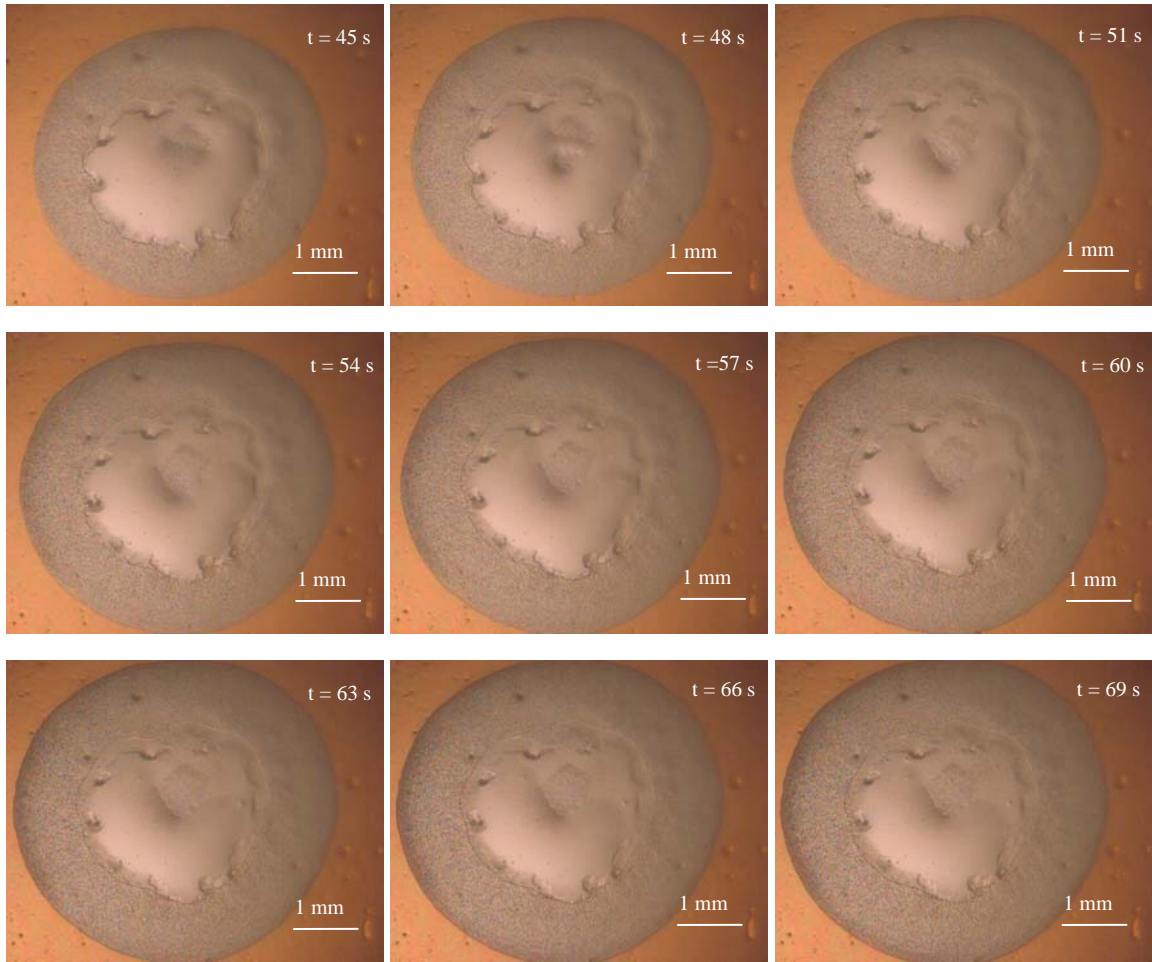


Fig. 5.3 Extracted images representing the sequence of spreading of eutectic *Sn-Pb* solder alloy on a highly polished surface (Met. Lab) (continued)

Analysis:

Figure 5.4 illustrates schematically the spreading contours of eutectic *Sn-Pb* solder alloy on a highly polished copper substrate. It provides a map of an area spread by solder during different stages of spreading. First spreading profile represents the solder before it melts. Next profile gives the spreading of the solder sample when temperature rises from the melting temperature to the peak temperature. The later two profiles provide the spreading at the peak temperature. Finally, the last contour gives the final area spread. As noticed from figure 5.4, solder alloy melts and spreads uniformly in a form resembling almost circular front.

Images extracted from the video were analyzed to obtain the rate of spreading of molten solder. Figure 5.5 shows the plot of A/A_0 versus time in seconds. Where A is the area of spread of solder at a given instance of time and A_0 is the initial area of solder at room temperature.

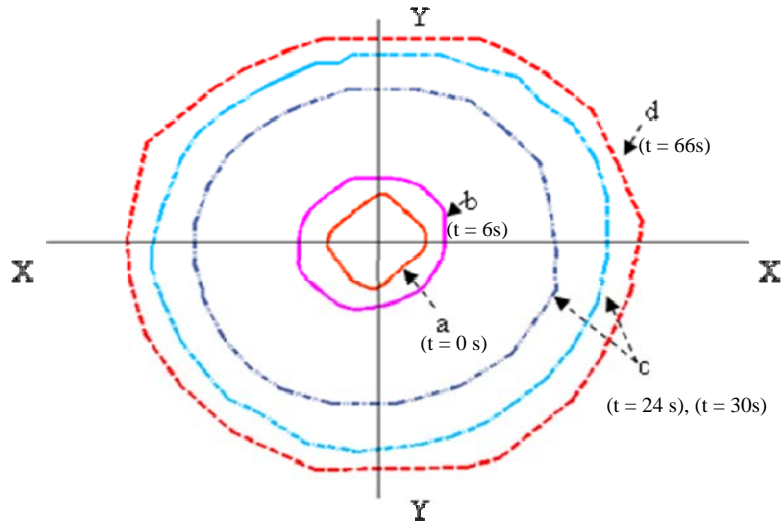


Fig. 5.4 Schematic representation of spreading of eutectic *Sn-Pb* solder alloy on polished surface (Met. Lab): a) solder before melting, b) spreading of solder at an instant during temperature rise from melting to peak temperature, c) Spreading of solder at peak temperature and d) Final area spread by molten solder

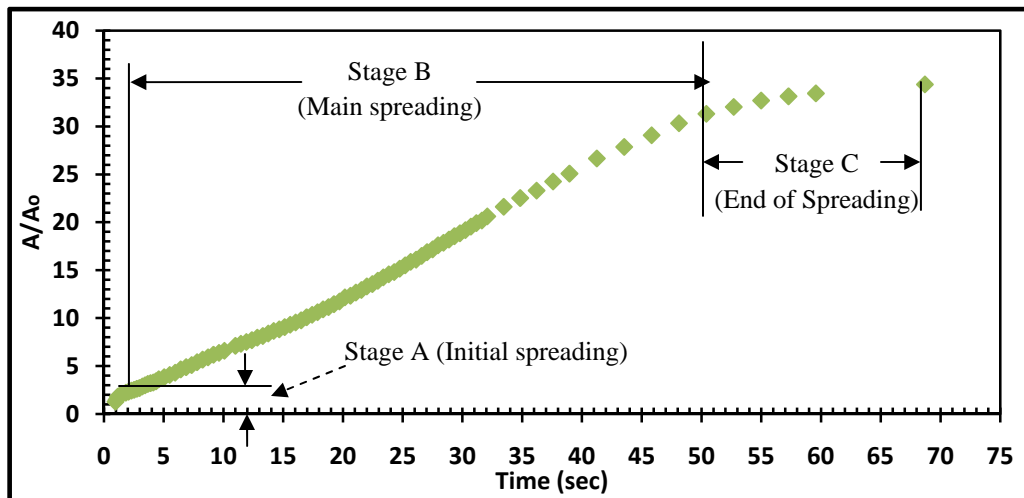


Fig. 5.5 A/A_0 Vs time (sec), eutectic *Sn-Pb* solder alloy spreading on polished surface (Met. Lab)

As shown in figure 5.5, spreading of solder alloy is divided into three stages. Stage A in the plot shows initial spreading of solder. The spreading is rapid for a short duration of time when solder melts and starts spreading. Spreading rate is almost linear during that period. Stage B resembles main solder spreading with the rate relatively slower than in stage A. This is the period when molten solder advances in almost circular front. Finally, stage C represents the final stage when area of spread becomes almost constant indicating end of spreading.

5.2 Eutectic *Sn-Pb* alloy spreading over Polished *Cu* surface (vendor)

Sample description:

Figure 5.6 shows the sample used in this experiment.



Fig. 5.6 Eutectic *Sn-Pb* over Polished Surface (vendor)

Solder alloy: 63Sn-37Pb Dimension: 0.5 mm x 0.5mm x 0.05 mm (approximately)

Substrate: Copper Dimension: 10 mm x 10 mm x 0.5 mm (approximately)

Surface: Polished surface (Vendor)

Duration of ultra pure N_2 flow: 120 mins

Observations:

Similar to previous experiment discussed, the sample in the hot-stage chamber is heated at the rate of $100^{\circ}\text{C}/\text{min}$. Solder melts around 189°C , a temperature higher than the nominal melting temperature of alloy (due to temperature uncertainty caused by thermal resistance as discussed in Chapter 4). Temperature of the hot-stage was maintained at the peak temperature of 213°C for a duration of 30 sec. Solder spreads over the substrate during this period. Sample was cooled down to room temperature at the rate $80^{\circ}\text{C}/\text{min}$. Movie recording during the experiment was started when temperature was 150°C during the heating segment of the cycle and stopped at 160°C in the cooling segment of the cycle.

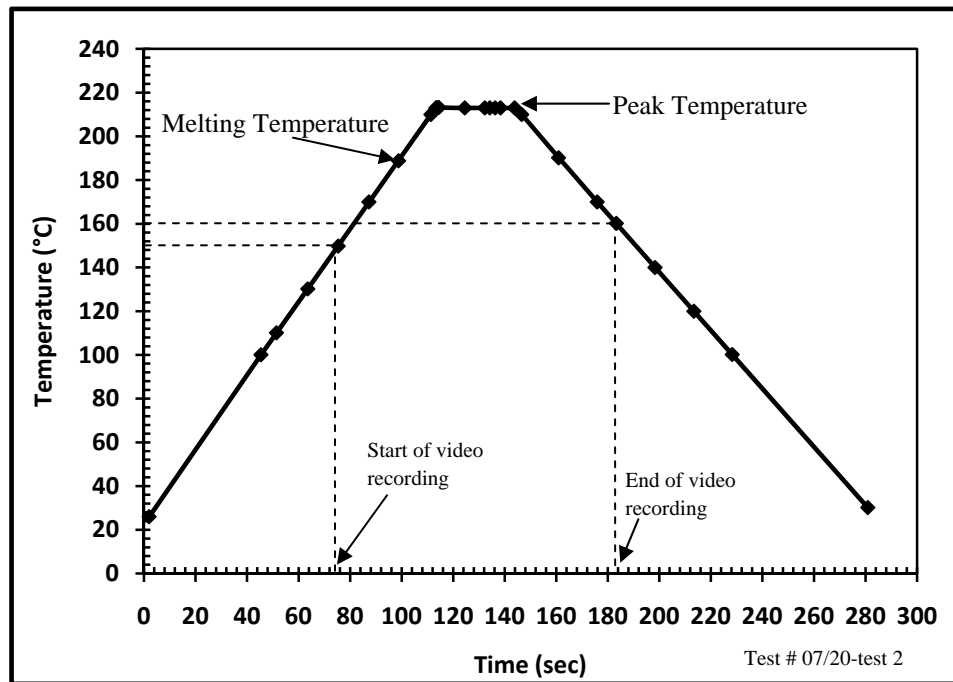


Fig. 5.7 Heating and Cooling cycle, eutectic *Sn-Pb* alloy on polished surface (vendor)

Figure 5.8 presents a series of photos, extracted from the movie. These frames represent spreading of the eutectic *Sn-Pb* solder alloy over the polished surface (vendor). Initial spreading appeared to be very similar to spreading in the experiment discussed earlier. Spreading front was almost circular during the period when the temperature rises from

melting temperature to the peak temperature. But, as the time progresses the shape of the spreading front becomes irregular.

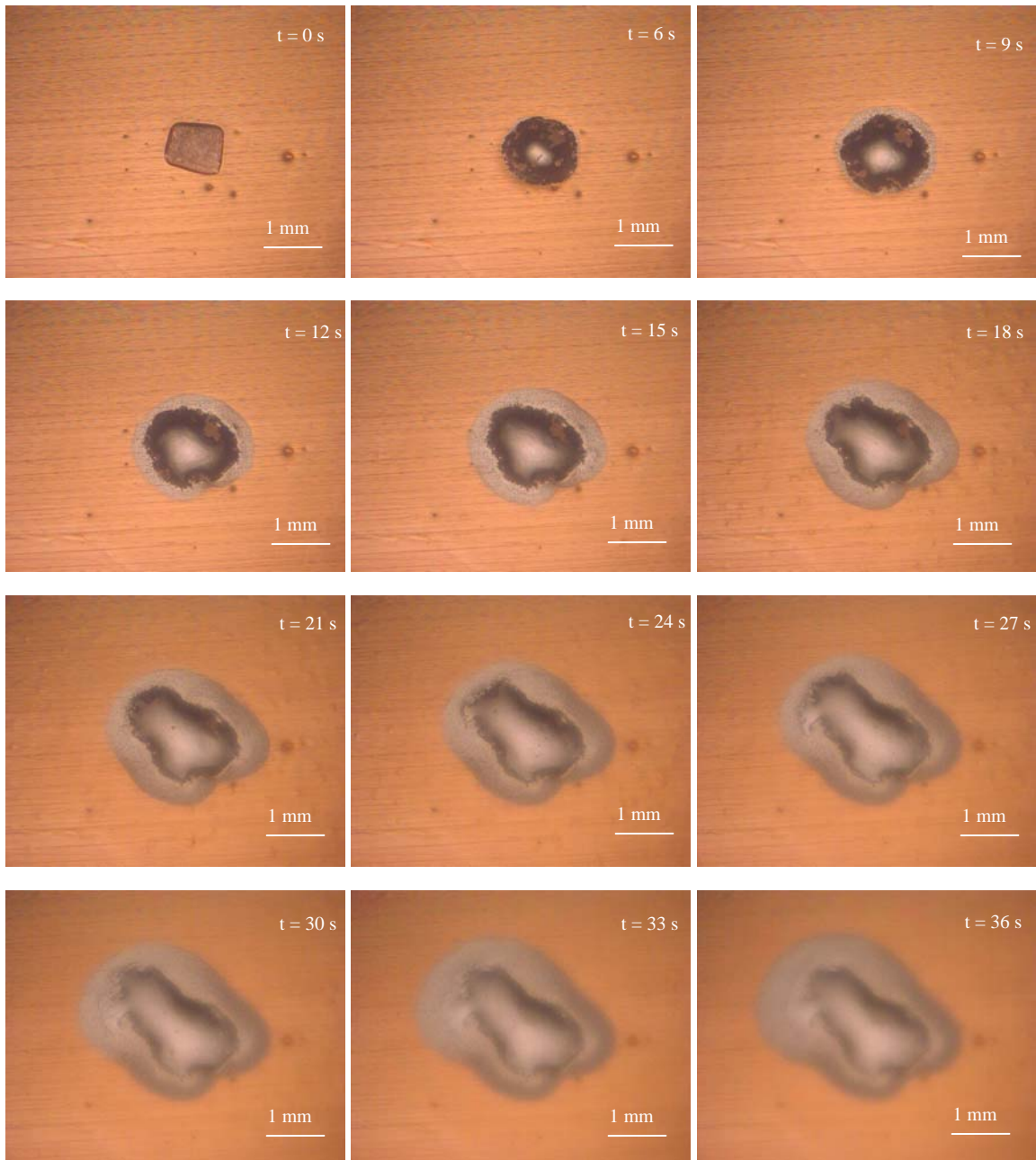


Fig. 5.8 Extracted images representing the sequence of spreading of eutectic *Sn-Pb* solder alloy on a polished surface (vender)

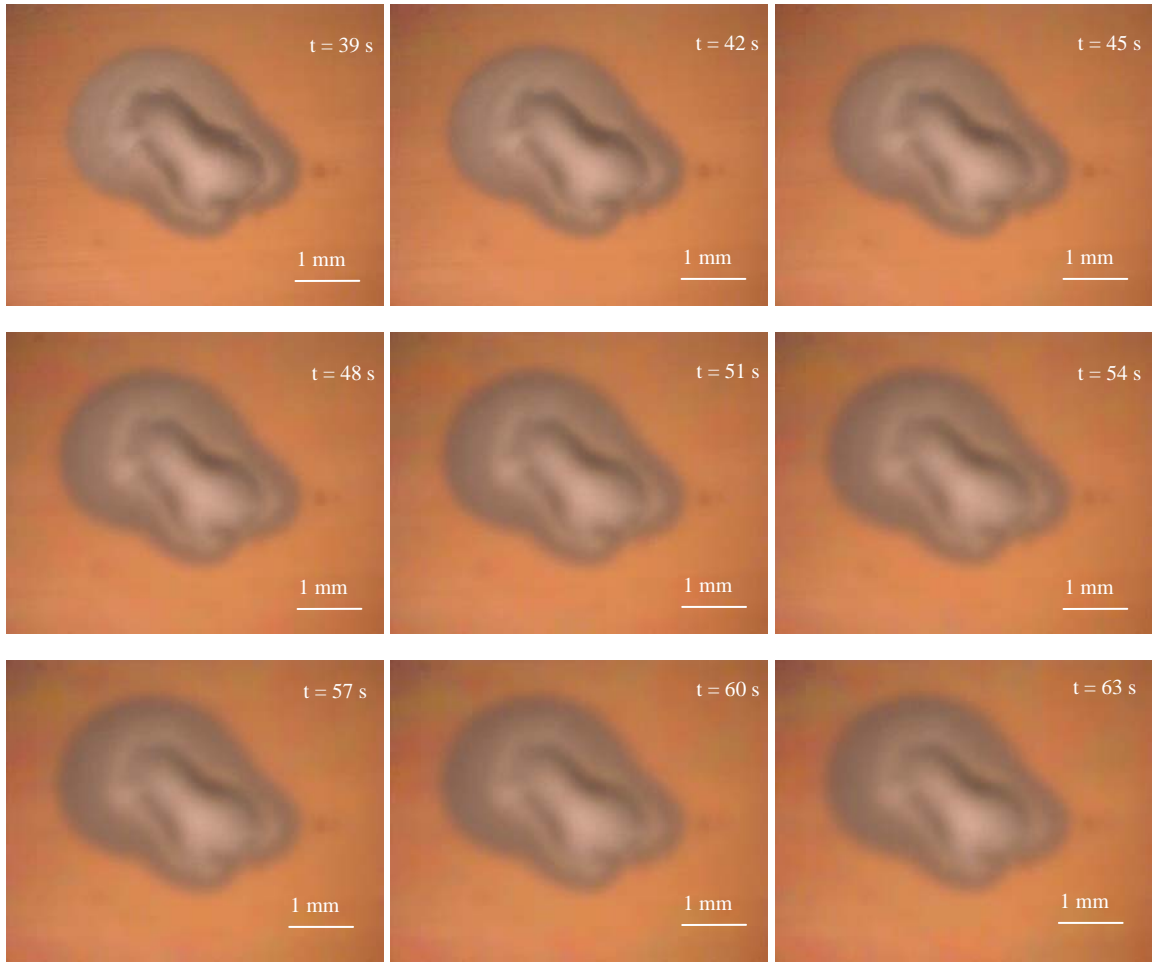


Fig. 5.8 Extracted images representing the sequence of spreading of eutectic *Sn-Pb* solder alloy on a polished surface (vendor) (continued)

Analysis:

Figure 5.9, provides a clear idea of the spreading presented in figure 5.8. This schematic representation maps solder spreading during different stages in the test, as explained in the analysis section of the experiment discussed earlier. It shows the irregularity in the spreading of solder alloy in the final stage when compared to initial stage. This non-uniformity in spreading can be attributed to irregularities in the form of micro groove lines (discussed in chapter 3) present in the surface which promote preferential direction of spreading.

Digital images extracted from the video were analyzed to understand the rate of spreading of solder on the current copper substrate. Figure 5.10 gives the plot of A/A_0 versus time in seconds.

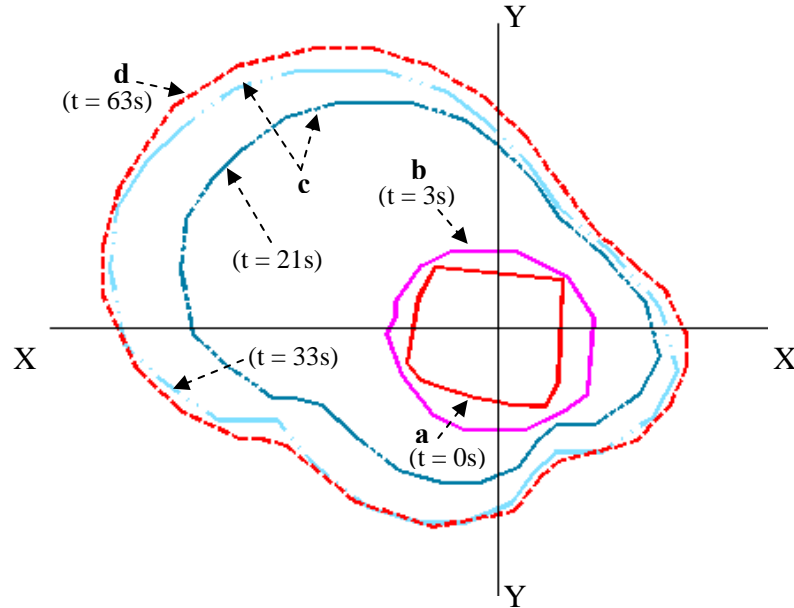


Fig. 5.9 Schematic representation of spreading of eutectic *Sn-Pb* solder alloy on polished surface (vender): a) solder before melting, b) spreading of solder at an instant during temperature rise from melting temperature to peak temperature, c) Spreading of solder at peak temperature and d) Final area spread by molten solder

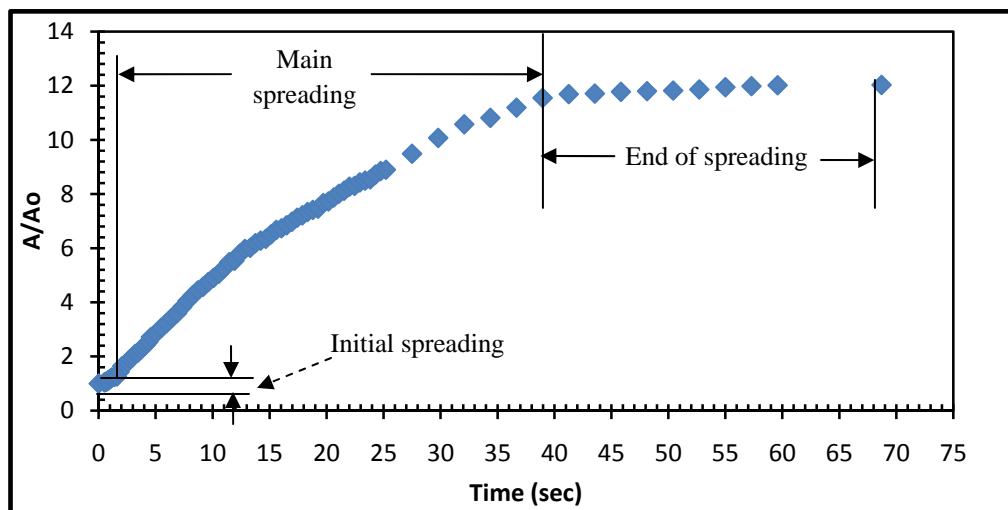


Fig. 5.10 A/A_0 vs time (sec), eutectic *Sn-Pb* solder alloy spreading on a polished surface (vender)

Figure 5.10 indicates initial spreading, like in earlier experiment, was rapid for a short duration of time. Spreading rate was almost linear during this period. After this solder spreads at a slower rate than initially for a long duration of time. Subsequently, the area of spread reaches a constant value, indicating the end of spreading.

5.3 Eutectic *Sn-Pb* alloy spreading over Unpolished *Cu* surface

Sample description:

Figure 5.11 shows the sample used in this experiment, as positioned on the substrate and covered with flux.

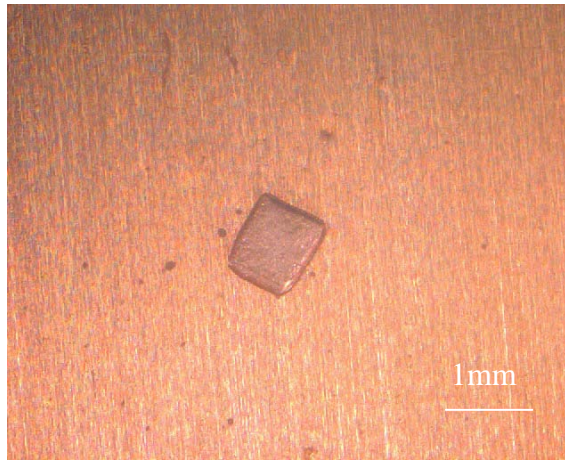


Fig. 5.11 Eutectic *Sn-Pb* over unpolished Surface

Solder alloy: 63Sn-37Pb Dimension: 0.5 mm x 0.5mm x 0.05 mm (approximately)

Substrate: Copper Dimension: 10 mm x 10 mm x 0.5 mm (approximately)

Surface: unpolished Surface

Duration of ultra pure N_2 flow: 120 mins

Observations:

Similar to previous experiments discussed, the sample in hot-stage chamber is heated at the rate of $100^{\circ}\text{C}/\text{min}$. Solder melts around 189°C , a temperature higher than actual melting temperature of this alloy. The temperature of the hot-stage was maintained at peak temperature of 213°C for a duration of 30 sec. Solder spreads over the substrate during this period. The sample is cool down to the room temperature at the rate of $80^{\circ}\text{C}/\text{min}$. Movie recording during the experiment was initiated when temperature was 150°C during heating segment and stopped at 160°C in cooling segment.

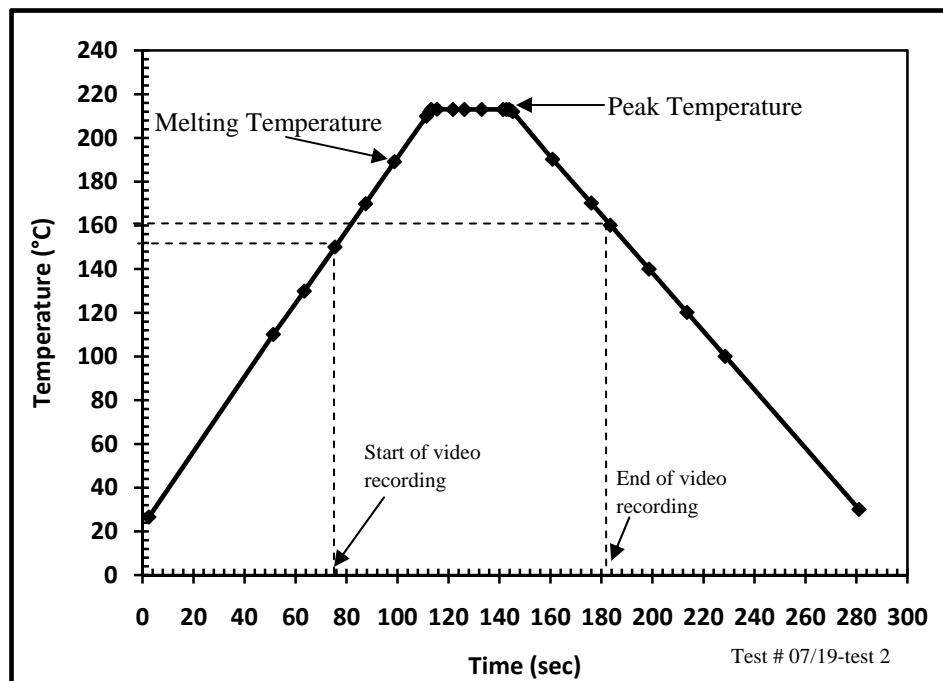


Fig. 5.12 Heating and Cooling cycle, eutectic *Sn-Pb* alloy on unpolished surface

Figure 5.13 presents a series of photos, extracted from the movie. These frames represent spreading of eutectic *Sn-Pb* solder alloy over the unpolished surface. Similar to earlier experiments the initial spreading of solder appears regular in this experiment. But, as the time progresses spreading solder moves in the form of an irregular front.

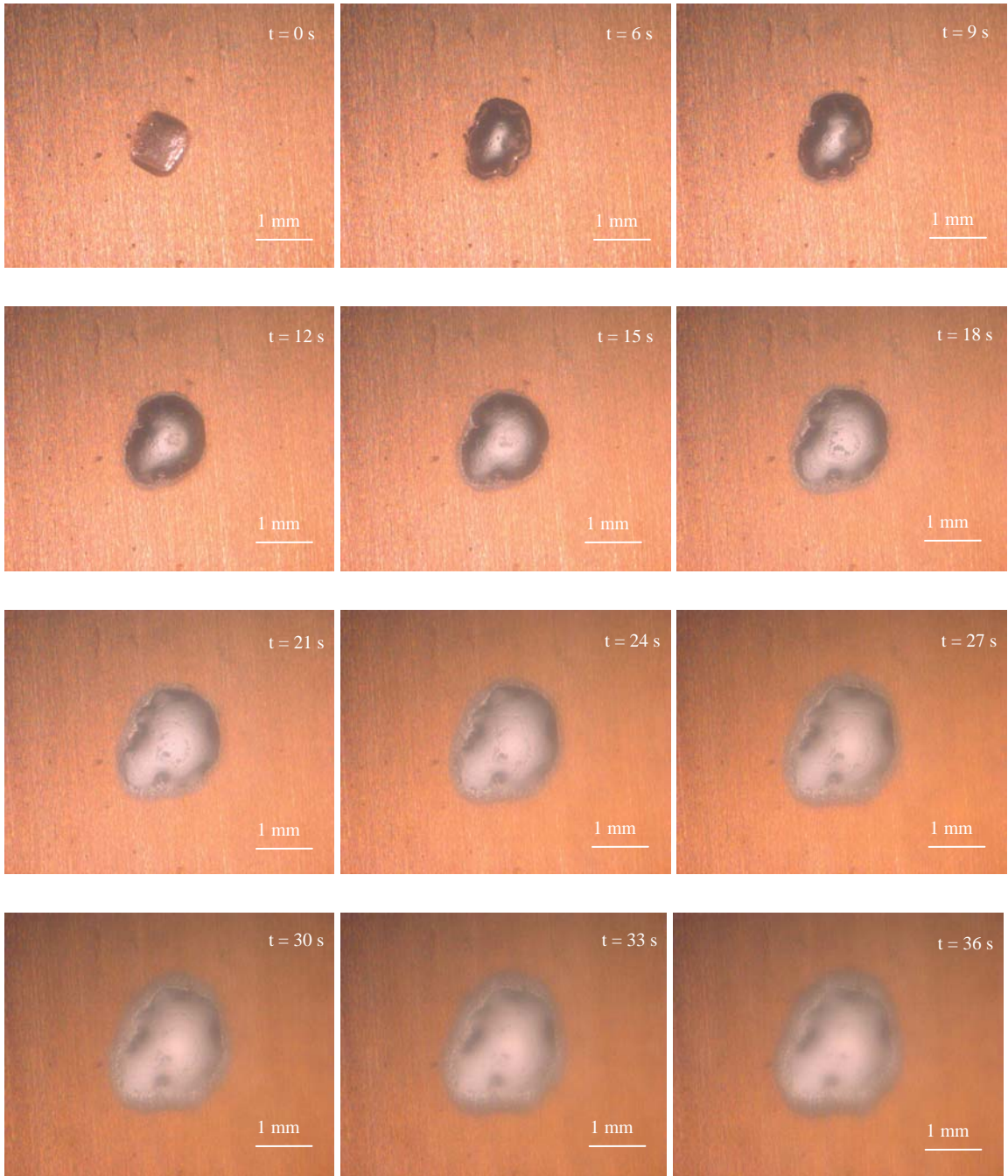


Fig. 5.13 Extracted images representing the sequence of spreading of eutectic *Sn-Pb* solder alloy on unpolished surface

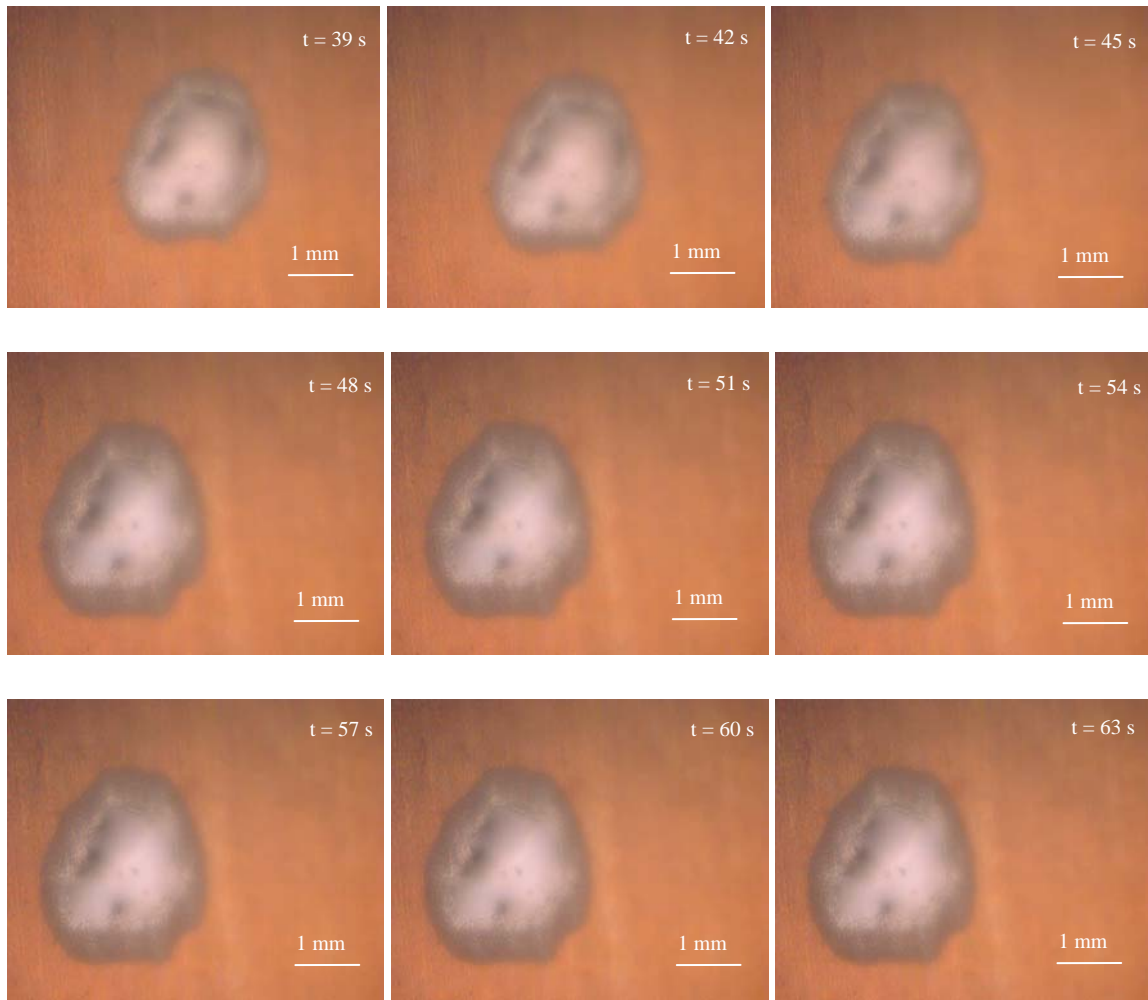


Fig. 5.13 Extracted images representing the sequence of spreading of eutectic *Sn-Pb* solder alloy on unpolished surface (continued)

Analysis:

Figure 5.14 shows the spreading of the solder alloy on the unpolished copper substrate. The irregularity in the spreading can be clearly observed in this figure. Digital images extracted from the video recorded were analyzed to understand the kinetics of spreading of solder in current experiment. Figure 5.15 give the plot of A/A_0 versus time in seconds. Where A is the area of solder spread at a given instance of time and A_0 is the initial area of solder at room temperature.

Figure 5.15 shows initial spreading, similar to previous two experiments, was rapid for the duration of time when solder melts and starts to spread. After that spreading increase

uniformly with time and later the area of spread becomes constant indicating end of spreading of solder on the substrate.

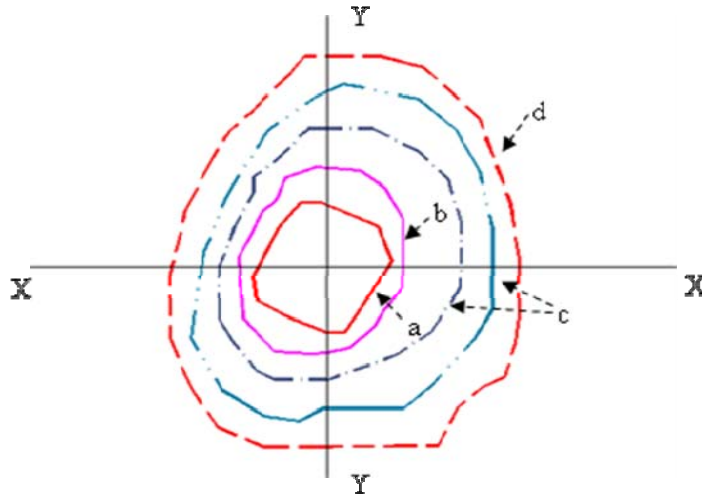


Fig. 5.14 Schematic representation of spreading of eutectic *Sn-Pb* solder alloy on unpolished surface: a) solder before melting ($t = 0s$), b) spreading of solder at an instant ($t = 3s$) during temperature rise from melting to peak temperature, c) Spreading of solder at peak temperature ($t = 21s$ & $t = 33s$) and d) Final area spread by molten solder ($t = 63 s$)

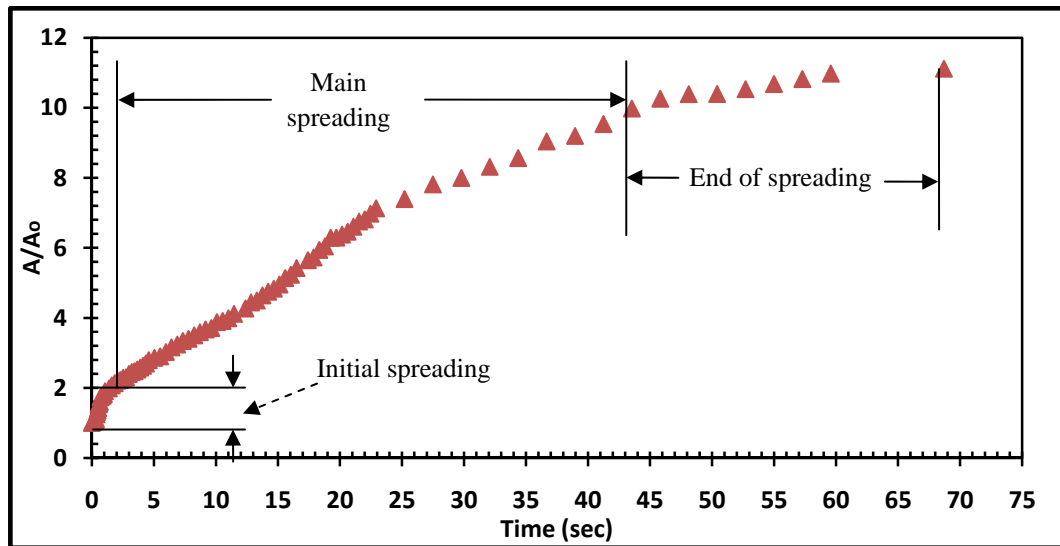


Fig. 5.15 A/A_0 Vs time (sec), eutectic *Sn-Pb* solder alloy spreading on unpolished surface

Chapter 6 Hot-stage experiments involving Lead-free solders

6.1 Pure Sn spreading over highly polished Cu surface (Met lab)

Sample description:

Figure 6.1 shows the sample used in this experiment, positioned on the substrate and covered with flux.

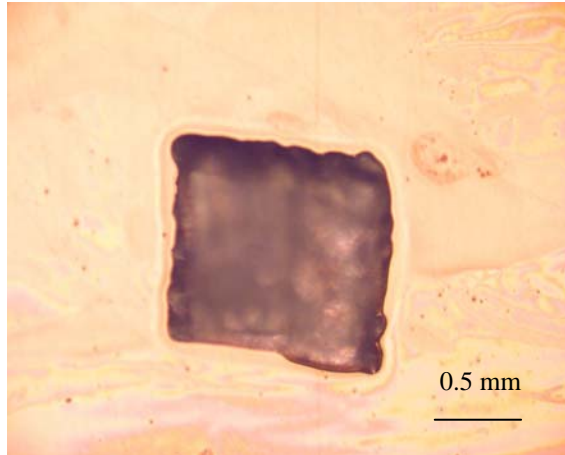


Fig. 6.1 Pure Sn over highly polished Surface (Met lab)

Solder alloy: Pure Sn Dimension: 0.5 mm x 0.5mm x 0.05 mm (approximately)

Substrate: Copper Dimension: 10 mm x 10 mm x 0.5 mm (approximately)

Surface: Highly polished Surface (Met. Lab)

Duration of ultra pure N_2 flow: 120 mins

Observations:

The sample was placed in the hot-stage chamber and heated at the rate of 100°C/min up to the peak temperature. Solder melts around 236°C which is higher than the nominal melting point of the solder i.e. 232°C (due to temperature uncertainty caused by thermal resistance as discussed in Chapter 4). The temperature of the hot-stage was maintained at the peak temperature of 262°C for a duration of 10 sec. It was then cooled to room temperature at the rate of 80°C/min. During the experiment, movie capturing was

initiated when the temperature reached 200°C, during the heating cycle, and terminated at around 180°C in the cooling cycle. Figure 6.2 shows the rate of temperature rise and fall during heating and cooling cycle respectively.

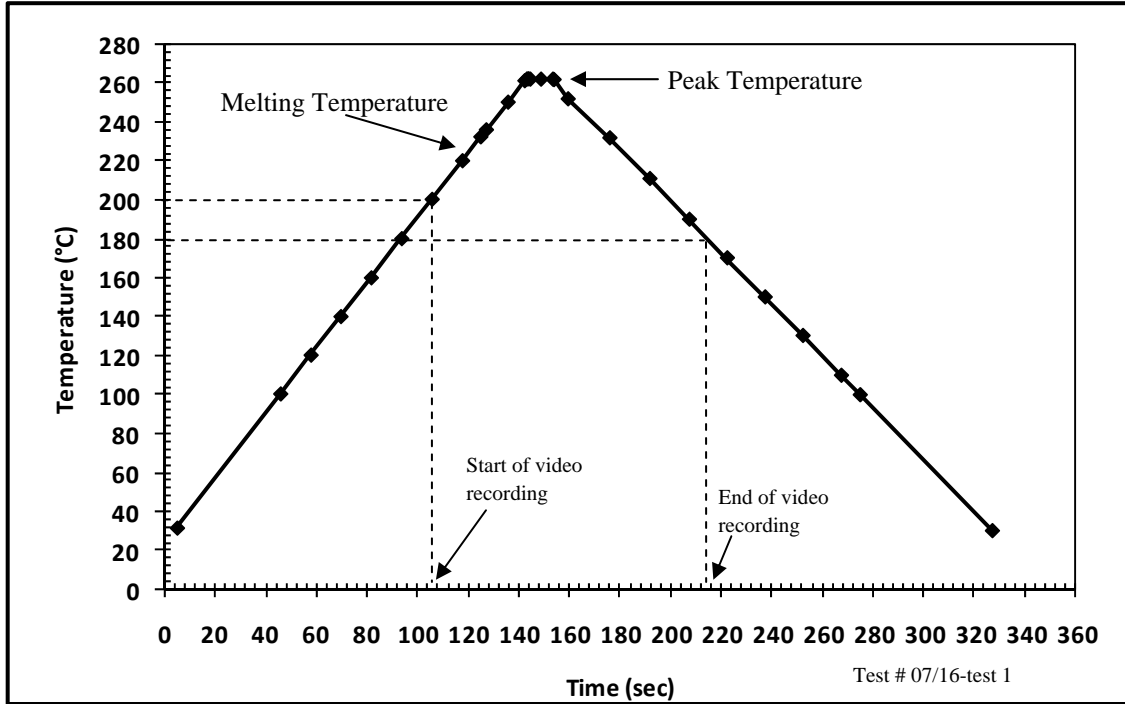


Fig. 6.2 Heating and cooling cycle, pure Sn over highly polished surface (Met. lab)

Figure 6.3 presents a series of photos, extracted from the movie. First image in the series depicts the sample at the onset of melting of solder and the last one shows the final spread of the solder. A little change in the shape of solder was observed at the end of the test vs. any intermediate instant of time suggesting a lack of spreading of pure tin over the surface. Major spreading in this test appears at the melting temperature of the solder whereas no significant spread was found with rise in temperature, subsequently.

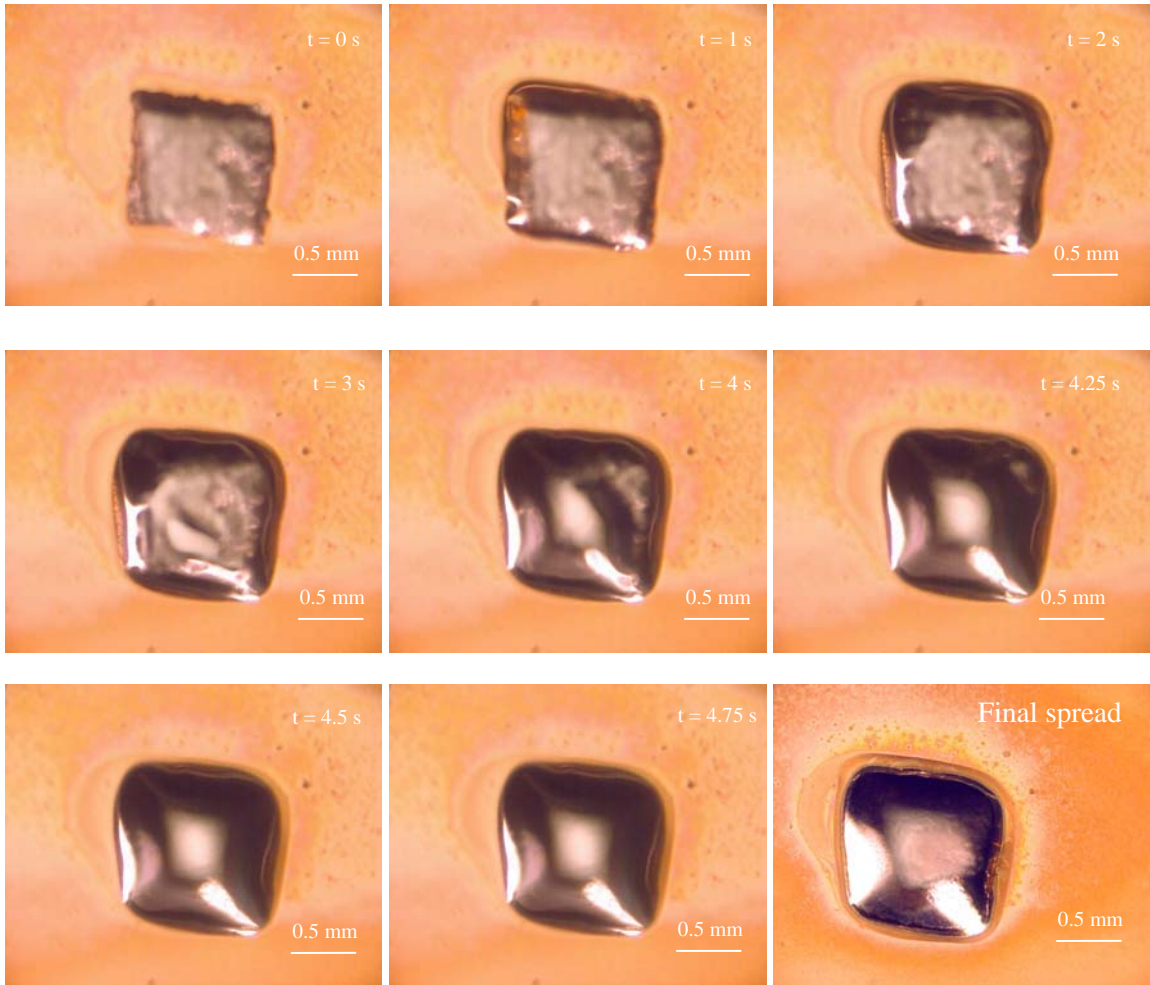


Fig. 6.3 Extracted images representing the sequence of spreading of pure *Sn* on highly polished surface (Met. Lab)

Analysis:

A schematic representation of solder spreading in this experiment was illustrated in figure 6.4. The schematic shows spreading of pure *Sn* at three different stages in the test – a) at the melting temperature b) at the peak temperature and c) the final area spread at the end of the test. Figure 6.4 gives a clear picture of a lack of spreading of molten pure *Sn* over a highly polished copper substrate. The area of spread in all the three cases was almost the same.

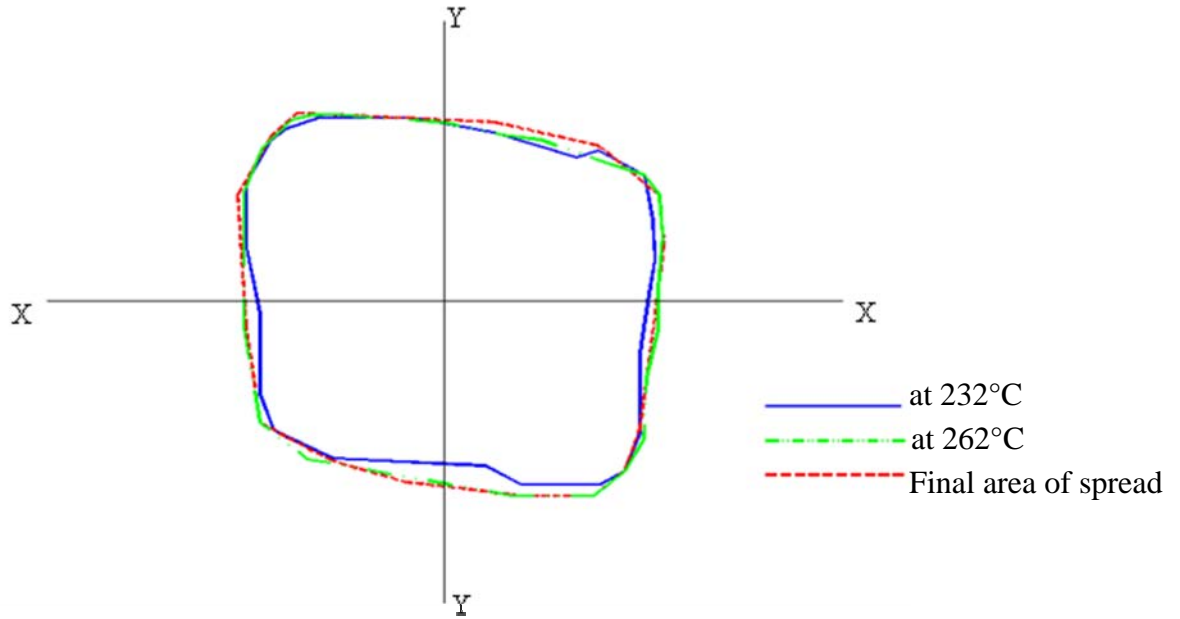


Fig. 6.4 Schematic representation of pure *Sn* spreading on highly polished surface (Met. lab)

Digital images extracted from the movies were analyzed to understand the spreading kinetics of molten *Sn* over the polished surface. Figure 6.5 provides the plot of A/A_o versus time. A is the area of spread of pure *Sn* at a given instance of time and A_o is the initial area of pure *Sn* at room temperature.

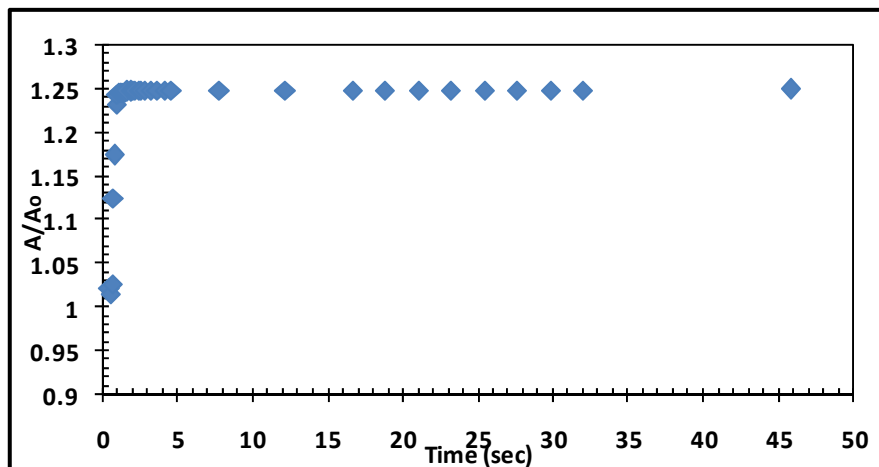


Fig. 6.5 A/A_o Vs time (sec), pure *Sn* spreading on highly polished surface (Met. lab)

Initially, spreading takes place for a short duration of time when pure *Sn* melts and starts to spread. After this stage, area spread by molten solder is almost constant. Thus, the pattern clearly indicates lack of spreading of Pure *Sn* on the selected substrate.

6.2 Pure *Sn* spreading over Polished *Cu* surface (Vendor)

Sample description:

Figure 6.6, shows the sample used in this experiment.

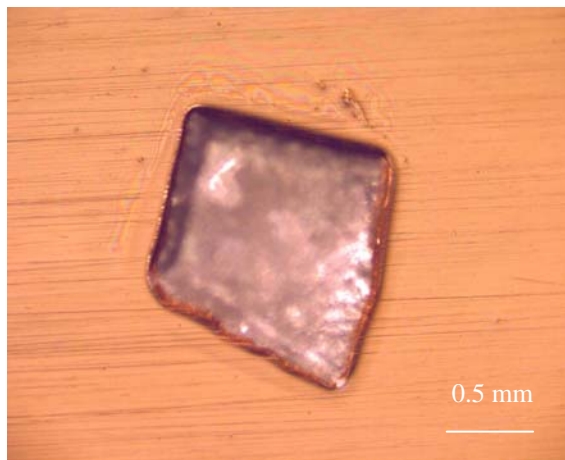


Fig. 6.6 Pure *Sn* over Polished Surface (vendor)

Solder alloy: Pure *Sn* Dimension: 0.5 mm x 0.5mm x 0.05 mm (approximately)

Substrate: Copper Dimension: 10 mm x 10 mm x 0.5 mm (approximately)

Surface: Polished Surface (vendor)

Duration of ultra pure N_2 flow: 120 mins

Observations:

The sample was kept in the hot-stage chamber and heated at the rate of $100^\circ\text{C}/\text{min}$ upto the peak temperature. The temperature of the hot-stage was maintained at peak temperature of 262°C for a duration of 10 sec. It was then cooled to the room temperature at the rate of $80^\circ\text{C}/\text{min}$. Video recording during the experiment was initiated when the temperature was at 200°C during the heating segment of the cycle and terminated at the

same temperature in the cooling segment of the cycle. Figure 6.7 shows the rate of temperature rise and fall during heating and cooling cycle.

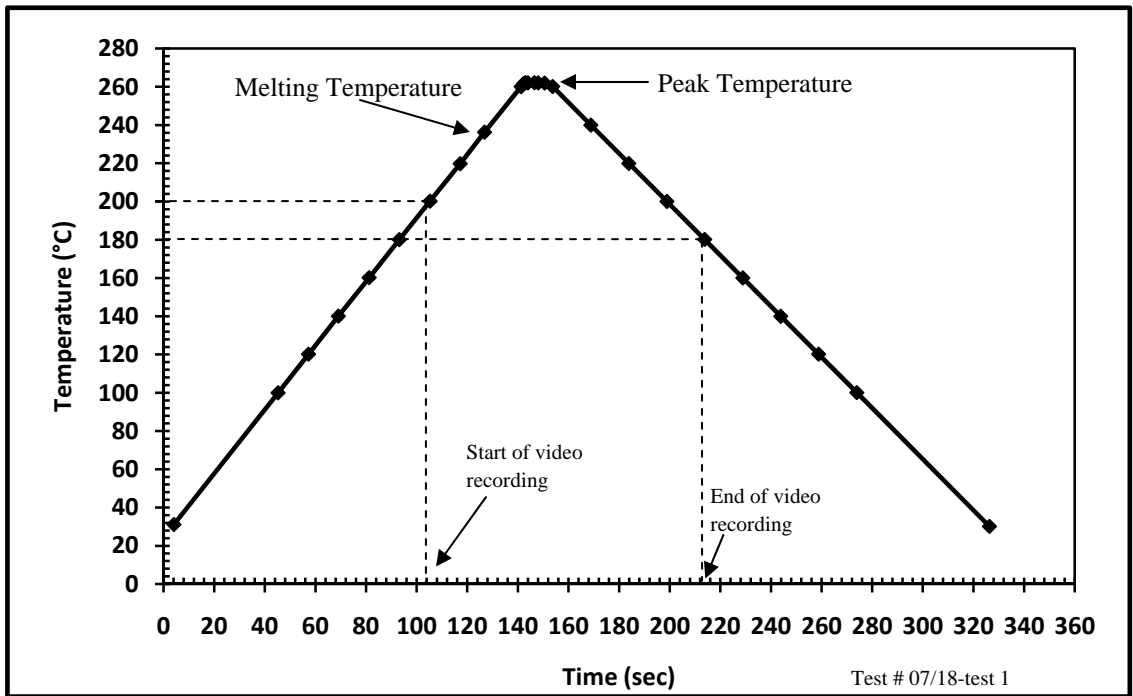


Fig. 6.7 Heating and cooling cycle, pure Sn over polished surface (vendor)

The images in figure 6.8 show the sequence of spreading of pure Sn over the polished surface received from a vendor. In this case, also no significant spreading of pure Sn was observed.

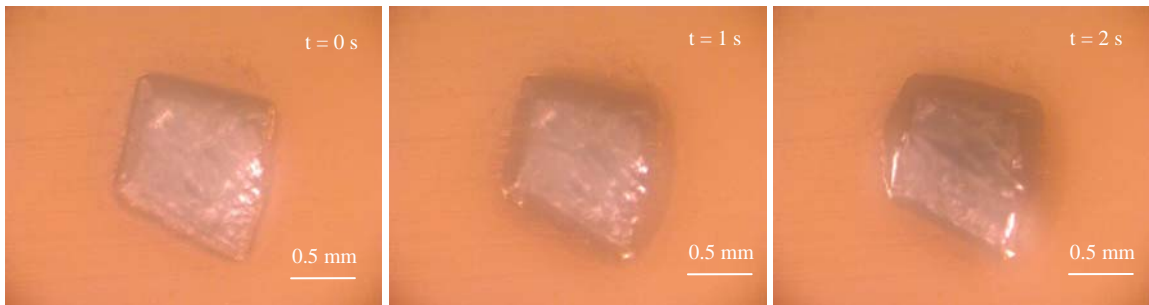


Fig. 6.8 Extracted images representing the sequence of spreading of pure Sn on polished surface (vendor)

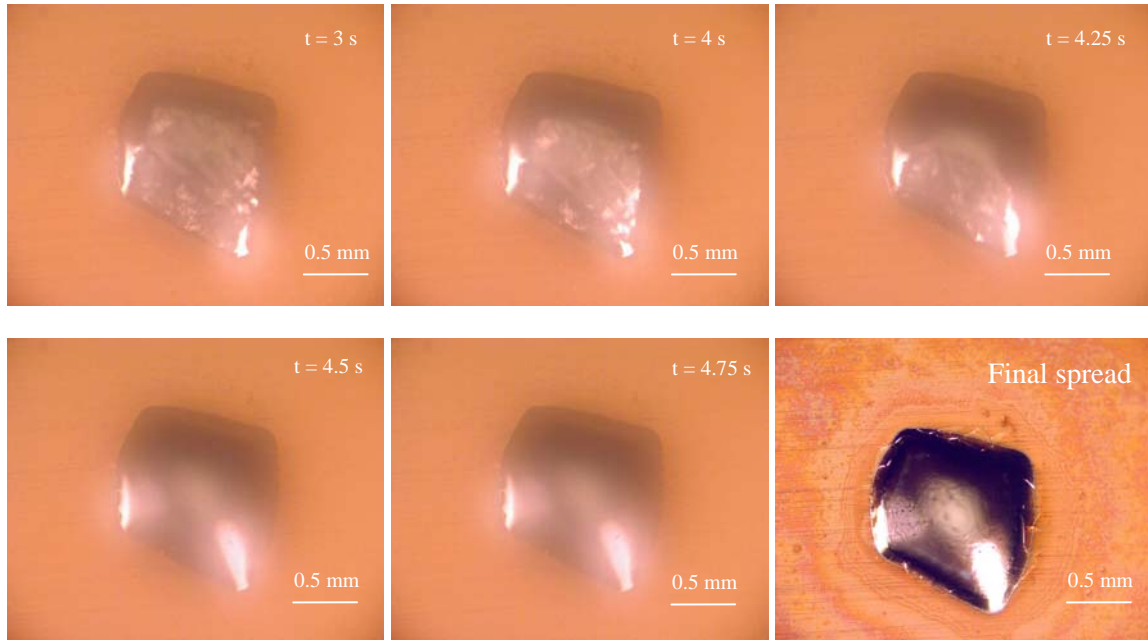


Fig. 6.8 Extracted images representing the sequence of spreading of pure *Sn* on polished surface (vendo) (contined)

Analysis:

Figure 6.9 gives a schematic representation of solder spreading in this experiment. It illustrates the spreading of pure *Sn* at three different stages as explained in the previous experiment's analysis section. Also, this sequence gives a good notion of a lack spreading of pure *Sn* over polished copper substrate.

Digital images extracted from the movies were analyzed to understand the spreading kinetics of molten *Sn* over the polished surface. Figure 6.10 provides the plot of A/A_0 versus time. Initially, spreading takes place for a very short duration of time. This was the period when pure *Sn* melts and starts to spread. After this stage no significant spreading occurs with the advancement of time. Area of spread is almost constant throughout this period.

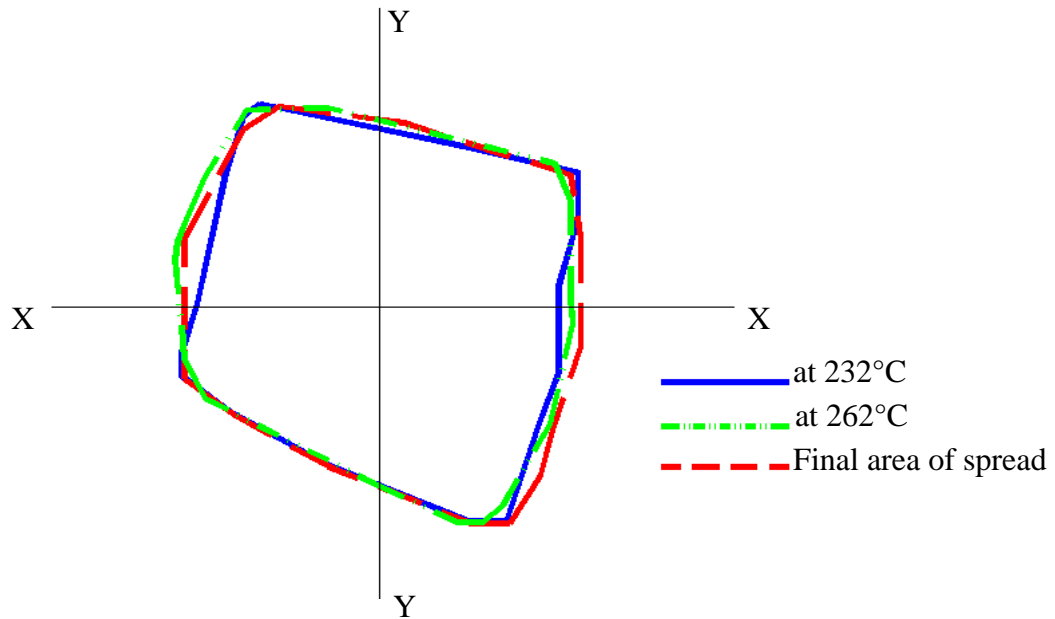


Fig. 6.9 Schematic representation of pure *Sn* spreading on a polished surface (vendedor)

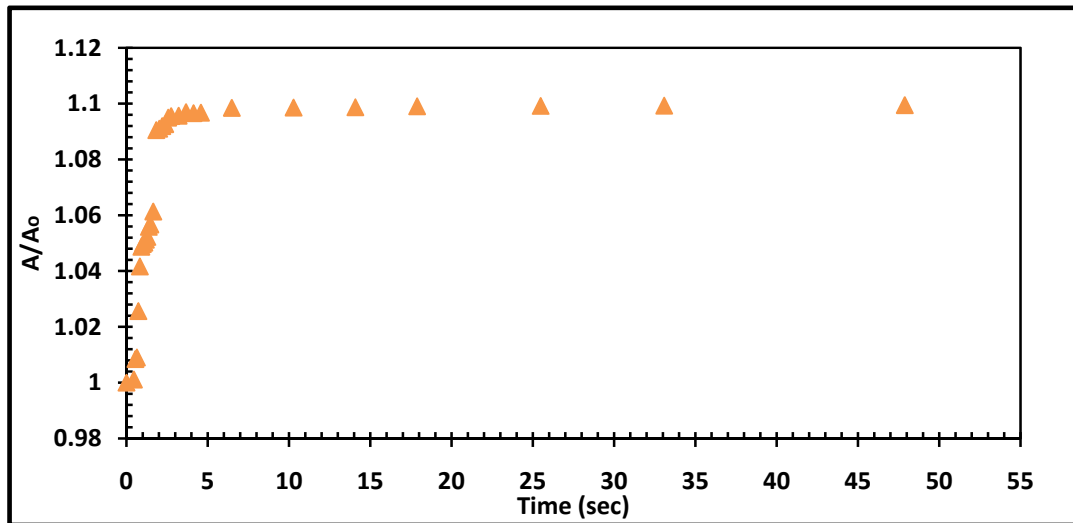


Fig. 6.10 A/A_0 Vs time (sec), pure *Sn* spreading on a polished surface (vendedor)

6.3 Pure Sn spreading over unpolished Cu surface

Sample description:

Figure 6.11, shows the sample used in this experiment, positioned on the substrate and covered with flux.

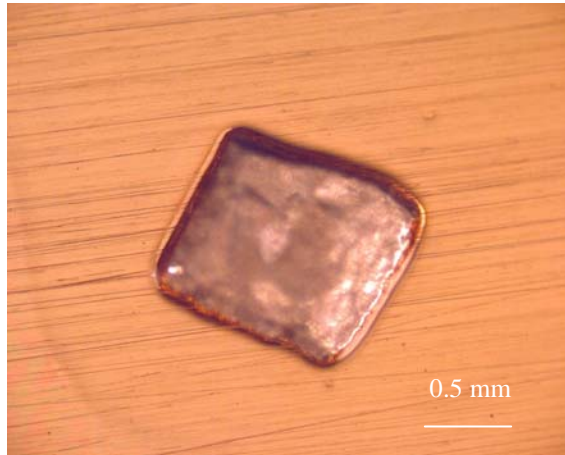


Fig. 6.11 Pure Sn over unpolished Surface

Solder alloy: Pure Sn Dimension: 0.5 mm x 0.5mm x 0.05 mm (approximately)

Substrate: Copper Dimension: 10 mm x 10 mm x 0.5 mm (approximately)

Surface: Unpolished Surface

Duration of ultra pure N_2 flow: 120 mins

Observations:

The sample placed in the hot-stage chamber was heated at the rate of $100^\circ\text{C}/\text{min}$ up to the peak temperature. Solder melts around 236°C . Temperature of hot-stage was maintained at peak temperature, 262°C , for a duration of 10 sec. It was then cooled to the room temperature at the rate of $80^\circ\text{C}/\text{min}$. Movie recording during the experiment was initiated when the temperature reached 170°C during heating cycle and stopped at around same temperature in cooling cycle. Figure 6.12 shows the rate of temperature rise and fall during heating and cooling segments of the cycle respectively.

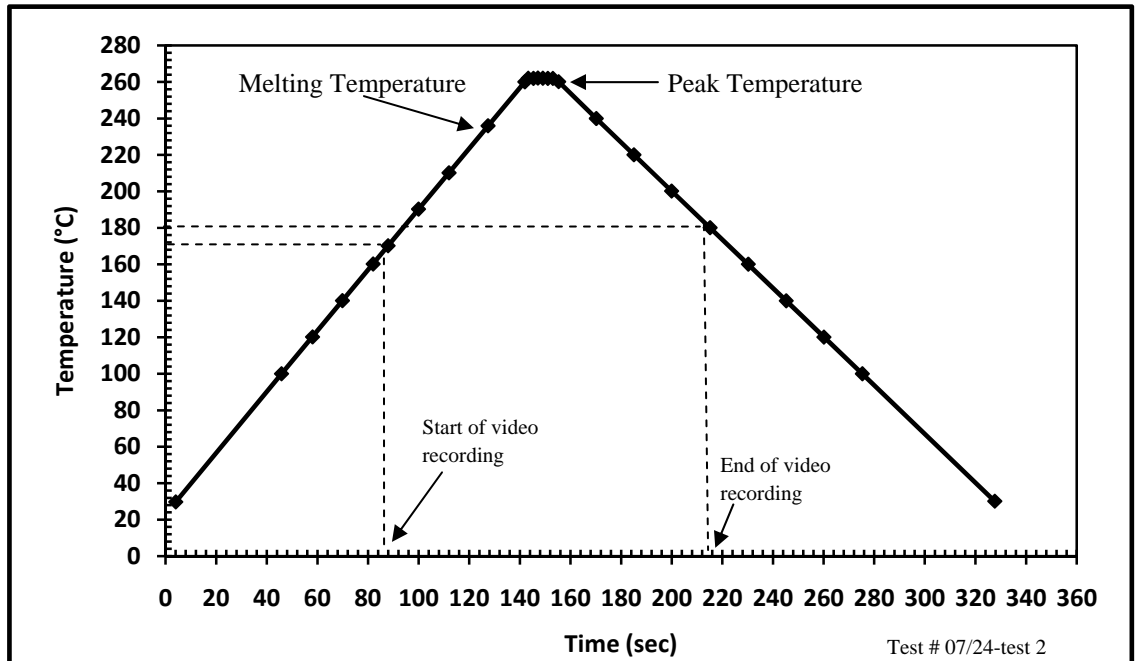


Fig. 6.12 Heating and cooling cycle, pure *Sn* over an unpolished surface

Figure 6.13 presents a series of photos, extracted from the movie, representing a sequence of spreading of pure *Sn* over the unpolished surface of a copper substrate. The images show similarity to those obtained in two previous experiments where no significant spreading took place.

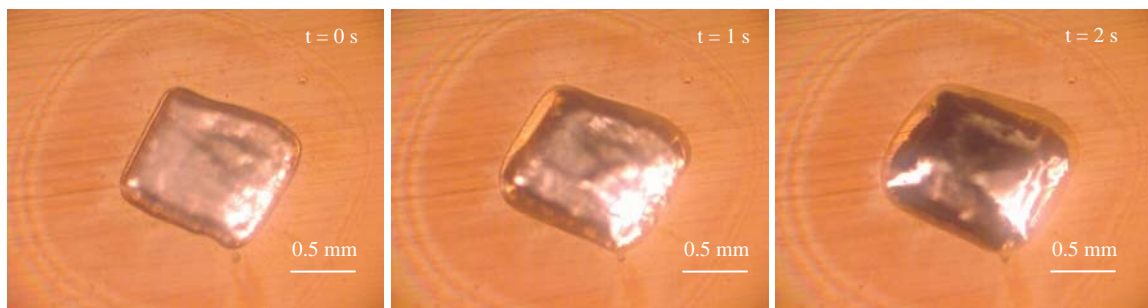


Fig. 6.13 Extracted images representing the sequence of spreading of pure *Sn* on an unpolished surface

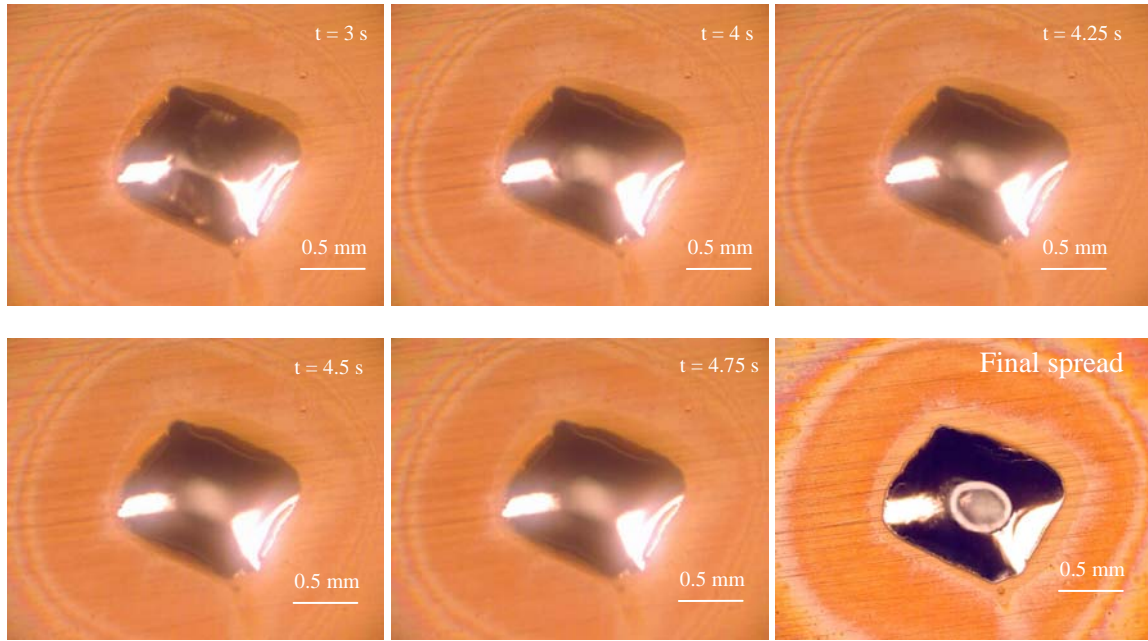


Fig. 6.13 Extracted images representing the sequence of spreading of pure *Sn* on an unpolished surface (continued)

Analysis:

Figure 6.14 provides a schematic representation of spreading of pure *Sn* on an unpolished surface. Similar to previous experiments discussed, figure 6.14 indicates a lack of spreading of pure *Sn* on the surface. Spreading area at different stages appears almost same. Figure 6.15 gives the plot of A/A_0 versus time.

It is observed that pure *Sn* spreads only during the time when it melts. The spreading rate during that period is almost linear, indicating fast spreading. Thereafter spreading area becomes constant as time progresses, suggesting no significant spreading during that stage.

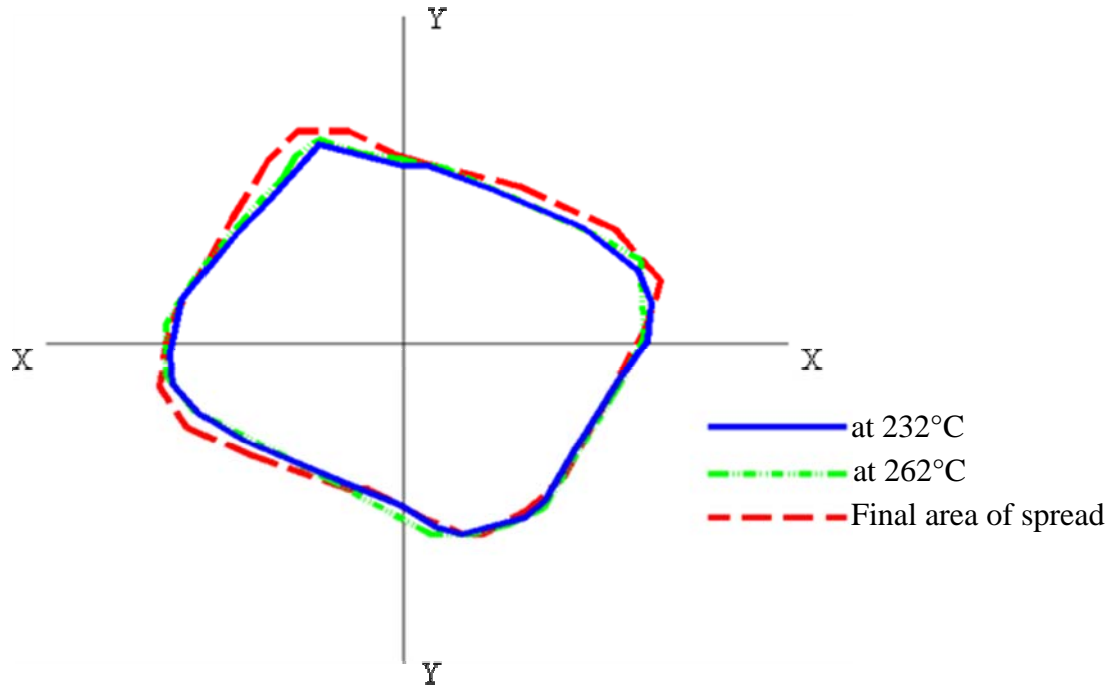


Fig. 6.14 Schematic representation of pure *Sn* spreading on an unpolished surface

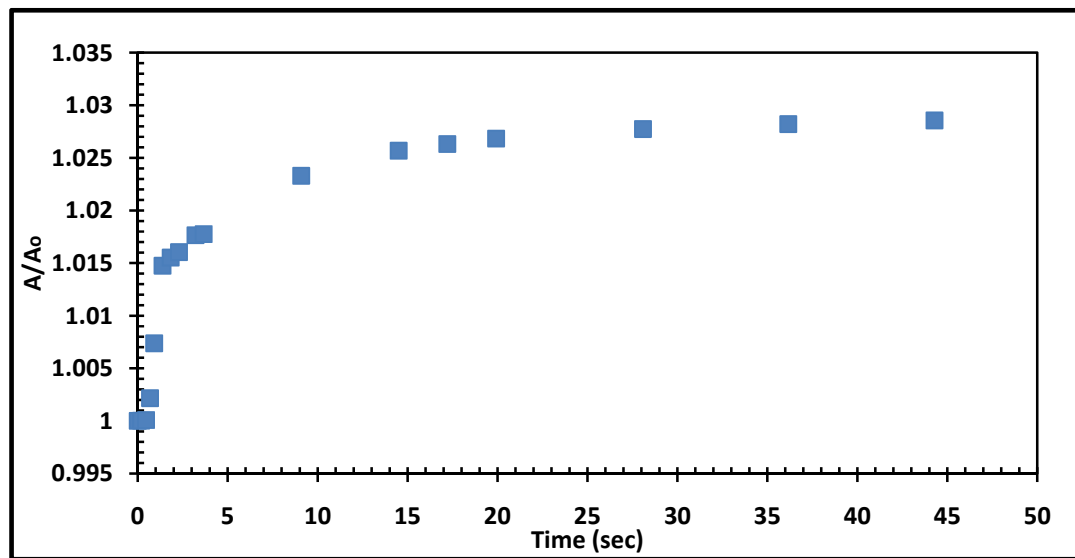


Fig. 6.15 A/A_0 Vs time (sec), pure *Sn* spreading on an unpolished surface

6.4 Eutectic *Sn-Cu* solder alloy spreading over a highly polished *Cu* surface (Met. Lab)

Sample description:

Figure 6.16 shows the sample used in this experiment, positioned on substrate and covered with flux.

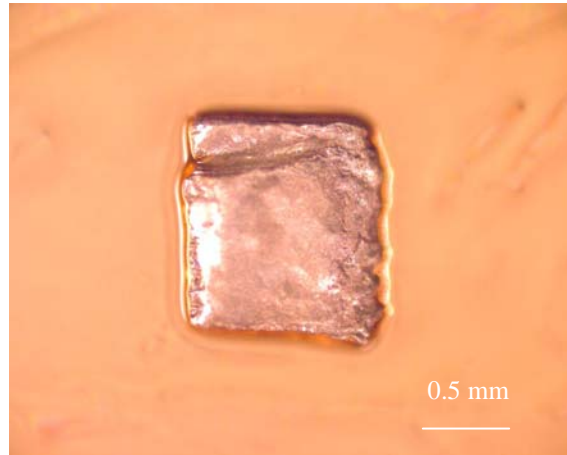


Fig. 6.16 Eutectic *Sn-Cu* solder alloy over a highly polished surface (Met. Lab)

Solder alloy: Eutectic *Sn-Cu* Dimension: 0.5 mm x 0.5mm x 0.05 mm (approximately)

Substrate: Copper Dimension: 10 mm x 10 mm x 0.5 mm (approximately)

Surface: Highly polished Surface (Met. Lab)

Duration of ultra pure N_2 flow: 120 mins

Observations:

The sample placed in hot-stage chamber was heated at the rate of 100°C/min. Solder melts around 230°C, which is higher than actual melting temperature i.e. 227°C. Temperature of hot-stage was maintained at peak temperature of 257°C for a duration of 10 sec. It was then cooled to room temperature at the rate of 80°C/min. Movie recording during the experiment starts when temperature was around 201°C during heating cycle and stopped at around 190°C in cooling cycle. Figure 6.17 shows the rate of temperature rise and fall during heating and cooling cycle respectively.

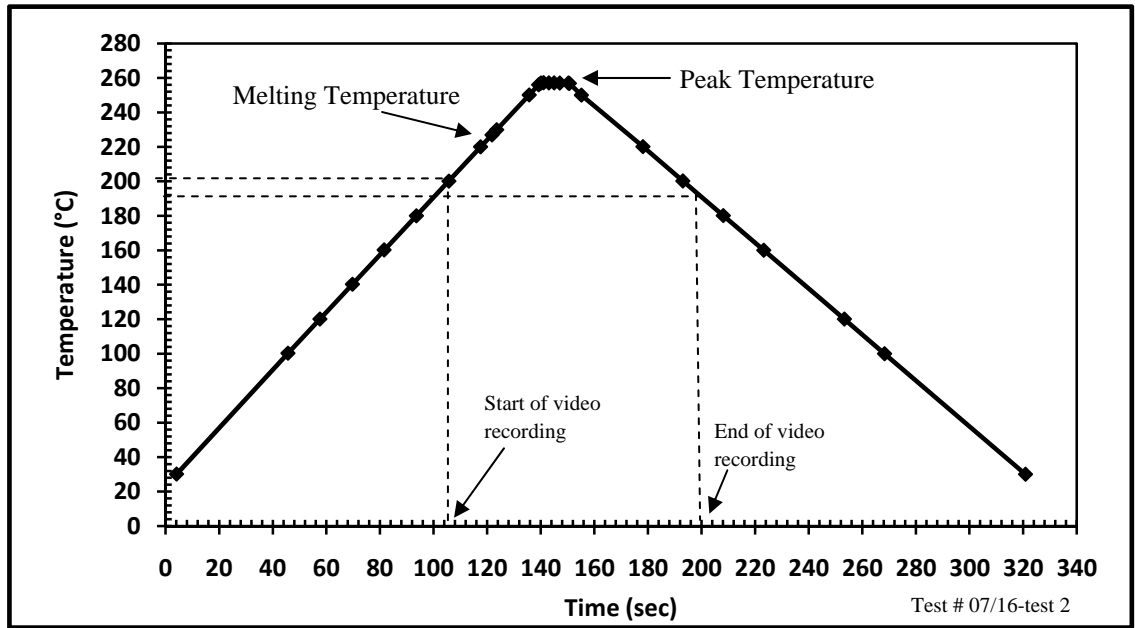


Fig. 6.17 Heating and cooling cycle, eutectic *Sn-Cu* solder alloy over a highly polished surface (Met. lab)

Figure 6.18 presents a series of photos, extracted from the movie, representing a sequence of spreading of the eutectic *Sn-Cu* alloy over the highly polished surface. Very little change in the shape of the solder alloy was noticed during the experiment. This suggests lack of spreading in this case. Spreading behavior of eutectic *Sn-Cu* solder alloy appears very similar to the spreading of pure *Sn* on a copper substrate.



Fig. 6.18 Extracted images representing the sequence of spreading of eutectic *Sn-Cu* solder alloy on a highly polished surface (Met. lab)

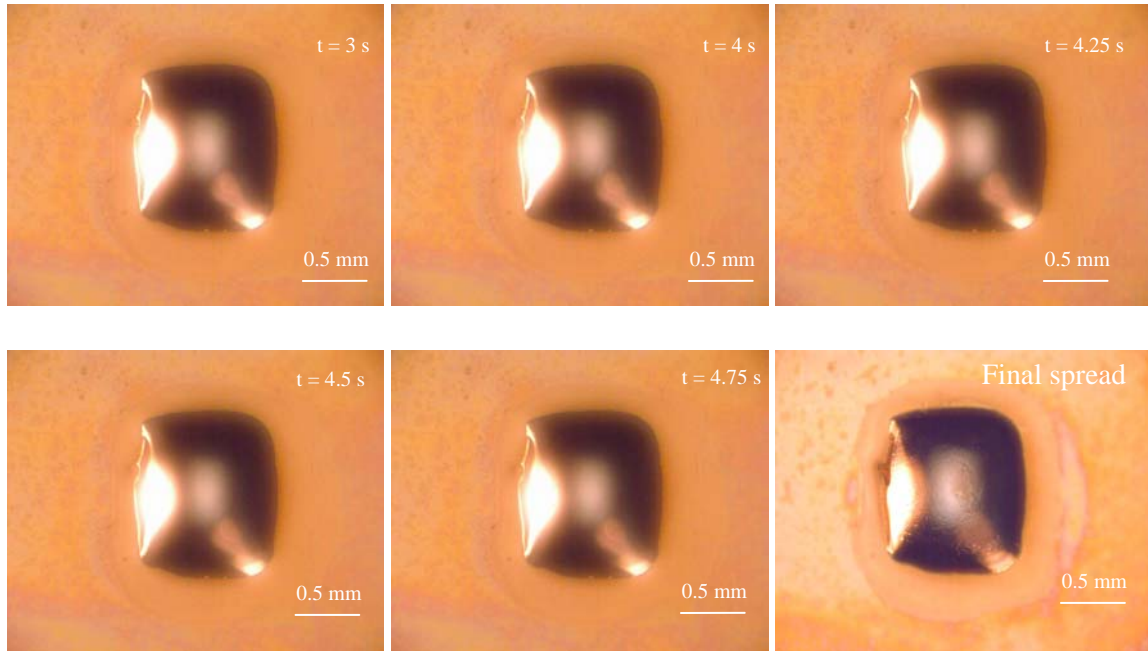


Fig. 6.18 Extracted images representing the sequence of spreading of eutectic *Sn-Cu* solder alloy on highly polished surface (Met. lab) (continued)

Analysis:

Figure 6.19 gives schematic representation of spreading of the eutectic *Sn-Cu* solder alloy on the polished *Cu* substrate. It maps the spreading of solder at three stages, as discussed earlier in this chapter, a) at the melting temperature, i.e 227°C, b) at peak temperature of 257°C and at the end of the test. Figure 6.19, shows that the area of spread in the three stages is almost similar, indicating lack of spreading of the eutectic *Sn-Cu* alloy on the *Cu* substrate.

Images extracted from the movie were analyzed to understand the kinetics of spreading. Figure 6.20, A/A_o versus time, gives the kinetics of spreading in this test. It is observed that the pattern of spreading was similar to previous tests done on Pure *Sn* spreading on *Cu* substrates. Sizeable spreading was observed only at the initial stage when solder melts and starts to spread for a very short duration of time. After that initial stage area of spread appears to be almost constant, indicating no major spreading after this initial period.

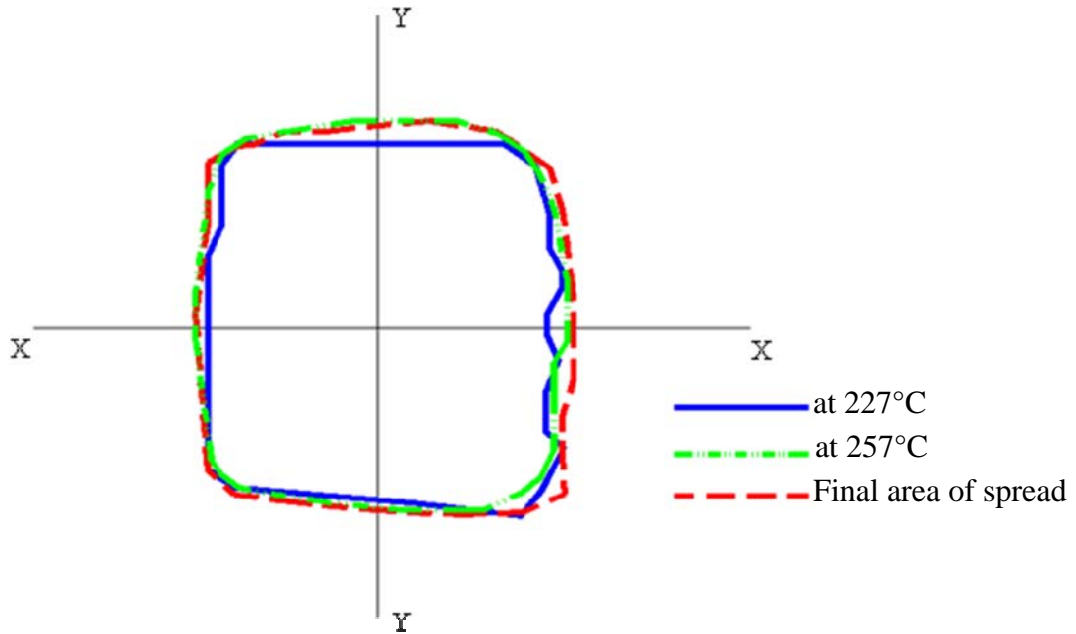


Fig. 6.19 Schematic representation of eutectic *Sn-Cu* solder alloy spreading on a highly polished surface (Met. lab)

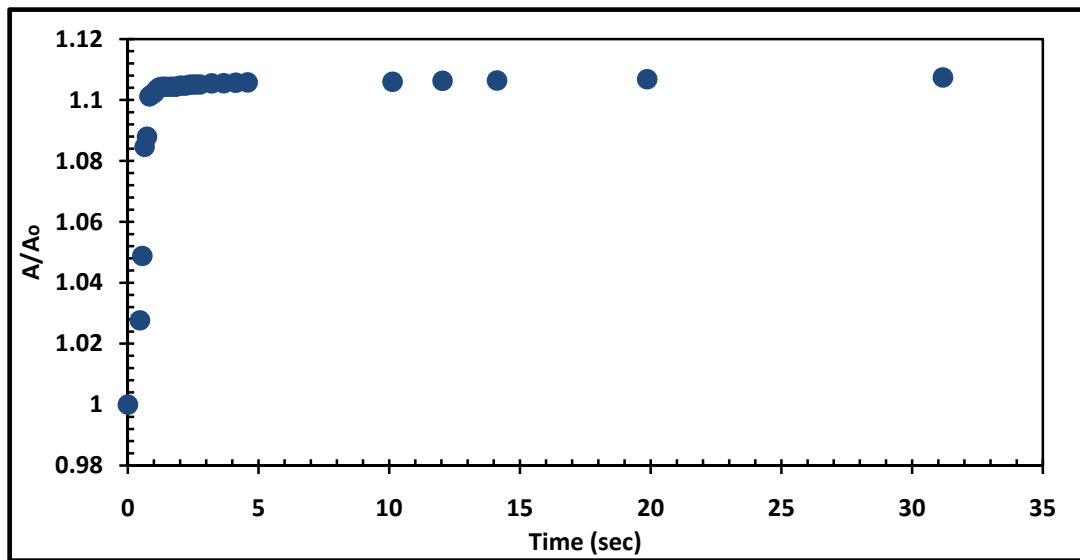


Fig. 6.20 A/A_0 Vs time (sec), eutectic *Sn-Cu* solder alloy spreading on a highly polished surface (Met. lab)

6.5 Eutectic *Sn-Cu* solder alloy spreading over a polished *Cu* surface (vendor)

Sample description:

Figure 6.21 shows the sample used in this experiment, positioned on the substrate and covered with flux.

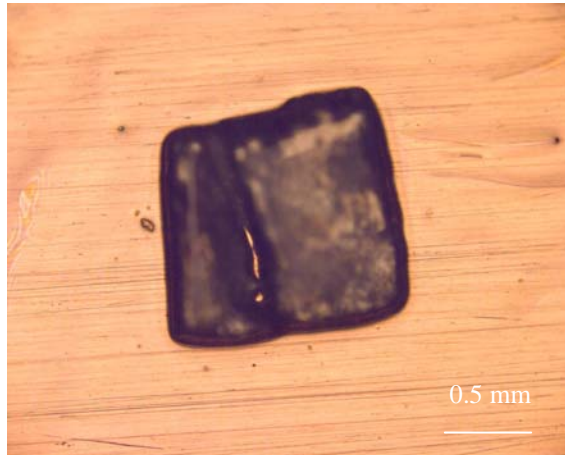


Fig. 6.21 Eutectic *Sn-Cu* solder alloy over polished Surface (vendor)

Solder alloy: Eutectic *Sn-Cu* Dimension: 0.5 mm x 0.5mm x 0.05 mm (approximately)

Substrate: Copper Dimension: 10 mm x 10 mm x 0.5 mm (approximately)

Surface: Polished Surface (Met. Lab)

Duration of ultra pure N_2 flow: 120 mins

Observations:

The sample placed in the hot-stage chamber was heated at the rate of 100°C/min up to the peak temperature. Solder melts around 230°C. Temperature of the hot-stage was maintained at peak temperature, 257°C, for a duration of 10 sec. It was then cooled to the room temperature at the rate of 80°C/min. Movie recording during the experiment starts when temperature was around 225°C during the heating segment of the cycle and terminated at around 180°C in the cooling segment of the cycle. Figure 6.22 shows the rate of temperature rise and fall during heating and cooling cycle respectively.

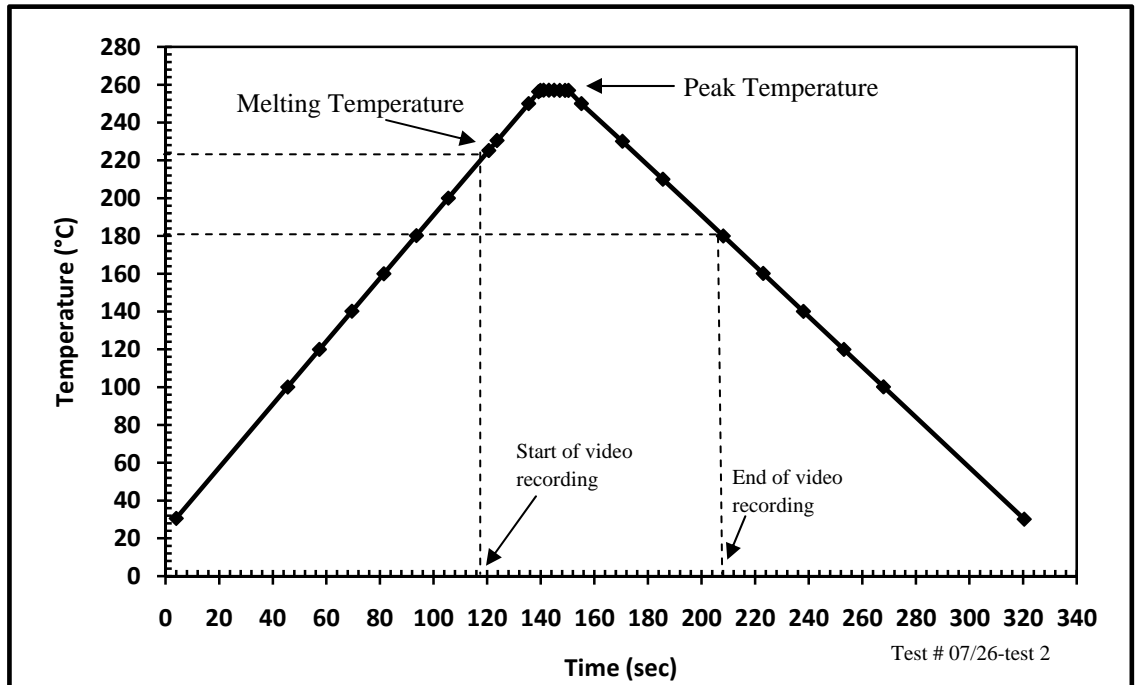


Fig. 6.22 Heating and cooling cycle, eutectic *Sn-Cu* solder alloy over a polished surface (vendor)

Figure 6.23 presents a series of photos, extracted from the movie, representing a sequence of spreading of the eutectic *Sn-Cu* alloy over the polished surface. Like in previous experiment, there was no major spread of solder over the substrate during the test.

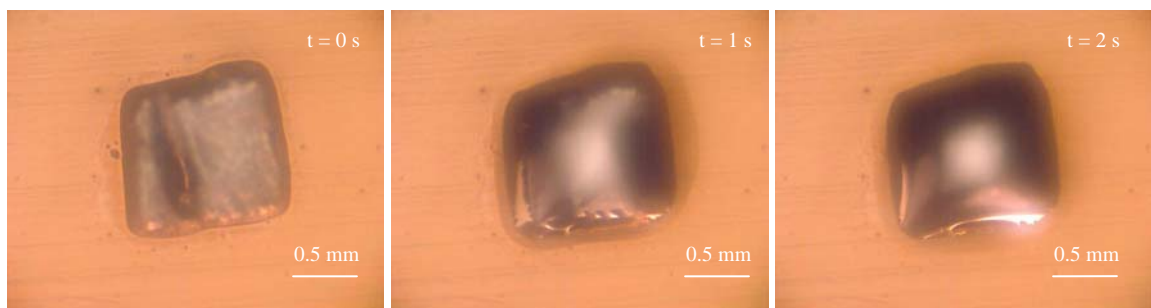


Fig. 6.23 Extracted images representing the sequence of spreading of eutectic *Sn-Cu* solder alloy on a polished surface (vendor)

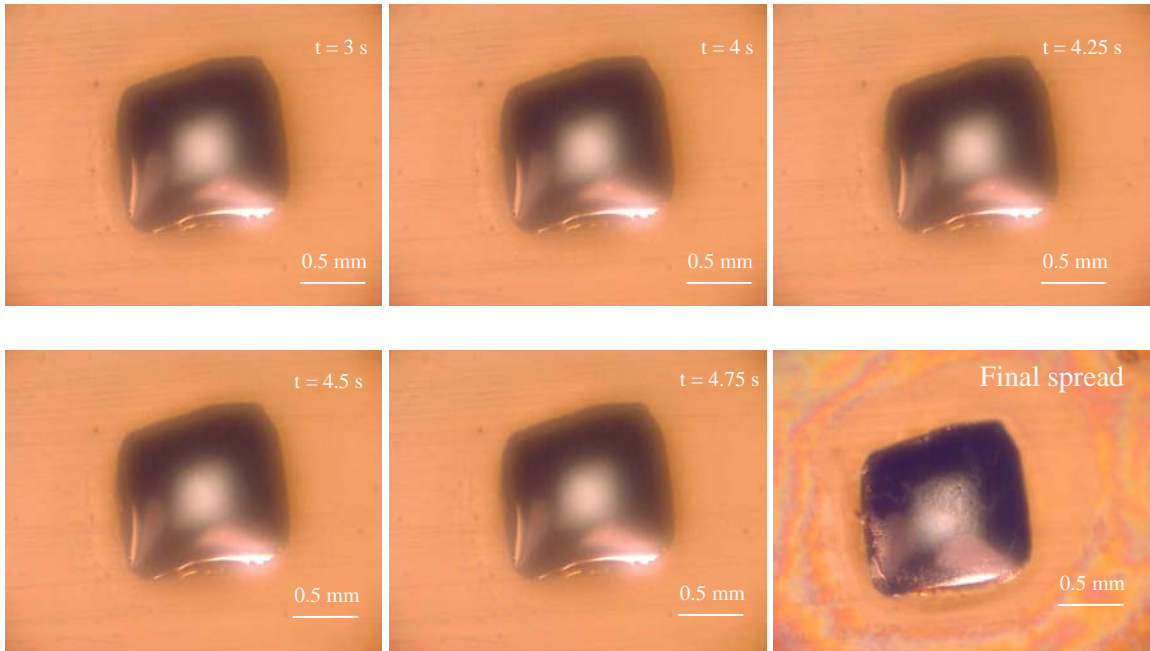


Fig. 6.23 Extracted images representing the sequence of spreading of eutectic *Sn-Cu* solder alloy on a polished surface (vender) (continued)

Analysis:

Figure 6.24 gives the schematic representation of spreading of the eutectic *Sn-Cu* solder alloy over the polished *Cu* substrate. Figure 6.24 shows that there was no major spreading of solder alloy during the test after melting. Figure 6.25 gives A/A_0 versus time plot. Digital images extracted from the movie were analyzed to obtain the set of data for plotting of A/A_0 versus time (Fig. 6.25).

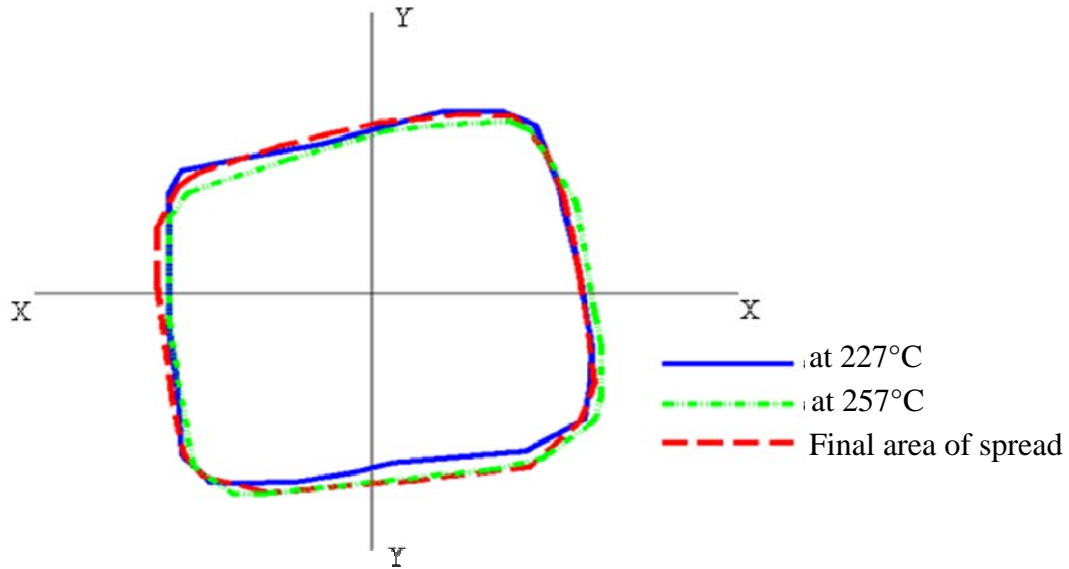


Fig. 6.24 Schematic representation of eutectic *Sn-Cu* solder alloy spreading on polished surface (vendor)

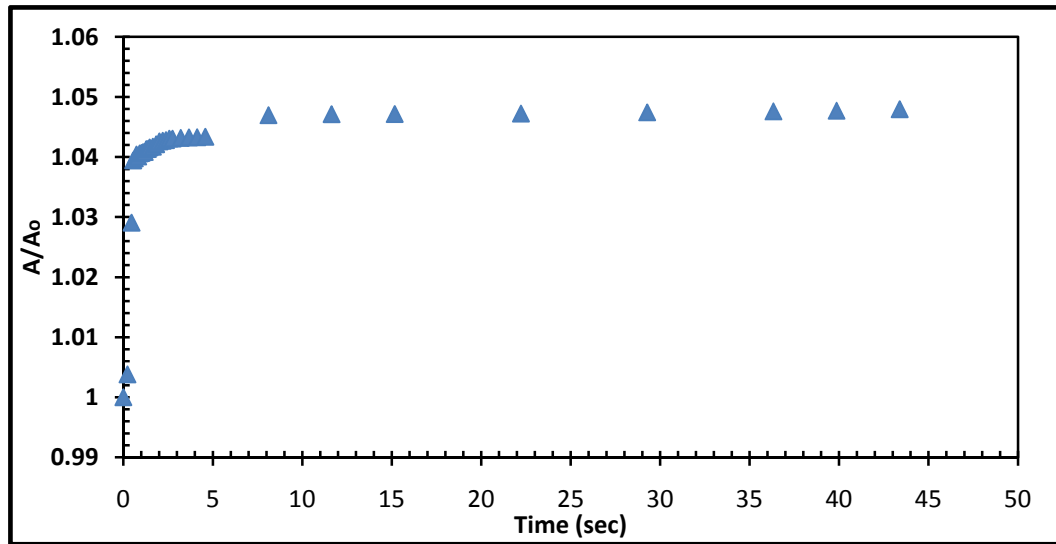


Fig. 6.25 A/A_0 Vs time (sec), eutectic *Sn-Cu* solder alloy spreading on polished surface (vendor)

Figure 6.25 shows spreading kinetics similar to the one observed in the previous experiment. Initial rapid increase in spreading area occurs when solder starts melting and spread for a very short duration of time. After the ultimate area of spread is reached no major spreading of solder is further registered.

Chapter 7 Summary of results and Discussion

7.1 Effect of the surface roughness of *Cu* substrates on the wetting behavior of eutectic *Sn-Pb* solder alloy

Figure 7.1 illustrates a comparison of the wetting behavior of the eutectic *Sn-Pb* solder alloy on a highly polished surface (Met. lab.), polished surface (vendor), and unpolished surface.

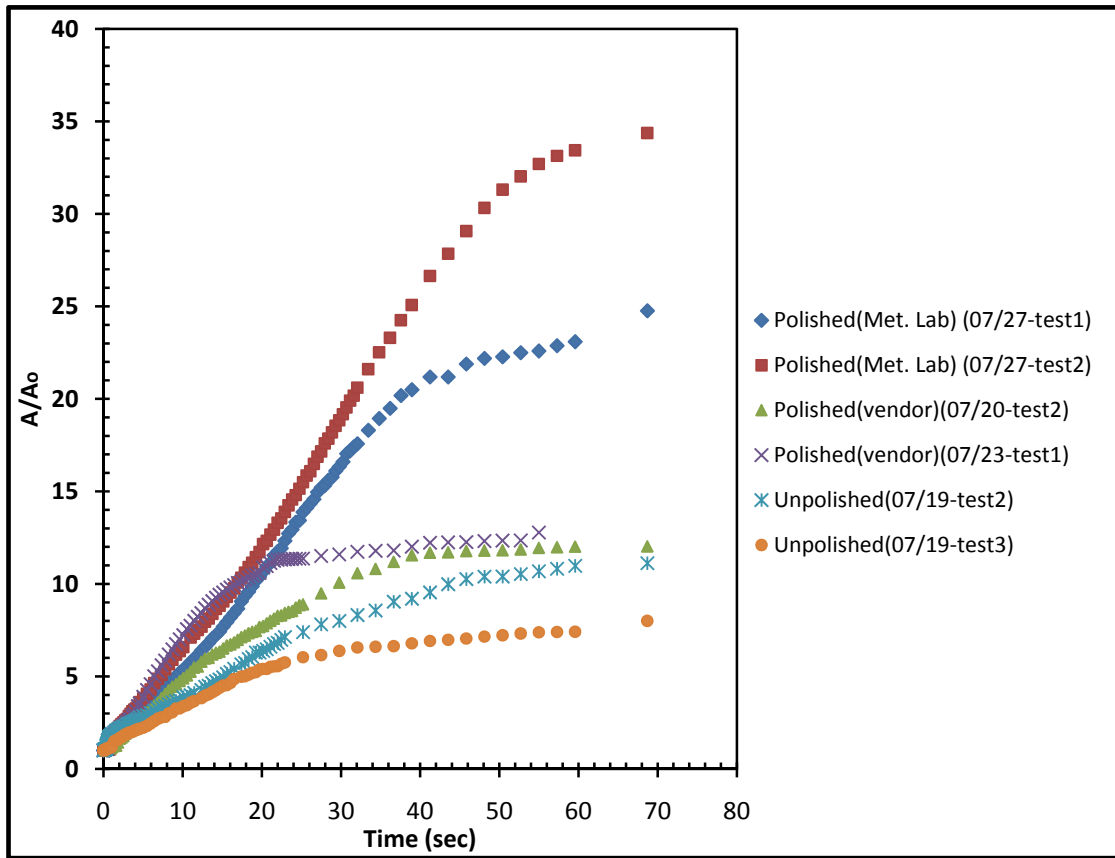


Fig. 7.1 Spreading behavior of eutectic *Sn-Pb* on *Cu* substrate with different surface roughnesses

A significant difference can be observed in the spreading behavior of the eutectic *Sn-Pb* solder over three different *Cu* substrates. The initial spreading appeared to be similar in all the three cases. However, as the time progresses the substrate with the least surface roughness showed a better spreading of the solder than the substrates with more rough surfaces.

Solder spreading on a highly polished surface (Met. lab) (the surface with the least roughness) shows most pronounced spreading with the final A/A_o value about four times higher than is the final A/A_o value of solder spreading on an unpolished surface. Figure 7.2 gives a comparison of the final A/A_o values of solder spreading on each of the three surfaces.

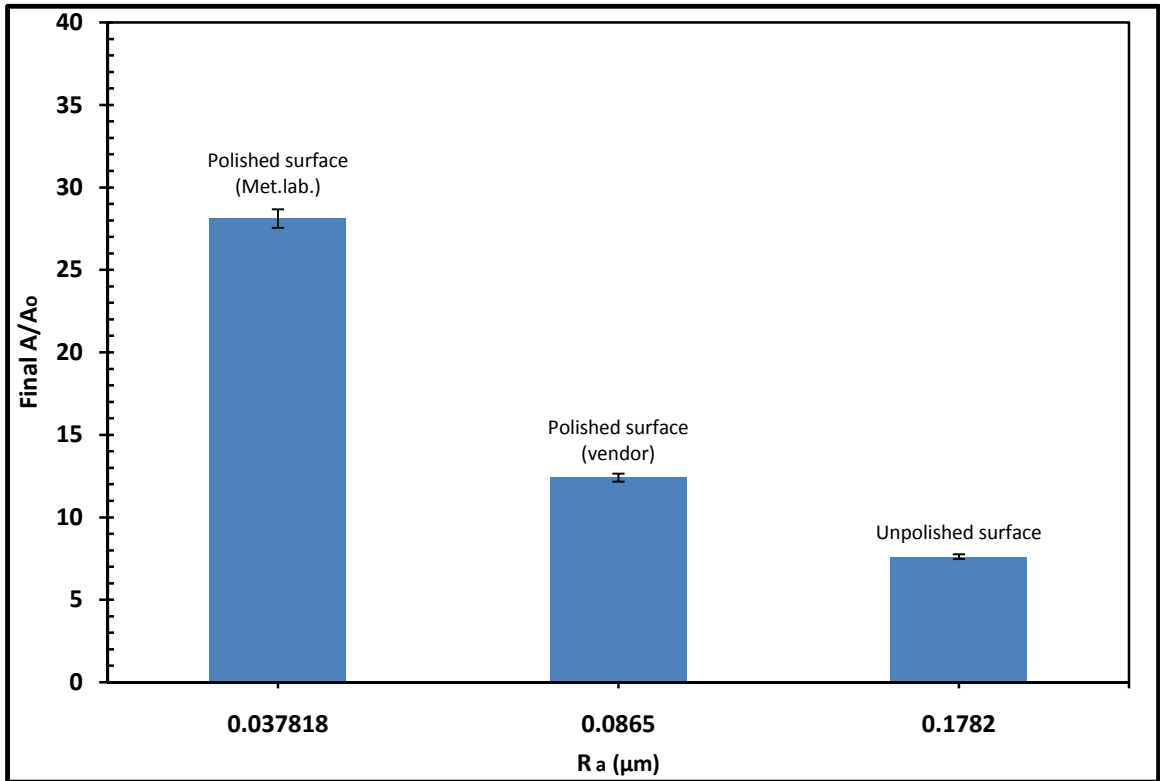


Fig. 7.2 Final A/A_o vs Average roughness (R_a)

The trends from figures 7.1 and 7.2 undoubtedly demonstrate that spreading of the eutectic *Sn-Pb* solder alloy improves with a decrease in surface roughness of the substrate. The results are in a disagreement with initial hypothesis discussed in chapter 2, but in a good accordance with the model proposed by Shuttleworth and Bailey [Shuttleworth et al., 1948], experimental studies of [Hitchcock et al., 1981] and [Chen et al., 2000]. According to all these studies, the asperities present in the rough surface acts as series of energy barriers as liquid drop spreads on the surface. The ability of the liquid drop to overcome those barriers and spread depends upon the relative size of the barriers.

In this study, as shown in figure 7.3, solder spreading on a highly polished surface (Met. lab.) advances in form of almost regular circular front, indicating quite uniform spreading as a consequence of the hypothesized absence of retarding influences present on more rough surface in the given range of roughness (and no large grooves). This suggests an absence of energy barriers on this surface which can obstruct the spread of solder. In case of solder spreading on polished surface (vendor) and unpolished surface, solder advances in the form of a more or less irregular front, indicating a non-uniform spreading (figure 7.3). This non-uniformity can be attributed to the presence of micro groove lines present in the surface.

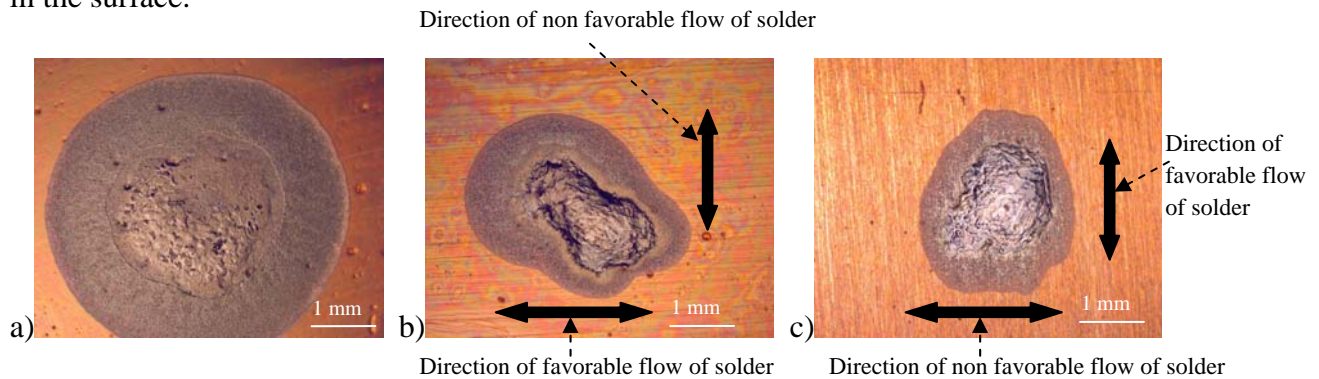


Fig. 7.3 Final area spread by eutectic *Sn-Pb* solder alloy on a) highly polished surface(Met. lab.) b) polished surface (vendor) c) unpolished surface.

The liquid front that must move along the direction perpendicular to the groove lines in case of polished surface (vendor) and unpolished surface should overcome more of the energy barriers of the valleys. Liquid front moving along the groove lines has low energy barriers. Thus, the liquid front moves well along the direction of groove lines when compared to moving in the direction perpendicular to them. As a result liquid front moves in form of an irregular shape. These lines are expected to cause improper spreading of solder on a polished surface(vendor) and an unpolished surface, when compared to spreading on a highly polished surface (Met. lab.).

7.2 Effect of surface roughness of *Cu* substrates on wetting behavior of the lead-free solder alloys

Figure 7.4 gives the summary of the wetting behavior of lead free solders, pure *Sn* and eutectic *Sn-Cu* alloy, on the *Cu* substrates used in the study.

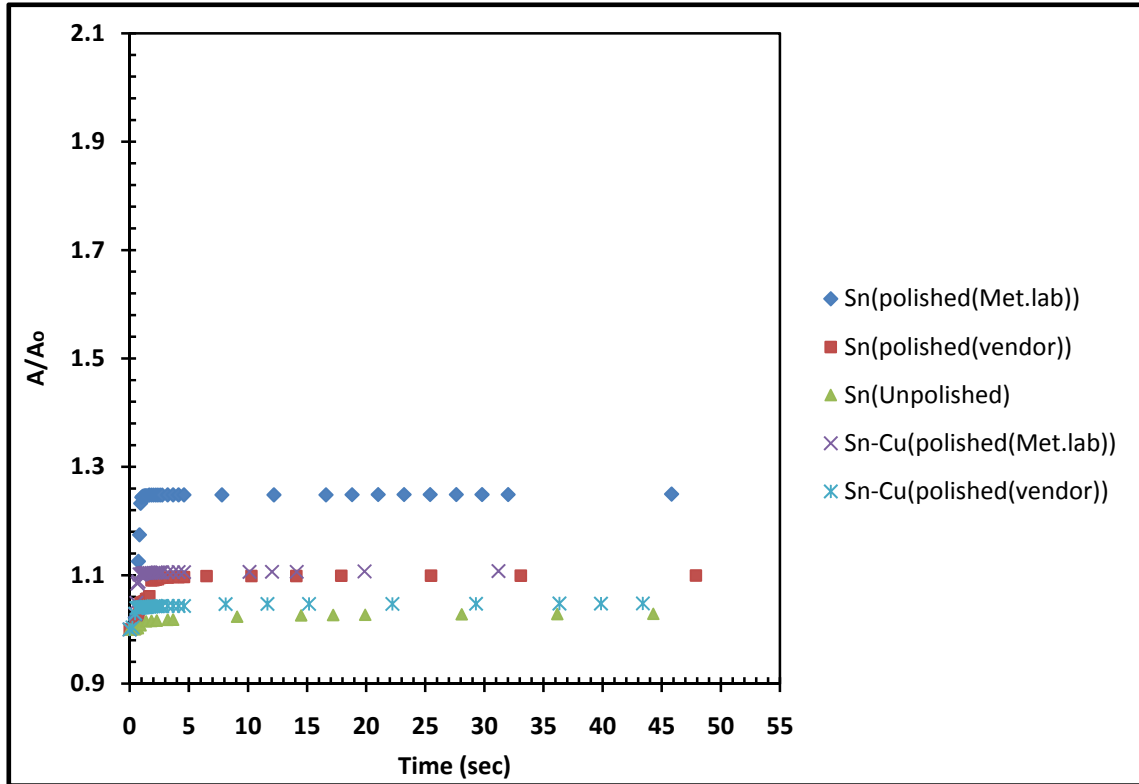


Fig. 7.4 Spreading behavior of pure *Sn* and eutectic *Sn-Cu* on *Cu* substrates with different surface roughness

From figures 7.4 and 7.1 one can notice a significant difference between the spreading kinetics of lead free solders vs. eutectic *Sn-Pb* solder alloys. It can be observed that no significant spreading takes place in case of lead free solders on *Cu* substrates, irrespective of varying surface roughness.

Pure *Sn* on highly polished surface (Met. lab) features a little larger final A/A_o value when compared to the one on a polished surface (vendor) and an unpolished surface. Figure 7.5 gives a comparison of the final A/A_o versus surface roughness of *Cu* substrates. Similar to pure *Sn*, the eutectic *Sn-Cu* also have relatively more spreading on highly polished surface (Met. lab) than on a polished surface (vendor) (see figure 7.5). However, more experiments are needed to conclude lead-free solders selected spread well on highly polished surface.

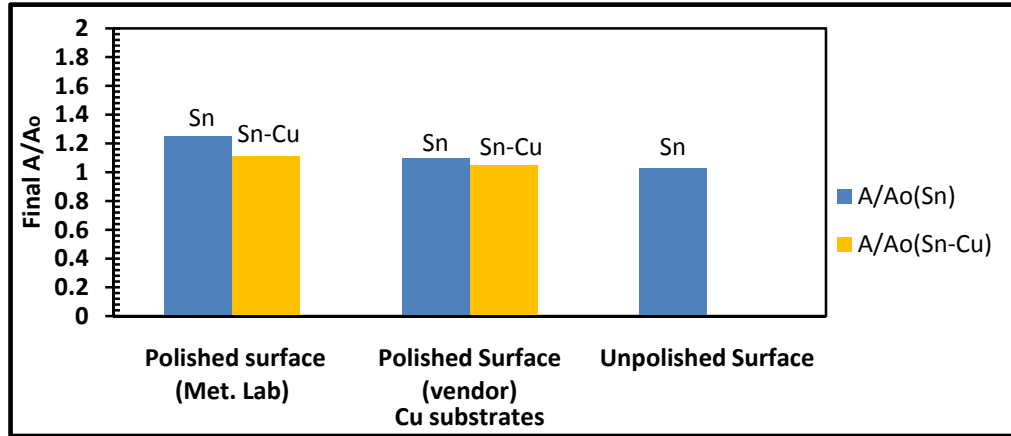


Fig. 7.5 Final A/A_o vs Cu substrates, Lead-free solders spreading on different Cu substrates

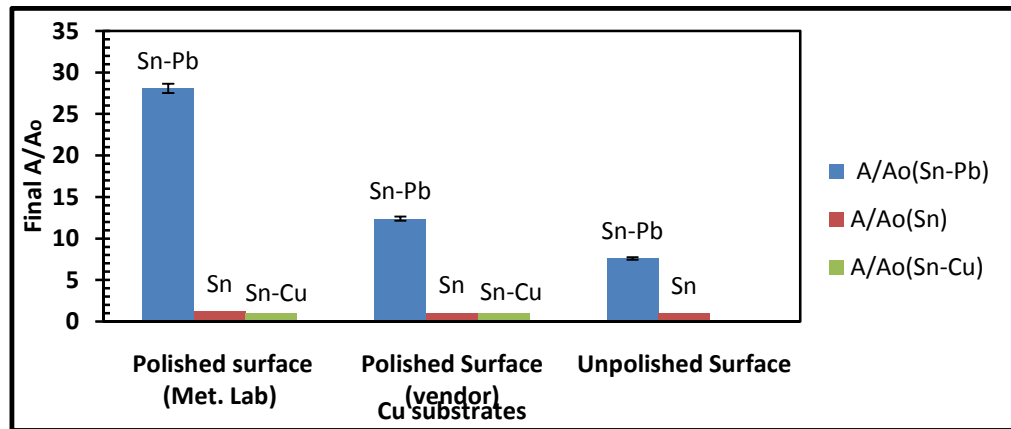


Fig. 7.6 Final A/A_o vs Cu substrates, Eutectic $Sn-Pb$ and Lead-free solders spreading on different Cu substrates

From figure 7.4 and 7.6, it can be noticed that there is no significant influence of surface roughness on the wetting characteristics of lead free solders. Final A/A_o values are almost constant with varying Cu substrate in case of lead free solders. That is not the case of lead solders (see figure 7.6). Therefore, an inference can be drawn that the surface roughness had no major effect on spreadability of lead free solders on Cu substrates for analyzed range of surface roughnesses.

Chapter 8 Conclusions and Future work

8.1 Summary and conclusions

The purpose of the present work was to observe and understand the influence of surface roughness of the *Cu* substrate on the wetting behavior of molten solder alloys. An important motivation behind this work was an expectation that an increase in surface roughness of the substrate would improve the wetting characteristics of solders. Eutectic *Sn-Pb*, eutectic *Sn-Cu* and pure tin solder alloys and three *Cu* substrates with different surface finish (highly polished surface, a less polished surface and unpolished surface) were considered in this study. Highly polished surface was prepared in Metallography laboratory of Center for Manufacturing, University of Kentucky while the other two substrates were obtained from a vendor. All the surfaces were characterized and measured using an optical profilometer. Profilometer results indicated that the highly polished surface was the smoothest and unpolished surface was the roughest among the three surfaces, as expected.

A number of hot-stage microscopy tests were conducted and data obtained to understand the kinetics of spreading of a solder on different substrates. Still digital images extracted from the movies of the spreading recordings during the hot-stage experiments were analyzed by using the Image-pro software. These data were used to generate the plots of the relative area of spread (A/A_o) versus time (where A was the area spread by solder at a given instance of time and A_o was the initial area of solder before spreading). These plots gave the trends of spreading behavior of solder alloys on *Cu* substrates with different surface roughnesses.

The following observations can be formulated

- 1.) Surface roughness of *Cu* substrates had a major influence on the spreading behavior of the eutectic *Sn-Pb* solder alloy.
- 2.) The eutectic *Sn-Pb* solder alloy spreads well over a very smooth surface (compared to rough surface).

- 3.) In case of the eutectic *Sn-Pb* solder spreading over surfaces in the range of roughness and directional pattern studied in this work, the results obtained were in disagreement with the initial hypothesis of this study, that the increase in roughness would assist spreading due to capillary effects.
- 4.) When compared to the eutectic *Sn-Pb* solder alloy lead-free solders, as expected, demonstrated no major spreading on the *Cu* substrates.
- 5.) Surface roughness of *Cu* substrate did not show any major influence on the spreading behavior of lead free solders (pure *Sn* and eutectic *Sn-Cu*).

Based on the above conclusions, final conclusions of this work are as follows:

- With decrease in surface roughness of *Cu* substrate, the spreadability of eutectic *Sn-Pb* solder alloy improves.
- Change in surface roughness of *Cu* substrate had no significant influence on the spreading behavior of lead free solders, pure *Sn* and eutectic *Sn-Cu*, used in this study.
- The initial hypothesis as discussed in Chapter 2, expected eutectic *Sn-Pb* solder alloy to spread well over the rough surface than compared to smooth surface. The hypothesis of this work was developed based on the studies done by [Yost et al., 1995] and [Nicholas et al., 1986]. According to these studies for very well wetting systems (such as eutectic *Sn-Pb* over *Cu* substrate) the spreading is better over the rough surface than compared to smooth surface. However, the results of this work over the limited range of surface roughnesses selected disprove the hypothesis. The eutectic *Sn-Pb* alloy was observed to spread well over the smooth surface than rough surface used in this work.

8.2 Future work

More extensive work needs to be done in order to understand and generalize the influence of surface roughness of *Cu* substrate on the wetting behavior of molten solders. Future works can involve:

- More hot-stage microscopy tests involving *Cu* substrates with extremely rough surfaces to understand the influence of open channel grooves.
- More hot-stage tests involving different lead free solders including ternary system alloys such as the *Sn-Ag-Cu* solder alloy (*93.6Sn-4.7Ag-1.7Cu*), and understanding the kinetics of spreading on *Cu* substrates.
- A study on kinetics of solder spreading along the grooves present in the rough surface, and how they influence the advancing front of a spreading solder alloy.

References

- Abtew, M., and Selvaduary, G., 2000, "Lead Free Solders in Microelectronics", *Material Sciences and Engineering, Vol 27*, pp 49 – 81
- Allenby, B.R. , Ciccarelli, J. P., Artaki, I., Fisher, J. R., Schoenthaler, D., Carroll, T. A., Dahringer, D. W., Degani, Y., Freund, R. S., Graedel, T. E., Lyons, A. M., Plewes, J. T. , Gherman, C., Solomon, H., Melton, C., Munie, G. C., and Socolowski, N., 1992, "An assessment of the use of lead in electronic assembly", *Surface Mount International Conference and Exposition. Proceedings of the Technical Program, 30 Aug.-3 Sept. 1992.*, pp. 1-28
- Cox, N and Schedtler, R., 2000, "Solder Reflow Technology Handbook", *Research International, Online, www.researchintl.com*, (visited during august 2007)
- Chen, Y., and Duh, J., 2000, "The effect of substrate surface roughness on the wettability of Sn-Bi solders", *Journal of Material Sciences: Materials in Electronics, Vol 11*, pp 279-283
- Cazabat, A. M., and Cohen Stuart, M. A., 1987, "Some experiments on wetting dynamics", *PCH Physico Chemical Hydrodynamics, Vol. 9*, pp 23-31
- Charles, H. K., 2003, "Electronics and the environment", *Electronic components and technology conference, IEEE*, pp 1705-1713
- Smith, E. B., 2004, "Health and environmental effects of lead and other commonly used elements in microelectronics", *Handbook of Lead-free Solder technology for Microelectronics assemblies, edited by Puttlitz, Karl J. and Stalter, Kathleen A.*, pp 49- 81
- EPA, 2007, "Electronics waste management in the United States", *a report, Final draft, U.S. Environmental Protection Agency(EPA), April 2007.*
- Evans, J. W., Kwon, D., and Evans, J. Y., 2007, "Chapter 3: Wetting and Joint Formation" *A guide to lead-free solders – Physical metallurgy and Reliability, Edited by Engelmaier, Werner, Published by Springer London.*

- Eustathopoulos, N., and Nicholas, M. G., 1999, *Wettability at High temperatures*, Published by Pergamon.
- Glasby, G. P., 2002, "Sustainable Development: need for new paradigm", *Environment, development and sustainability*, Vol. 4, pp 333-345
- Hupston, G., and Jacobson, D. M., 2004, *Principles of Soldering*, ASM International, Materials Park
- Huh, C., and Mason, S. G., 1977, "Effect of Surface Roughness on wetting (Theoretical)", *Journal of Colloid and Interface Science*, Vol. 60, pp 11-35
- Hitchcock, S. J., Carroll, N. T., and Nicholas, M. G., 1981, "Some effects of substrate roughness on wettability", *Journal of Material Sciences*, Vol 16, pp 714-732
- JCAA/JG-PP, 2006, "Lead-free solder project", *joint report, Joint council on Aging Aircraft(JCAA)/Joint group on pollution prevention(JG-PP)*.
- Lee, N.C., 1999, "Getting ready for Lead-free solders", *Soldering and Surface mount technology*, Vol9, pp 65-69
- Lee, N.C., 1999, "Lead-Free Soldering –Where the World is Going," *Advancing Microelectronics*, September/October, pp. 29-36.
- Landry, K., Rado, C., Voitovitch, R., and Eustathopoulos, N., 1997, "Mechanish of reactive wetting: question of triple line configuration", *Acta Metallurgica*, Vol. 45, pp 3079-3085
- Manko, H. H., 1979, *Solder and Soldering*, 2nd Edition, McGraw-Hill, New York.
- Miric, A. Z. and Grusd, A., 1998, "Lead-free solders", *Soldering and Surface mount technology*, Vol.10, pp 18-25
- Moser, Z., Gasior, W., and Debski, A., 2005, "Data base of Pb - free soldering materials, surface tension and density, experiment vs. modeling", *Data science journal*, Vol. 4, pp 195-208

- Napp, D., 1995, "Lead Free interconnect materials for Electronic Industry", 27th *International SAMP Technical conference, October 9-12, pp 238-244*
- Nicholas, M. G., and Crispin, R. M., 1986," Some effects of anisotropic roughening on the wetting of metal surfaces", *Journal of Material Sciences, Vol. 21, pp 522-528*
- Naryanaswamy, R., 2006, Thesis Dissertation, *College of Engineering, University of Kentucky.*
- Plasantzas, G., and Hosson, J. T. M. D., 2001," Wetting on rough surfaces", *Acta Materialia, Vol. 49, pp 3533-3538*
- Puttliz, K. J., 2004, "Sn-Ag and Sn-Ag-X Solders and properties", *Handbook of Lead-free Solder technology for Microelectronics assemblies, edited by Puttliz, Karl J. and Stalter, Kathleen A., pp 239-279*
- RoHS directives, 2003, "Directive 2002/95/EC of European Parliament and of the Council of 27 January 2003 on the restriction of the use of certain hazardous substances in electrical and electronic equipment", *Official Journal of European Union, February.*
- Shuttleworth, R., and Bailey, G. L., 1948, "The spreading of liquid over rough solid", *Discussion Faraday Society, Vol. 3, pp 16-22*
- Suganuma K., 2001, "Advances in Lead Soldering in Electronics", *Current Opinion in Solid States and Material Sciences, Vol. 5, pp 55-64*
- Sattiraju, S. V., Dang, B., Johnson, W. R., Li, Y., Smith, J. S., and Bozak, M. J., 2002, "Wetting characteristics of Pb-free solder alloys and PWB finishes", *IEEE Transactions on electronics packaging manufacturing, Vol. 25, pp 168-184*
- Stevenson, J. O., Roberts, J. L., Davidson, R. N., Yost, F.G., and Hosking, F. M., 1997, "The effect of lead content and surface roughness on wetting and spreading of low-lead and no-lead solders on copper-clad FR-4 laminates", *Advances in electronic packaging, ASME, Vol. 2, pp 1335-1345.*

- Singler, T. J., Meschter, S. J., and Spalik, J., 2004, "Solder wetting and spreading", *Handbook of Lead-free Solder technology for Microelectronics assemblies*, edited by Puttlitz, Karl J. and Stalter, Kathleen A., pp 331-430
- Shankara, J., 2005, Thesis Dissertation, *College of Engineering, University of Kentucky*.
- Vianco, T. P., 1993, "Development of alternatives to lead-bearing solders", in: *Proceedings of the Technical Program on Surface Mount International, 19 August - 2 September, San Jose, CA*
- Wang, H., Wang, F., Gao, F., Ma, X., and Qian, Y., 2007a, "Reactive wetting of Sn-0.7Cu-xZn lead free solders on Cu substrate using wetting balance", *Journal of Alloys and Compound*, Vol. 433, pp302-305.
- Wang, H.Q., Zhao, H., Sekulic, D.P., and Qian, Y., 2007b, "A comparative study of Reactive wetting of lead and lead-free solder on Cu and (Cu₆Sn₅)/Cu substrates", *under review by Journal of Electronic Materials*.
- Warren, J. A., Boettinger, W. J., and Roosen, A. R., 1998, "Modeling Reactive wetting", *Acta Metallurgica*, Vol. 46, pp 3247-3264
- Wang, H., Gao, F., Ma, X., and Qian, Y., 2006, "Reactive wetting of solders on Cu and Cu₆Sn₅/Cu₃Sn/Cu substrates using wetting balance", *Scripta Materialia*, Vol. 55, pp 823-826.
- Wenzel, R. N., 1936, "Resistance of solid surfaces to wetting by water", *Industrial and engineering chemistry*, Vol. 28, pp 988-994
- WEEE directives, 2003, "Directive 2002/96/EC of European Parliament and of the Council of 27 January 2003 on waste electric and electronic equipment (WEEE)", *Official Journal of European Union, February*.
- Wu, C. M. L., Yu, D. Q., Law, C. M. T., and Wang, L., 2004, "Properties of Lead-free solder alloys with rare Earth elements addition", *Material Science and Engineering*, Vol44, pp 1-44.

Yost, F. G., Michael, J. R., and Eisenmann, E. T., 1995, “ Extensive wetting due to roughness”, *Acta Materialia*, Vol. 43, pp 299-305

Yost, F. G., Hosking F. M., and Frear D. R., 1993, “Introduction: The Mechanics of Solder alloy wetting and spreading”, *The Mechanics of solder alloy wetting and spreading*, pp 1-7

Yost, F. G., 2000, “Kinetics of reactive wetting”, *Scripta Materialia*, Vol. 42, pp 801-806

Yost, F. G., Sackinger, P. A., O’Tool, E. J., and Swiler, T. R., 1998, “Model determination and validation for reactive wetting processes”, *Technical report, SAND97-3122*

Zen, G. K., and Tu, K. U., 2002, “Six Cases of Reliability study Pd-Free Solder joints in Electronics Packaging Technology”, *Material Science and Engineering*, pp 55-105

<http://www.metallurgy.nist.gov/phase/solder/pbsn.html>, 2007a, online, visited during august 2007.

<http://www.metallurgy.nist.gov/phase/solder/cusn.html>, 2007b, online, visited during august 2007.

<http://www.metallurgy.nist.gov/phase/solder/agsn.html>, 2007c, online, visited during august 2007.

<http://www.metallurgy.nist.gov/phase/solder/bisn.html>, 2007d, online, visited during august 2007.

<http://www.metallurgy.nist.gov/phase/solder/agcusn.html>, 2007e, online, visited during august 2007.

<http://www.metallurgy.nist.gov/phase/solder/agbisn.html>, 2007f, online, visited during august 2007.

Worldwide consumer electronics market, 2006, *Market research report, Published by RNCOS*.

Appendix A

Surface Characterization using optical profilometer

Measurements were taken at ten different points on each surface and their average values are listed in table 3.2. The maximum deviation of R_a and PV values from their respective mean values was around $0.023\mu\text{m}$ and $0.957\mu\text{m}$ respectively. Following are the measurement data of three surfaces studied under profilometer.

Data of surface measurements of highly polished surface (Met. Lab)

S.No.	distance(mm)	$PV(\mu\text{m})$	$R_a(\mu\text{m})$
1	0	1.916	0.021
2	1	4.55	0.028
3	2	2.449	0.015
4	3	2.066	0.031
5	4	2.288	0.054
6	5	4.691	0.096
7	6	2.733	0.034
8	7	2.145	0.039
9	8	2.943	0.049
10	9	2.22	0.019

Average	
$PV(\mu\text{m})$	$R_a(\mu\text{m})$
2.788	0.038

Standard Deviation	
$PV(\mu\text{m})$	$R_a(\mu\text{m})$
0.957	0.023

Data of surface measurements of polished surface (vendor)

S.No.	Distance(mm)	$PV(\mu\text{m})$	$R_a(\mu\text{m})$
1	0	3.614	0.09
2	1	5.674	0.088
3	2	5.495	0.083
4	3	5.396	0.081
5	4	4.815	0.08
6	5	4.529	0.087
7	6	4.869	0.087
8	7	4.825	0.086
9	8	5.243	0.091
10	9	4.742	0.092

Average	
$PV(\mu\text{m})$	$R_a(\mu\text{m})$
4.920	0.087

Standard Deviation	
$PV(\mu\text{m})$	$R_a(\mu\text{m})$
0.591	0.004

Data of surface measurements of unpolished surface

S.No.	Distance(mm)	PV(μm)	R_a (μm)
1	0	5.642	1.76
2	1	6.658	1.8
3	2	6.425	1.72
4	3	6.503	1.839
5	4	5.75	1.739
6	5	8.517	1.981
7	6	6.122	1.756
8	7	6.663	1.725
9	8	5.654	1.871
10	9	6.676	1.74

Average	
PV(μm)	R_a (μm)
38.513	1.793

Standard Deviation	
PV(μm)	R_a (μm)
0.837	0.004

Appendix B

Temperature uncertainty in Hot-stage experiments

The solder alloys in the hot-stage experiments were observed to melt at the temperature higher than their melting temperature. This uncertainty is caused due to a thin glass plate inserted in between sample and the silver block to protect the silver block. This glass acts as thermal resistance, slightly reducing conduction from the heating source to sample. The data of temperature uncertainty observed during the experiments is as follows.

Temperature uncertainty observed in the hot-stage experiments

S. No.	Test #	Solder alloy	Substrate	Observed melting temperature (°C) of solder alloy	Nominal Melting temperature (°C) of solder alloy	Temperature Uncertainty (°C)
1	07/27-test1	63Sn-37Pb	Highly polished	187	183	4
2	07/27-test2	63Sn-37Pb	Highly polished	187	183	4
3	07/20-test2	63Sn-37Pb	polished	192	183	9
4	07/23-test1	63Sn-37Pb	polished	188	183	5
5	07/19-test2	63Sn-37Pb	unpolished	189	183	6
6	07/19-test3	63Sn-37Pb	unpolished	193	183	10
7	07/16-test1	Pure Sn	Highly polished	236	232	4
8	07/18-test1	Pure Sn	polished	236	232	4
9	07/24-test2	Pure Sn	unpolished	236	232	4
10	07/16-test2	99.3Sn-0.7Cu	Highly polished	230	227	3
11	07/26-test2	99.3Sn-0.7Cu	polished	230	227	3

Average	5.09
----------------	------

Appendix C

Temperature vs. time data for the hot-stage experiments involving eutectic *Sn-Pb* solder alloy

Data of temperature vs. time, eutectic *Sn- Pb* alloy over a highly polished surface refer figure 5.2

S.No.	Time (sec)	Temperature (°C)
1	4.5	30.6
2	46.062	100.2
3	57.984	120
4	70.015	140.2
5	76.031	150.1
6	81.937	160
7	88.062	170.3
8	94.078	180.2
9	99.984	190.1
10	106.109	200.1
11	112.015	210
12	113.984	213
13	116.078	213
14	116.843	213
15	123.297	213
16	128	213
17	135	213
18	142	213
19	144.406	213
20	147.359	210
21	153.609	200.1
22	161.703	190
23	169.14	180.2
24	176.578	170.1
25	184.015	160.3
26	191.672	150
27	198.906	140.4
28	214	120.1
29	281.422	30.2

Data of temperature vs. time, eutectic *Sn- Pb* alloy over a polished surface refer figure 5.7

S.No.	Time (sec)	Temperature (°C)
1	2	26
2	45.422	100.1
3	51.437	110.1
4	63.578	130.2
5	75.39	149.8
6	87.312	170
7	98.797	188.8
8	111.375	210
9	113.344	213
10	113.672	213.1
11	114.437	213.2
12	124.5	213
13	132.265	213
14	134.234	213
15	136.312	213
16	138.39	213
17	143.859	213
18	146.594	210
19	160.922	190.2
20	175.906	170
21	183.344	160.2
22	198.328	140
23	213.422	120
24	228.297	100.2
25	280.922	30.2

Data of temperature vs. time, eutectic *Sn- Pb* alloy over an unpolished surface refer figure 5.12

S.No.	Time (sec)	Temperature (°C)
1	2.5	26.6
2	51.297	110.1
3	63.453	129.9
4	75.484	150.1
5	87.516	169.9
6	98.781	189.1
7	111.359	209.9
8	112.672	211.9
9	113.219	213
10	115.516	213.1
11	121.75	213
12	126.234	213
13	133.016	213
14	141.437	213
15	142.75	213
16	143.844	213
17	145.156	212
18	160.797	190.2
19	176	170.2
20	183.437	160.1
21	198.641	140
22	213.516	120.2
23	228.5	100.1
24	281	30.1

Appendix D

Temperature vs. time data for the hot-stage experiments involving lead-free solder alloys

Data of temperature vs. time, pure Sn over a highly polished surface refer figure 6.2

S.No.	Time (sec)	Temperature (°C)
1	5.062	31.5
2	45.969	100.4
3	58	120.3
4	69.812	140.1
5	81.844	160
6	93.875	180.1
7	105.906	200.3
8	117.937	220.1
9	125.156	232.4
10	127.344	236
11	135.984	250.2
12	142.547	261.2
13	143.422	262.1
14	144.078	262.2
15	144.734	262
16	149	262
17	153.703	262
18	154.141	261.8
19	159.719	251.9
20	176.234	231.9
21	192.094	211
22	207.734	190.1
23	222.719	170.3
24	237.703	150.2
25	252.687	130.4
26	267.891	110
27	275.328	100
28	327.625	30.2

Data of temperature vs. time, pure Sn over a polished surface refer figure 6.7

S.No.	Time (sec)	Temperature (°C)
1	2	26.4
2	45.234	100
3	57.265	120.2
4	69.078	140.1
5	81.218	160.2
6	93.14	180.1
7	105.281	200.2
8	117.203	219.8
9	126.828	236.3
10	141.265	260.1
11	142.25	261.7
12	143.015	262.2
13	144	262.1
14	146.515	262.2
15	148.047	262.1
16	150.562	262
17	153.734	260.2
18	168.828	240
19	183.812	219.9
20	198.906	200.1
21	213.781	180.2
22	228.875	160.1
23	243.859	140
24	258.843	120.2
25	273.937	100.1
26	326.328	30.1

Data of temperature vs. time, pure Sn over an unpolished surface refer figure 6.12

S.No.	Time (sec)	Temperature (°C)
1	4.015	29.7
2	45.797	100
3	58.047	120.2
4	69.859	140.1
5	82	160.2
6	87.906	170.2
7	99.937	190.3
8	111.969	210.2
9	127.39	236
10	141.953	260.1
11	143.265	262.1
12	145.344	262
13	147.094	262.2
14	149.062	262.1
15	151.031	262
16	153	262
17	155.297	260.2
18	170.172	240
19	185.047	220.1
20	199.922	200.2
21	215.14	180.1
22	230.234	160.1
23	245.219	140
24	260.094	120.1
25	275.297	100
26	327.609	30.1

Data of temperature vs. time, eutectic *Sn-Cu* solder alloy over a highly polished surface refer figure 6.17

S.No.	Time (sec)	Temperature (°C)
1	4.141	30.2
2	45.703	100.3
3	57.625	120.1
4	69.766	140.3
5	81.578	160.2
6	93.61	180
7	105.75	200.1
8	117.563	220
9	121.828	226.9
10	123.578	229.9
11	135.719	250.1
12	139.219	256
13	140.094	257
14	141.078	257.2
15	143.047	257.1
16	145.016	257.1
17	147.094	257
18	150.375	257
19	150.703	256.8
20	155.188	250
21	178.156	220.1
22	193.031	200.2
23	208.125	180.1
24	223.219	160
25	253.313	120.1
26	268.297	100
27	320.875	30.1

Data of temperature vs. time, eutectic *Sn-Cu* solder alloy over a polished surface refer figure 6.22

S.No.	Time (sec)	Temperature (°C)
1	4	30.6
2	45.594	100.1
3	57.406	120
4	69.547	140.2
5	81.469	160
6	93.609	180.2
7	105.531	200
8	120.625	225.2
9	123.687	230.5
10	135.5	250
11	139.219	256.3
12	139.875	257
13	141.078	257.1
14	143.047	257.1
15	145.015	257.1
16	147.094	257
17	149.062	257
18	150.375	257
19	155.187	250
20	170.5	230.1
21	185.594	210
22	208.14	180
23	223.031	160.2
24	238.031	140.1
25	253.14	120
26	267.906	100.2
27	320.422	30.2

Appendix E

A/A_0 vs. time data for the hot-stage experiments involving eutectic *Sn-Pb* alloy

A/A_0 Vs Time data for eutectic *Sn-Pb* solder alloy spreading on highly polished surface, Refer Fig. 5.5

S.No.	Time (sec)	A/A_0	S.No.	Time (sec)	A/A_0	S.No.	Time (sec)	A/A_0
1	0	1	33	9.625	6.374	65	24.750	15.149
2	0.458	1.036	34	10.083	6.585	66	25.209	15.505
3	0.688	1.042	35	11.000	7.104	67	25.667	15.865
4	0.779	1.046	36	11.458	7.316	68	26.125	16.095
5	0.871	1.095	37	11.917	7.509	69	26.583	16.492
6	0.962	1.269	38	12.375	7.696	70	27.042	16.879
7	1.054	1.485	39	12.833	7.959	71	27.500	17.166
8	1.146	1.801	40	13.292	8.131	72	27.959	17.597
9	1.375	1.996	41	13.750	8.387	73	28.417	17.859
10	1.833	2.211	42	14.208	8.654	74	28.875	18.195
11	2.062	2.323	43	14.667	8.828	75	29.333	18.548
12	2.292	2.428	44	15.125	9.060	76	29.792	18.848
13	2.521	2.519	45	15.583	9.310	77	30.250	19.174
14	2.750	2.625	46	16.042	9.541	78	30.709	19.542
15	2.979	2.705	47	16.500	9.768	79	31.167	19.907
16	3.208	2.865	48	16.959	10.087	80	31.625	20.175
17	3.438	2.989	49	17.417	10.341	81	32.084	20.612
18	3.667	3.126	50	17.875	10.617	82	33.459	21.616
19	3.896	3.210	51	18.333	10.915	83	34.834	22.525
20	4.125	3.2780	52	18.792	11.149	84	36.209	23.304
21	4.354	3.407	53	19.250	11.455	85	37.584	24.253
22	4.583	3.618	54	19.709	11.728	86	38.959	25.077
23	5.042	3.831	55	20.167	12.160	87	41.250	26.651
24	5.500	4.066	56	20.625	12.333	88	43.542	27.853
25	5.958	4.301	57	21.083	12.669	89	45.834	29.074
26	6.417	4.645	58	21.542	12.933	90	48.125	30.327
27	6.875	4.879	59	22.000	13.305	91	50.417	31.310
28	7.333	5.096	60	22.459	13.545	92	52.709	32.027
29	7.792	5.398	61	22.917	13.895	93	55.000	32.700
30	8.250	5.664	62	23.375	14.249	94	57.292	33.139
31	8.708	5.908	63	23.833	14.567	95	59.583	33.443
32	9.167	6.177	64	24.292	14.806	96	68.705	34.378

**A/A_0 Vs Time data for eutectic *Sn-Pb* solder alloy spreading on polished surface,
Refer Fig. 5.10**

S.No.	Time (sec)	A/A_0
1	0	1
2	0.504	1.069
3	0.595	1.250
4	0.688	1.414
5	0.779	1.513
6	0.871	1.629
7	0.963	1.736
8	1.054	1.791
9	1.146	1.822
10	1.375	1.926
11	1.604	2.058
12	1.833	2.087
13	2.062	2.190
14	2.291	2.258
15	2.521	2.338
16	2.750	2.417
17	2.979	2.532
18	3.208	2.635
19	3.437	2.708
20	3.667	2.862
21	3.896	2.947
22	4.125	3.139
23	4.354	3.394
24	4.583	3.546
25	5.042	3.894
26	5.500	4.269
27	5.958	4.579

S.No.	Time (sec)	A/A_0
28	6.416	5.009
29	6.875	5.277
30	7.333	5.607
31	7.791	5.853
32	8.250	6.187
33	8.708	6.458
34	9.167	6.744
35	9.625	7.002
36	10.083	7.230
37	10.541	7.555
38	11.000	7.740
39	11.458	8.004
40	11.917	8.222
41	12.375	8.424
42	12.833	8.678
43	13.292	8.881
44	13.750	9.071
45	14.208	9.251
46	14.667	9.412
47	15.125	9.532
48	15.583	9.687
49	16.041	9.803
50	16.500	9.934
51	16.958	10.051
52	17.416	10.139
53	17.875	10.235
54	18.333	10.342

S.No.	Time (sec)	A/A_0
55	18.792	10.463
56	19.250	10.520
57	19.708	10.587
58	20.167	10.881
59	20.625	10.961
60	21.083	11.124
61	21.541	11.251
62	22.001	11.298
63	22.458	11.310
64	22.917	11.327
65	23.375	11.340
66	23.833	11.347
67	24.292	11.355
68	24.750	11.358
69	25.209	11.365
70	27.500	11.508
71	29.791	11.591
72	32.083	11.732
73	34.375	11.784
74	36.667	11.803
75	38.959	12.010
76	41.250	12.222
77	43.542	12.242
78	45.833	12.258
79	48.125	12.310
80	50.417	12.337
81	68.705	12.772

**A/A_0 Vs Time data for eutectic *Sn-Pb* solder alloy spreading on unpolished surface,
Refer Fig. 5.15**

S.No.	Time(sec)	A/A_0
1	0	1
2	0.046	1.037
3	0.092	1.038
4	0.138	1.040
5	0.183	1.077
6	0.229	1.044
7	0.275	1.069
8	0.320	1.107
9	0.3667	1.240
10	0.412	1.312
11	0.458	1.363
12	0.504	1.421
13	0.550	1.529
14	0.596	1.568
15	0.642	1.603
16	0.688	1.730
17	0.779	1.763
18	0.871	1.781
19	0.962	1.822
20	1.054	1.904
21	1.375	1.985
22	1.604	2.072
23	1.833	2.131
24	2.062	2.207
25	2.292	2.226
26	2.521	2.289
27	2.750	2.298
28	2.979	2.396
29	3.208	2.450
30	3.438	2.476

S.No.	Time(sec)	A/A_0
31	3.667	2.527
32	3.896	2.579
33	4.125	2.630
34	4.354	2.695
35	4.583	2.791
36	5.042	2.859
37	5.500	2.901
38	5.958	3.022
39	6.417	3.155
40	6.875	3.237
41	7.333	3.339
42	7.792	3.400
43	8.250	3.500
44	8.708	3.588
45	9.167	3.668
46	9.625	3.710
47	10.083	3.879
48	10.542	3.911
49	11.000	3.988
50	11.458	4.114
51	12.375	4.266
52	12.833	4.441
53	13.292	4.493
54	13.750	4.641
55	14.208	4.747
56	14.667	4.832
57	15.125	4.951
58	15.583	5.136
59	16.042	5.231
60	16.500	5.420

S.No.	Time(sec)	A/A_0
61	17.417	5.648
62	17.875	5.723
63	18.333	5.940
64	18.792	6.037
65	19.250	6.285
66	19.709	6.292
67	20.166	6.379
68	20.625	6.460
69	21.083	6.599
70	21.542	6.750
71	22.000	6.813
72	22.459	6.974
73	22.917	7.126
74	25.209	7.391
75	27.500	7.810
76	29.792	7.996
77	32.084	8.313
78	34.375	8.561
79	36.667	9.037
80	38.959	9.195
81	41.250	9.534
82	43.542	9.978
83	45.834	10.256
84	48.125	10.388
85	50.417	10.393
86	52.709	10.529
87	55.000	10.677
88	57.292	10.818
89	59.584	10.973
90	68.705	11.113

Appendix F

A/A_o vs. time data for the hot-stage experiments involving lead-free solder alloys

A/A_o Vs time data for pure Sn spreading on highly polished surface, Refer Fig. 6.5

S.No.	Time (sec)	A/A_o
1	0	1
2	0.458	1.022
3	0.550	1.015
4	0.642	1.027
5	0.733	1.126
6	0.825	1.175
7	0.917	1.233
8	1.008	1.244
9	1.100	1.246
10	1.192	1.246
11	1.283	1.246
12	1.375	1.246
13	1.467	1.246
14	1.650	1.248
15	1.833	1.248
16	2.017	1.248
17	2.200	1.248

S.No.	Time (sec)	A/A_o
18	2.383	1.248
19	2.567	1.248
20	2.750	1.248
21	3.208	1.248
22	3.667	1.248
23	4.125	1.248
24	4.583	1.248
25	7.795	1.248
26	12.199	1.248
27	16.603	1.248
28	18.805	1.249
29	21.007	1.249
30	23.209	1.249
31	25.411	1.249
32	27.613	1.249
33	29.805	1.249
34	45.834	1.250

A/A_0 Vs Time data for pure Sn spreading on polished surface, Refer Fig. 6.10

S.No.	Time (sec)	A/A_0
1	0	1
2	0.458	1.001
3	0.550	1.009
4	0.642	1.009
5	0.733	1.026
6	0.825	1.042
7	0.917	1.049
8	1.008	1.050
9	1.100	1.050
10	1.192	1.051
11	1.283	1.052
12	1.375	1.056
13	1.467	1.057
14	1.650	1.061
15	1.833	1.090

S.No.	Time (sec)	A/A_0
16	2.017	1.091
17	2.200	1.092
18	2.383	1.093
19	2.567	1.095
20	2.750	1.096
21	3.208	1.096
22	3.667	1.097
23	4.125	1.097
24	4.583	1.097
25	6.483	1.099
26	10.283	1.099
27	14.083	1.099
28	17.883	1.099
29	33.083	1.099
30	47.883	1.099

A/A_0 Vs Time data for pure Sn spreading on unpolished surface, Refer Fig. 6.15

S.No.	Time (sec)	A/A_0
1	0	1
2	0.183	1.000
3	0.458	1.000
4	0.688	1.002
5	0.917	1.007
6	1.375	1.015
7	1.833	1.016
8	2.292	1.016
9	3.208	1.018
10	3.667	1.018
11	9.082	1.023
12	14.498	1.026
13	17.206	1.026
14	19.914	1.027
15	28.083	1.028
16	36.160	1.028
17	44.284	1.028

A/A_0 Vs Time data for eutectic *Sn-Cu* solder alloy spreading on highly polished surface, Refer Fig. 6.20

S.No.	Time (sec)	A/A_0
1	0	1
2	0.458	1.028
3	0.550	1.049
4	0.642	1.085
5	0.733	1.088
6	0.825	1.101
7	0.917	1.102
8	1.008	1.102
9	1.100	1.103
10	1.192	1.104
11	1.283	1.104
12	1.375	1.104
13	1.467	1.104
14	1.650	1.104

S.No.	Time (sec)	A/A_0
15	1.833	1.104
16	2.017	1.105
17	2.200	1.105
18	2.383	1.105
19	2.567	1.105
20	2.750	1.105
21	3.208	1.105
22	3.667	1.105
23	4.125	1.106
24	4.583	1.106
25	10.124	1.106
26	12.038	1.106
27	14.124	1.106
28	31.178	1.107

A/A_0 Vs Time data for eutectic Sn-Cu solder alloy spreading on polished surface(vendor), Refer Fig. 6.25

S.No.	Time (sec)	A/A_0
1	0	1
2	0.229	1.004
3	0.458	1.029
4	0.550	1.039
5	0.642	1.040
6	0.733	1.040
7	0.825	1.040
8	0.917	1.041
9	1.008	1.041
10	1.100	1.041
11	1.192	1.041
12	1.283	1.041
13	1.375	1.041
14	1.467	1.042
15	1.650	1.042
16	1.833	1.042

S.No.	Time (sec)	A/A_0
17	2.017	1.043
18	2.200	1.043
19	2.383	1.043
20	2.567	1.043
21	2.750	1.043
22	3.208	1.043
23	3.667	1.043
24	4.125	1.043
25	4.583	1.043
26	8.111	1.047
27	11.639	1.047
28	15.168	1.047
29	22.224	1.047
30	29.280	1.047
31	36.336	1.048
32	43.395	1.048

Appendix G

Final A/A_o Vs Cu substrates data for spreading of solder alloys on different copper substrates

S.No.	Surface	Surface Roughness		Final A/A_o		
		$PV(\mu\text{m})$	$R_a(\mu\text{m})$	Eutectic $Sn-Pb$	Pure Sn	Eutectic $Sn-Cu$
1	Polished surface (Met. Lab)	2.788	0.038	28.097	1.250	1.107
2	Polished Surface (vendor)	4.920	0.087	12.400	1.099	1.048
3	Unpolished Surface	6.461	0.179	7.606	1.029	

Nomenclature

Chemical symbols:

<i>Sn</i>	tin
<i>Pb</i>	Lead
<i>Cu</i>	Copper
<i>Ag</i>	Silver
<i>Bi</i>	Bismuth
<i>HCL</i>	Hydrochloric acid
<i>N₂</i>	Nitrogen

Unit symbols:

atm	atmosphere
° C	Celsius
m	meter
mm	millimeter
nm	nanometer
µm	micrometer
min	minute
sec	second
mg/dl	milligram/deciliter

Symbols:

γ_{sv}	Surface energy at the interface of solid surface and vapor
γ_v	Surface energy at the interface of liquid and vapor
γ_{sl}	Surface energy at the interface of solid surface and liquid
θ	Dynamic contact angle
θ_e	Equilibrium contact angle
θ_o	Equilibrium contact angle on smooth surface
θ_r	Apparent equilibrium contact angle on rough surface
ϕ	Lower contact angle of dissolution
α	Angle of steepness on rough surface
R_a	Average surface roughness
R_p	Maximum peak height
R_v	Maximum valley depth
λa	Average distance between peaks on rough surface
PV	Maximum peak to valley height
t	time
A_o	Initial area of solder
A	Area of spread at a given instance of time
A/A_o	Relative area of spread

VITA

Name: Dinesh Reddy Nalagatla

Date of Birth: July 5th 1984

Place of Birth: Rajampet, Andhra Pradesh, India

Professional Positions held:

- 1) Student Research Assistant, Osmania University, India, 2004-2005
- 2) Graduate Research Assistant, University of Kentucky, US, 2006-2007

Educational Institutions Attended:

- 1) Osmania University, India, 2001 - 2005.

Degree Awarded: Bachelor's in Mechanical Engineering

- 2) University of Kentucky, U.S.A. 2005 - 2007